Author/s:
Khoury, DS;Aogo, R;Randriafanomezantsoa-Radohery, G;McCaw, JM;Simpson, JA;McCarthy, JS;Haque, A;Cromer, D;Davenport, MP

Title:
Within-host modeling of blood-stage malaria

Date:
2018-09-01

Citation:
Khoury, D. S., Aogo, R., Randriafanomezantsoa-Radohery, G., McCaw, J. M., Simpson, J. A., McCarthy, J. S., Haque, A., Cromer, D. & Davenport, M. P. (2018). Within-host modeling of blood-stage malaria. Immunological Reviews, 285 (1), pp.168-193. https://doi.org/10.1111/imr.12697.

Article type : Invited Review

Within-host modelling of blood-stage malaria

David S. Khoury[1], Rosemary Aogo[1], Georges Randriafanomezantsoa-Radohery[1], James M. McCaw[2,3,4], Julie A. Simpson[3], James S. McCarthy[5], Ashraful Haque[5], Deborah Cromer[1], Miles P. Davenport[1].

1. Kirby Institute, UNSW Sydney, Sydney, Australia.
2. School of Mathematics and Statistics, University of Melbourne
3. Centre for Epidemiology and Biostatistics, Melbourne School of Population and Global Health, University of Melbourne
4. Peter Doherty Institute for Infection and Immunity, The Royal Melbourne Hospital and University of Melbourne
5. QIMR Berghofer Medical Research Institute, Herston, Queensland, Australia.

Corresponding Author:
Miles P. Davenport
Address: Kirby Institute Level 6, Wallace Wurth Building, UNSW Sydney NSW 2052
Phone: +61 2 9385 2762
Email: m.davenport@unsw.edu.au
David S. Khoury
Address: Kirby Institute Level 6, Wallace Wurth Building, UNSW Sydney NSW 2052
Phone: +61 2 9385 0980

29 Email: dkhoury@kirby.unsw.edu.au

30

31

Running Title: Within-host modelling of blood-stage malaria

Summary

Malaria infection continues to be a major health problem worldwide and drug resistance in the major human parasite species, Plasmodium falciparum, is increasing in South East Asia. Control measures including novel drugs and vaccines are in development, and contributions to the rational design and optimal usage of these interventions are urgently needed. Infection involves the complex interaction of parasite dynamics, host immunity, and drug effects. The long lifecycle (48 hours in the common human species) and synchronized replication cycle of the parasite population present significant challenges to modelling the dynamics of Plasmodium infection. Coupled with that, variation in immune recognition and drug action at different lifecycle stages leads to further complexity. We review the development and progress of 'within-host' models of Plasmodium infection, and how these have been applied to understanding and interpreting human infection and animal models of infection.

Keywords

Malaria, Within host, Mathematical modelling, Parasite Development, Immunity, Antimalarial.

Introduction

Mathematical models of viral infections such as HIV and hepatitis C have been extensively studied from the molecular level to the epidemiological level, drawing on a broad range of modelling strategies and data analysis techniques (1-5). This has contributed to the development of highly effective control strategies at the host and population levels for both HIV and hepatitis C, among other important viral infections. Although a significant body of work, modelling to understand the within-host dynamics of malaria infections has enjoyed significantly less attention from modellers compared with viral infections. Here we discuss the key aspects of within-host malaria infection, highlighting the application of different modelling approaches, the parallels with models of viral dynamics, as well as important and interesting differences specific to malaria parasite biology. With more than 200 million cases of malaria each year, leading to approximately half a million deaths, the vast majority of which (more than 90%) occur in Africa and in children under five (6), malaria is a global health priority. Our intention with this review is to spark the interest of the infection modelling community to commence a renewed investigation of this important and complex pathogen.

The blood-stage of malaria infection can be modelled as a variant of the 'basic model' of infection used for viral dynamics (7-13). However, the peculiarities of the parasite lifecycle – a prolonged development within the host red blood cell (RBC) followed by rupture, and the synchronised nature of parasite replication in many species, lend themselves to application of more complex modelling approaches such as age-structured ordinary differential/difference equation models (14-16), delay differential equation models (17), or partial differential equation models (18-20). By discussing, the similarities and differences between viral infections and malaria we hope to show the reader both the potential for the application of

existing virological modelling techniques to malaria, and the opportunities for developing new modelling approaches to address some of malaria's unique challenges.

Outline of the parasite lifecycle

The malaria parasite (Plasmodium genus) infects a wide variety of host species and has a complex lifecycle involving sexual reproduction occurring in the insect vector (21), and two stages of infection within a human (or animal host), a liver-stage (22) and blood-stage (23-25) (illustrated in fig. 1). Five species infect humans (Plasmodium falciparum, P. vivax, P. malariae, P. ovale, and P. knowlesi). Here we focus mainly on the most pathogenic species infecting humans, P. falciparum, and refer to differences with the other major human species, as well as peculiarities of commonly used animal models, where relevant.

Human infection is initiated by mosquito transmission of the sporozoite form of P. falciparum during a blood meal (fig. 1a). The sporozoites find and enter the host peripheral circulation, and rapidly transit to the liver where they infect liver cells (hepatocytes) (fig. 1b) (22). The liver stage of infection lasts around a week in humans, is asymptomatic, and at present there are few experimental approaches for in vivo detection of parasites in the liver. The parasite replicates within the liver cell before rupturing to release ≈40,000 extracellular parasite forms, known as merozoites, into the host circulation (fig. 1b), where they may invade red blood cells (RBCs) to initiate blood-stage infection (fig. 1c) (24). Then follows a series of cycles of replication, rupture, and re-invasion of the RBC (fig. 1c). This so-called erythrocytic lifecycle is the primary focus of this review (25). Some asexual parasite forms commit to an alternative developmental pathway and become sexual forms (gametocytes) (fig. 1d) (23). Gametocytes can be taken up by mosquitos during a blood meal where they

undergo a cycle of sexual development to produce sporozoites (21) (fig. 1e), which completes the parasite lifecycle.

Asexual parasite development within RBCs is characterised by a series of morphological stages, readily identified by microscopy (fig. 1c) (23). The youngest stage is known as the ring stage, describing the appearance of the parasite vacuole as a ring-like structure within the recently infected RBC. As the parasite grows it assumes a larger and denser appearance termed the trophozoite stage. Following mitotic division of the growing parasite it reaches the final intraerythrocytic stage, the schizont, when the morphological appearance of small structures within the infected RBC signals the formation of between 8-32 daughter merozoites within the schizont. The schizont then ruptures to release daughter merozoites into the circulation, where they rapidly invade another host RBC, initiating the next cycle of replication.

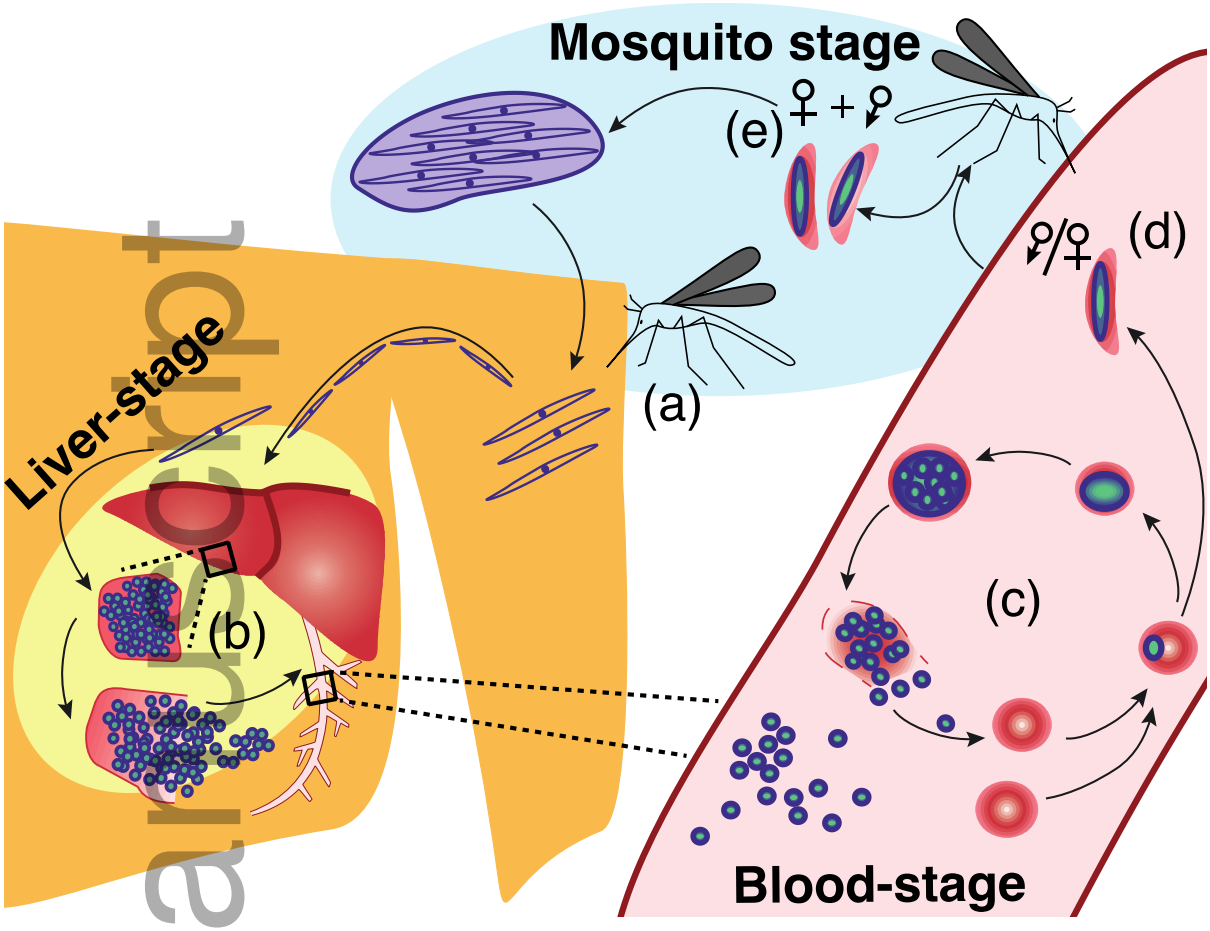

Figure 1: Illustration of the Plasmodium lifecycle. (a) infection in a human or animal host is initiated by a bite from an infectious mosquito. Sporozoite parasite forms are injected and traverse the blood stream to the liver where they infect liver cells. (b) This initiates the liver-stage of infection, which lasts around a week in humans. Once mature, these infected liver cells rupture to release ≈40,000 merozoites into the blood. (c) Merozoites invade red blood cells (RBCs) inside which the parasite matures into a schizont. Schizonts rupture to release between 8-32 merozoites that can infect more RBCs. This asexual proliferation in the blood of the host is called the blood-stage of infection and is the stage of the parasites lifecycle that leads to pathogenesis. (d) Some parasite can commit to sexual development in the RBC, producing gametocytes. (e) Gametocytes are taken up by mosquitos during a blood meal, where sexual development occurs resulting in sporozoite formation.

Parasite multiplication: The standard within-host model of Plasmodium parasite replication

The malaria parasite asexual cycle described above (fig. 1c) is very similar to the replication cycle of many viruses, such as HIV. Both involve cycles of infecting cells ($CD4^+$ T cells or RBC), and short-lived extracellular stages (free virus, or merozoites). The "classical" model of within-host parasite multiplication in malaria infections was formulated by Anderson et al.

in 1989 (9), and has a similar formulation to the standard viral replication model for HIV (26) (fig. 2). This model tracks target cells, parasitised cells and extracellular parasites (7, 8). Using these models as a starting point we will discuss some of the key similarities and differences between viral infections and malaria, paying special attention to the key opportunities for applied mathematicians and other quantitative experts to bring insights into some of the many outstanding problems in malaria research.

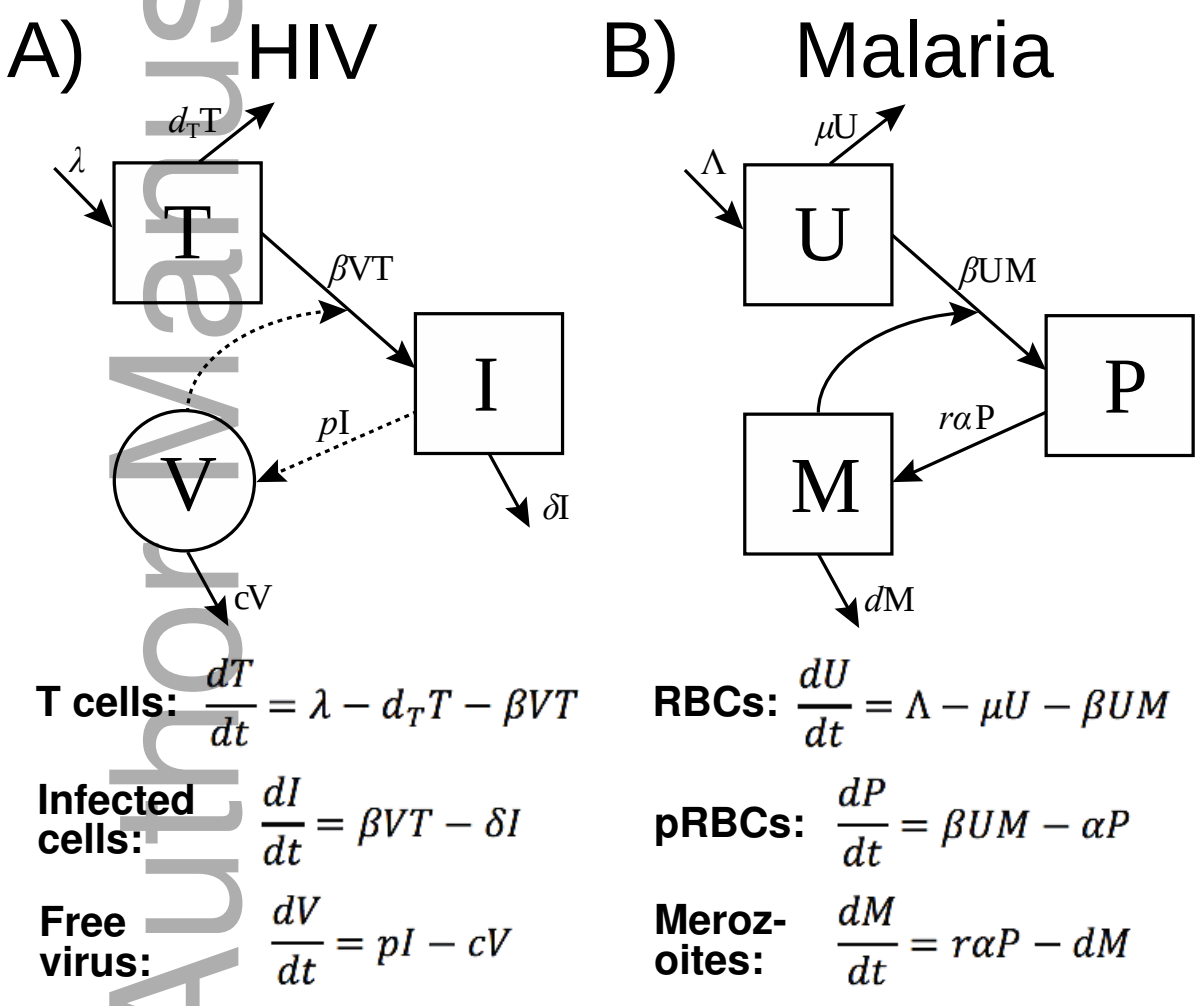

Figure 2: Schematic and equations of the standard models of within-host HIV and malaria infections. (A) The standard model of HIV infection. Target $CD4^+$ T cells, T, are produced at rate λ and die at a natural death rate d_T. The infection of T cells depends on the availability of T cells, the amount of free virus, V, and infectivity β. Infected cells, I, are lost at rate δ. Infected cells produce virus at rate p, and virus is cleared at rate c. The solid lines indicate a transition of state (e.g. uninfected T cells becomes infected), whereas, the dashed

lines indicate an interaction that does not 'use up' the contributing population. For example, virus production does not directly lead to the loss of the infected cell. Similarly, the infection of T cells is related to the virus level but virus is not used up by infection in this standard version of the model. (B) The standard model of Plasmodium infection. Uninfected red blood cells (RBCs), U, are produced at rate Λ and lost at rate μ. Parasitised RBCs (pRBCs), P, are created when a merozoite, M, infects a RBC. This process depends on the availability of uninfected RBCs, merozoites, and the infectivity β. Parasitised RBCs rupture at rate α, with each rupturing pRBC producing r merozoites. Merozoites are lost at rate d.

Modelling the replication cycle of Plasmodium

The standard model illustrated in figure 2 highlights a key difference in most models of viral infections and malaria infection. Whereas, HIV virus production is often treated as continuous and proportional to the number of infected cells (i.e. virus production does not lead to cell death, though this is not always the case). On the other hand, merozoite production only occurs when a mature parasitised RBC (pRBC) ruptures, releasing a brood of merozoites (of size r) (fig. 2). The standard model of Plasmodium infection tries to capture this by including the production of merozoites as proportional to the loss of pRBCs (fig. 2B). Interestingly, there is some debate about whether a continuous production of virus is realistic for some viral infections (27-30), but that is a question for modellers in virology. For modellers of Plasmodium infections, the issue of correctly modelling the rupturing of mature pRBCs has been a major point of discussion, and for good reason given the unique synchronous character of many Plasmodium infections.

The problem of lifetimes

Issues with the standard model of Plasmodium infection were first highlighted by Saul (31), and is related to the distribution of possible life-times of pRBCs. In particular, Saul noted that the parameter in this model that was defined as describing the number of merozoites produced per infected cell (r) gave a dramatic over estimate of the growth rate of infected cells. Even though the model correctly captures the idea that r merozoites are produced at the

end of a pRBCs lifecycle, the model fails to capture realistic life-times of the pRBCs. The model uses an exponential process to describe the rate of rupture of pRBCs, and the rate of rupture (α) is chosen so that on average the life-time of pRBC matches the known time life-time of pRBCs (approximately 48 hours for P. falciparum and P. vivax). Despite this formulation of the model (with parasite rupture as an exponential process) giving a correct average life-time of pRBCs, it also ensures that many pRBCs will have a much shorter life-time (some even reaching maturity and rupturing almost instantly after invasion of the RBC), and some will have a much longer life-time. This means that some pRBCs will rupture immediately (and release r merozoites), and others will take much longer (even months), and still release r merozoites. This is not realistic, given the asexual lifecycle time is known to be relatively constant, and fast pRBC rupture leads to unrealistically high parasite growth rates.

Modelling parasite life-times

This observation by Saul (31), led to a number of other approaches to modelling parasite development and replication within a host. These other approaches included, a model that added many compartments representing a progression through a parasites lifecycle (which we refer to as the n-compartment model, fig. 3A) (14-16), delay differential equations to capture the time it takes infected cells to mature before producing merozoites (17), and the use of partial differential equations (PDE) to track the age structure of the pRBC population (18-20) (which we refer to as the PDE model, fig. 3B).

The n-compartment model has some interesting properties. The standard model (fig. 2B) produced an exponential distribution in the life-times of pRBCs with mean equal to 1 over the rate of pRBC rupture ($1/\alpha$). However, the n-compartment model produces an Erlang distribution in pRBCs life-times, with the same mean, but with life-times more narrowly

204 distributed around this mean as the number of compartments (N) increases (32, 33). This
205 provides a useful way to control the variation in the parasite lifecycle. As N approaches
206 infinity the distribution approaches the Dirac delta function, causing all pRBCs to have
207 identical life-times.
208
209 The PDE model tracks the movement of the age-density of the parasite population through
210 time. That is, with each step forward in time resulting in an equivalent increase in all
211 parasites' ages. This model captures parasite invasion of RBCs in the boundary condition,
212 which illustrates the birth of pRBCs of age zero, and merozoite creation is related to the
213 number of mature pRBCs rupturing at age 48 h (fig. 3B). Alternatively, a parasite rupture rate
214 that depends on the age of parasites can be included in this model. In this case the production
215 of merozoites (fig. 3B), becomes a more complicated expression related to the integral of the
216 rupture rate multiplied by the age-density of parasites (see (19, 34)). This PDE model is a
217 more general formulation of an older model of parasite replication found in the literature,
218 which tracked a normal distribution of pRBCs of different ages as they progress through time
219 (35). Further, this PDE model is equivalent to the n-compartment model as the number of
220 compartments approaches infinity, in that all pRBCs have identical life-times.
221
222 This issue of correctly capturing the life-times of pRBCs when modelling Plasmodium
223 infections is perhaps most important because the lifecycle of infection within an individual
224 host is often synchronous.
225

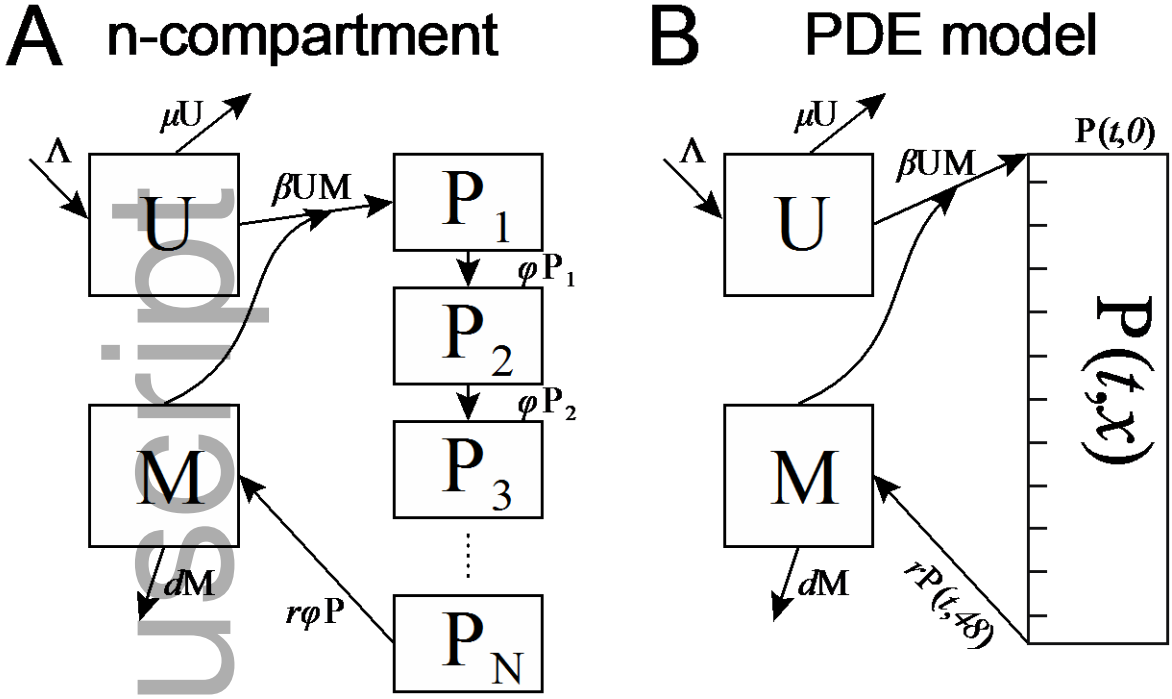

$$\frac{dP_1}{dt} = \beta UM - \phi P_1$$

$$\frac{dP_i}{dt} = \phi P_{i-1} - \phi P_i \qquad i = 2, \ldots, N$$

$$\frac{dM}{dt} = r\phi P_N - dM$$

$$\frac{\partial P}{\partial t} + \frac{\partial P}{\partial x} = 0$$

$$P(t,0) = \beta UM$$

$$\frac{dM}{dt} = rP(t,48) - dM$$

Figure 3: Schematic and equations for two age-structured models of Plasmodium infection. (A) An ordinary differential equation (ODE) model extending on the standard model in figure 2B. The parasitised RBC compartment from the standard model is split into N discrete stages of development. The rate of transition between stages is given by ϕ, and chosen such that $\phi = N/48$, to ensure an average parasitised red blood cell (pRBC) life-time of 48 hours. The form of the equations for merozoites, M, is equivalent to that in the standard model except only the mature pRBC compartment, P_N, contributes to merozoites production. We refer to this model as the n-compartment model. (B) A partial differential equation (PDE) model of parasite development. In this model P represents the age-density of pRBCs at time t, where x is parasite age in hours. The structure of this PDE is such that for every hour of time that passes all parasites will mature by one hour. The infection of RBCs is defined by the boundary condition of the PDE. The equation describing merozoites has the same form as the classical model except that production of merozoites at any given time is proportional to mature pRBCs, $P(t, 48)$. The total pRBCs at any given time is given by $\int_0^{48} P(t,x)\,dx$. We refer to this model as the PDE model. In both model (A) and (B) the uninfected RBC equation, U, is identical to that shown in the classic model in figure 2B.

Synchronous Parasite Replication

Very early studies of malaria (even before it was agreed that it was caused by an infectious agent) noted patients experienced periodic fevers every 48 hours ('tertian fever', as seen with the most common human Plasmodium species, P. falciparum and P. vivax) or every 72 hours ('quartan fever', as seen with P. malariae) (36, 37). It became commonly accepted that this periodicity in fever was the result of synchronous cycles of simultaneous rupture of infected RBC, releasing pyrogenic toxins into the circulation (36). The stereotypic pattern of periodic fevers in Plasmodium infection may not be universal, for a range of reasons, including multiple, out-of-phase, releases of merozoites from the liver or multiple concurrent infections. However, synchrony has been confirmed in experimental human Plasmodium infections where it has been possible to track parasite numbers in individuals that have received deliberate infection either for treatment of neurosyphilis (before the discovery of penicillin), or more recently for drug and vaccine development (38-42). In these studies it is clear that parasite numbers increase periodically (fig. 4A). Importantly, we observe that the standard model proposed in figure 2B cannot account for the periodic structure of the growth of parasites observed in individuals infected with P. falciparum. This creates an issue because some of the traditional concepts of infection, such as the 'growth rate', become less meaningful when applied to a synchronous infection (Box 2). However, models similar in construction to both the n-compartment and PDE models have been used to capture synchronous infection dynamics (43, 44).

The synchronous nature of many malaria infections raise some important questions that remain to be resolved. In particular, how does the parasite co-ordinate or maintain a synchronous infection? And why do some Plasmodium species mature and rupture

268 synchronously in some individuals? What advantage is gained by the parasite? (Be aware that
269 there are examples of highly synchronous (45) and asynchronous Plasmodium falciparum
270 infections (46) recorded in the literature).

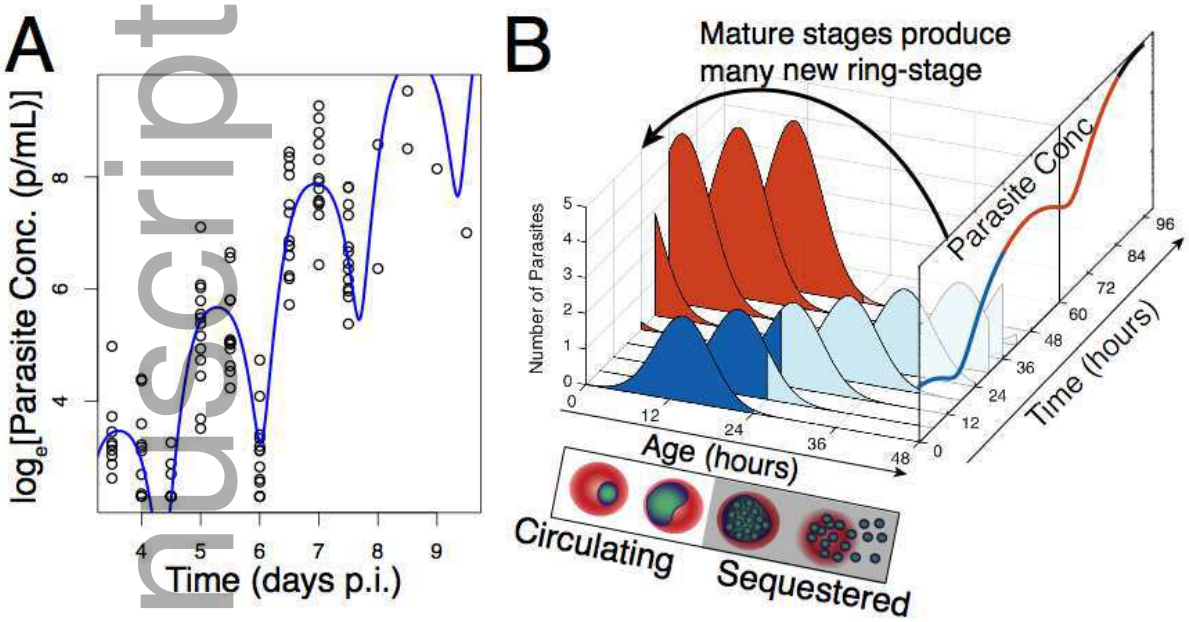

271

272 **Figure 4: Synchronous infection Plasmodium falciparum infection and sequestration in**
273 **humans.** (A) Parasite concentration data of individuals (n=13) infected with P. falciparum
274 3D7 parasites in a controlled human malaria infection study (CHMI, Box 4) (42). Data prior
275 to treatment is shown. The blue line indicates a model similar to that presented in fig. 3B,
276 which has been fit to the data using mixed effects approaches. The laboratory strain of P.
277 falciparum used in this challenge study has a 40 hour lifecycle (43). (B) An illustration of
278 waves of semi-synchronous pRBCs maturing through the ring, trophozoite and schizont
279 stage. The first generation of pRBCs is shown in blue. As this population reaches 24 hours
280 into its lifecycle the pRBCs sequester (shown in pale blue). Once these pRBCs rupture they
281 release merozoites that infect more RBCs, generating a new generation of pRBCs (shown in
282 red). The ratio of the peak of the second wave of pRBCs compared with the peak of the first
283 generation is equivalent to the parasite multiplication rate (PMR). In circulation we typically
284 do not distinguish between parasites based on age, and so we only see the total circulating
285 parasite concentration oscillating as it increases.
286

287 <u>How does the parasite maintain synchronous infection cycles?</u>

288 One simple mechanism by which parasites might establish and maintain synchronous
289 infection is by having fixed lifecycle times. If this were the case then merozoites (which only
290 have a very short life-time in which they remain viable, (approximately 10 minutes (47))
291 would be released from the liver stage and rapidly invade RBCs. Subsequent infected pRBCs

would all have a fixed 48 hour lifecycle, and they themselves would rupture releasing short-lived merozoites, which would then establish another generation of pRBCs with a fixed lifecycle. However, any deviation from this would tend to allow desynchronization of the parasite population over time. Further, it has recently become clear that host factors such as the level of immune response and nutrient availability may affect the lifecycle of the parasite (48, 49), which may lead to asynchrony. Thus, how synchrony is maintained in the face of variable lifecycle and exposure to host responses presents an interesting question for modelling.

One modelling study proposed to explain parasite synchrony by suggesting that fever itself may provide a synchronising force during infection (50). Using a difference equation version of the n-compartment model with 2 or 4 compartments, the paper explored the idea that if fever is lethal or inhibitory in some way to older parasites then it may remove any asynchronous 'tail' of parasites at every replication cycle, providing a simple explanation for the maintenance of synchronicity. That is, as the dominant population of parasitised RBCs reaches maturity in unison, they will rupture the RBCs and induce a burst in host inflammation leading to fever. This fever will then kill any 'slow' parasites that have not yet ruptured. This implies that during each cycle of parasite replication and rupture, any distribution in times to parasite rupture is trimmed by the tail of that distribution being destroyed. However, a weakness to this explanation is that it relies on fever being present to maintain a synchronous infection; recent development of controlled human malaria infections in volunteers has allowed us to study parasite synchrony in individuals with no fever. From this data, it is clear that parasite synchrony exists even before fever or other symptoms appear (fig. 4A).

317 The advantage of a synchronous infection

318 The length of the asexual cycle (and periodicity of fever) varies for each Plasmodium species,
319 with P. falciparum and P. vivax, the two most prevalent human species both having a 48-hour
320 lifecycle. However, the less common P. malariae has a 72-hour asexual cycle, and the
321 zoonotic P. knowlesi has a 24-hour asexual cycle. It is striking that the various species'
322 lifecycles, as reported in the literature, are all multiples of 24 hours. Murine studies (Box 1)
323 suggest that Plasmodium may synchronise with the host diurnal rhythm, and that falling out
324 of synchrony with the host may restrict parasite growth (reviewed in (51)). For example,
325 Reece and colleagues compared parasite growth in mice kept in a typical day-night cycle, and
326 another group housed in an artificial day-night cycle, 12 hour out of phase. When both groups
327 were infected with the same Plasmodium chabaudi parasite inoculum (a rodent species),
328 parasites proliferated more rapidly in the mice housed in the typical day night cycle (52).
329 This suggests that parasites replicating synchronously perform better if the mature parasites
330 rupture and merozoite release occurred at a particular time (i.e. in the evening). Further, it
331 seems that when infections are induced out of sync with the host circadian cycle that the
332 parasites shift their periodic pattern to become more synchronised with the host day-night
333 cycle (53). This indicates, not only that the parasite gains some benefit from keeping a
334 particular asexual cycle matched with host circadian factors, but that the parasite can alter its
335 asexual cycle time to bring it in line with the host circadian rhythm. It has been suggested
336 that this may be due to changes in host macrophage function, and the varying ability to clear
337 parasites from circulation at different times. However, very recent work suggests that host
338 feeding cycles and metabolic processes, and circadian fluctuations in the production of
339 inflammatory cytokines may be involved (54, 55).

340

While synchronised parasite replication is a common feature of human (and some animal) Plasmodium species, it is not universal. P. berghei for example, a common species studied in mice, will desynchronise over the course of infection (56). The 48-hour lifecycle in human infection can also be perturbed, as a commonly studied laboratory strain of P falciparum, known as 3D7, has been shown to grow with a 40 hour lifecycle both in vitro and in vivo (43, 57). The dynamics, mechanisms, and fitness advantages of synchronisation amongst the parasite population and with host cycles remains an exciting field on which modelling may be able to shed further light.

Box 1: Experimental models of malaria infection

Tracking the natural course of Plasmodium infections in humans is rarely possible without treatment (a few exceptions, Box 4). However, "animal models" are commonly used to study the course of Plasmodium infections, as well as host responses and other host-parasite factors that play an important role during infection. The most common animal models used to study malaria are mouse models. The rodent parasite species used in such studies include Plasmodium berghei, Plasmodium yoelii and Plasmodium chabaudi. Depending on the strain of each of these species and the mouse line used, these infections have very diverse phenotypes. For example, there are lethal and non-lethal strains of P. yoelii and P. chabaudi, and while P. berghei ANKA can cause rapid onset of illness and mortality within a week in C57BL6 mice, in Balb/c mice the infections are less virulent with mice surviving twice as long. Further, P. berghei ANKA infection in C57BL6 mice reaches a parasitemia of only about 10% by day 6 or 7 day of infection, at which point mice succumb to severe neurological symptoms. On the other hand, non-lethal P. yoelii XNL infection, in the same mice, reaches up to 50% parasitemia, but is completely

resolved by the mice without intervention, rendering the mice protected from subsequent challenges with the same parasite species. Other animal models are also used to study malaria, in particular, avian and primate malaria models (Owl monkeys, Aotus monkeys, squirrel monkeys) (58-60). However, these are far less common.

The applicability of conclusions from these animal studies to human infection has been discussed extensively (61, 62). There is some agreement that these models might be useful for studying immunological responses to infection, but there is also some criticism of these experimental models, in particular for their use in understanding the pathogenesis of neurological disease in severe malaria, since there are a number of features of the manifestation of disease in these models that is quite different to that seen in human infection (62). Animal models are very useful in that they allow us to assess host and parasite interactions beyond what would be possible in human infection. However, caution is always required when relating results from animal models to human infection.

Box 2: Growth rate, parasite multiplication rate (PMR) and R_0

Whereas we would typically talk about the growth rate of a viral infection (meaning the exponential rate, per unit time of viral growth), in the case of Plasmodium infection it is less clear how best to describe the "growth rate", because the parasite population typically increases with a periodic structure. The most commonly used term to describe parasite growth is the parasite multiplication rate (PMR) (or less commonly parasite multiplication factor (PMF)), which refers to the fold-increase in the parasite population per replication cycle (i.e. usually the fold increase in parasite

load over 48 hours in P. falciparum infection). The PMR can be interpreted as the average number of progeny of each infected RBC, over a single replicative cycle. This is similar to the within-host basic reproductive number (R_0) often discussed in viral infections, which represents the average number of progeny of an infected individual within its infectious life-time. Common estimates of the PMR in early infection in previously unexposed individuals have ranged between 8-17 for P. falciparum (39, 57, 63-65). The PMR is the average number of progeny of a single pRBC and so includes in it the probabilities that some pRBCs will not survive to produce merozoites, and that not all merozoites produced will successfully infect RBCs.

Where do all the parasites go? Sequestration in P. falciparum infection

An important feature of P. falciparum infection is that the late-stage pRBCs (older than approximately 24 hours (35)) are not typically observed in the peripheral circulation of infected individuals (66). This is because these late-stage pRBCs adhere to the walls of blood vessels causing them to accumulate in the microvasculature of host organs, including the brain, lungs, liver, spleen – making them undetectable in the circulating blood of a host (67). This is known as sequestration. Measures of parasite concentration (Box 3) that rely on counting infected cells in a sample of blood from the peripheral circulation are limited in that they only quantify the circulating forms of Plasmodium falciparum (rings and young trophozoites) but cannot detect sequestered forms (late trophozoites and schizonts). The sequestration of parasites is not merely an impediment to accurate measurement of parasite numbers in the blood. It is also thought to be directly responsible for much of the

pathogenesis of malaria, with parasite accumulation in organs such as the brain and lung believed to be important drivers of clinical illness (i.e. malaria – which is the name of the disease caused by infection with Plasmodium parasites, rather than the parasite itself) (68-72). Therefore, the ability to measure or estimate sequestered parasite biomass in host organs is an important goal for modellers.

Box 3: Measuring circulating parasite concentration

Malaria is not a parasite. Malaria is a disease caused by infection with Plasmodium parasites. A common clinical definition of malaria, is an individual presenting with a fever (temperature above 37.5^{o}C), and more than 5000 Plasmodium parasites/μL detected in the blood of the individual (73).

Microscopy: Plasmodium parasites are most commonly detected and quantified in an individual by preparing a blood smear and, using a microscope counting the number of infected RBCs (microscopy). Parasite counts performed by microscopy can either be given as the percentage of total RBCs that were infected (parasitemia), or as a concentration of parasites per unit volume (e.g. p/μL). In fact, one can readily convert between these two units by using the measured red cell count (typically approximately 5×10^{9}/mL), the hemoglobin level, or making assumptions based on patient age, weight and gender. Typically, rather than counting the number of infected RBCs as a fraction of uninfected RBCs, microscopists count the number of infected RBCs as a fraction of the number of white blood cells (WBCs) they observed on the microscope slide. This is most common because WBCs are readily counted, are less common (4.5 - 11.0$\times$ 10^{6}/mL). Therefore, when counting the fraction of RBCs infected it is much faster to count only a small number of WBCs rather than all of the

uninfected RBCs on the slide. One can then convert measures of infected RBCs per WBC into parasitemia. However, this conversion usually assumes a fixed ratio between RBCs and WBCs. This may be inaccurate, since we expect the number of WBCs in circulation to increase due to infection, and the number of RBCs to decline as Plasmodium infection commonly causes anaemia. Unless the white cell count is also measured some errors may be introduced by this approach.

PCR: It is generally reported that a thick film blood smear has a limit of detection, in the hands of an expert microscopist, of approximately 20 p/µL. However, there are instances in which it is desirable to measure parasites at lower concentrations than microscopy will allow, such as in control human malaria infection (CHMI, Box 4) studies. In these instances quantitative PCR (qPCR) can be used to quantify parasite concentrations as low as 20 p/mL (i.e. 1000 fold more sensitive than microscopy). An important difference to note with PCR approaches to measuring pRBCs is that these methods rely on amplifying and quantifying the amount of parasite DNA in a sample. Since pRBCs begin to synthesize parasite DNA during their development, individual pRBC may have up to 32 genomes (DNA copies). Thus, the amount of DNA in a sample is not necessarily equivalent to the number of pRBCs (which is what is measured by microscopy). In the case of P. falciparum this is not an important confounder, since the mature parasites stages that would have multiple genome copies (schizonts) are sequestered and not circulating, but in the case of other parasite species that do not sequester this factor may be a consideration.

Modelling to estimate the sequestered parasite load

Models of pRBC dynamics to estimate sequestration

A simple way to adapt the standard model (fig. 1) to explore sequestration is by splitting the pRBC compartment into circulating pRBC and sequestered pRBC compartments (19, 74, 75). Newly parasitised RBCs occupy the circulating blood compartment, transit to the sequestered compartment, and then rupture to produce merozoites, and ultimately give rise to a new generation of infected cells in the blood. Such a model was used to fit patient data from The Gambia, which monitored the parasite concentration in individuals with cerebral malaria following treatment (74). This model then estimated the sequestered parasite load in each individual, and found a correlation between the sequestered parasite load in an individual and risk of mortality. However, this model suffers from the issue of not accurately capturing the life-times of pRBCs, which we outlined above. The same authors also included sequestration into the n-compartment model (fig. 3A) by defining circulating parasites ($\bar{P}$) as the sum of all P_i compartments that correspond to parasites less than 24 hours old (fig. 5A) (44). The authors fitted this model to more parasite concentration data from patients treated for malaria and estimated the sequestered parasite loads. This model relies on the structure of the declines (or sometimes transient rises) in circulating parasite concentration after treatment in each individual in order to infer the number of sequestered pRBCs they harbour. However, it is assumed that drug affect is constant over the period of observation, which is unlikely, and in fact the constant drug effect may itself influence the shape of the decline in pRBCs after treatment, confounding this approach.

Sequestration can be readily incorporated into the PDE model (fig. 3B). In the PDE model, the circulating parasite load ($\bar{P}$) can be defined as the integral of the pRBCs population over the ages, x, between 0 and 24 hours (first half of the parasite lifecycle) (35, 43), which implies that all pRBCs between 24 and 48 hours are sequestered (fig. 5B). This model has been applied to fit data from studies in which volunteers received deliberate infections with

P. falciparum (43) (e.g. fig. 4A, Box 4). Unlike in a hospital setting, where malaria patients are quickly treated, in these deliberate infections, the natural course of pRBC multiplication before drug treatment can be tracked (fig. 4A). From these parasite growth curves one quickly observes, a) the synchronous rupture of mature pRBCs, b) that the release of merozoites is responsible for the periodic rises in parasite concentration in these individuals, and c) that the periodic troughs in parasite concentration correspond to the mass sequestration of pRBCs as they mature (fig. 4B). Given this direct connection between oscillations in the parasite growth curve and sequestration, one might expect that accurate estimates of the sequestered pRBC parasite load would be obtained when fitting models to this data.

There are alternative ways to model sequestration. In particular, the models discussed above all assumed that all parasites sequester instantaneously at a specific parasite age, rather than at as a process occurring at some rate (e.g. fig. 5C, (15, 35)). This might be reasonable for P. falciparum given the almost complete absence of late-stage pRBCs in peripheral circulation. However, other species, such as P. vivax and some Plasmodium species in animals, exhibit weak cytoadhesion properties (76, 77), allowing only partial sequestration of late-stage pRBCs. Further, some studies have suggested in P. falciparum infection that inflammation can expose more tissue sites to pRBC adherence (67, 72, 78). Hence, there may be scope for more mechanistic models of parasite sequestration in Plasmodium infections that consider the interaction of sequestration sites and pRBCs as well as the affinity of "binding" to these sites.

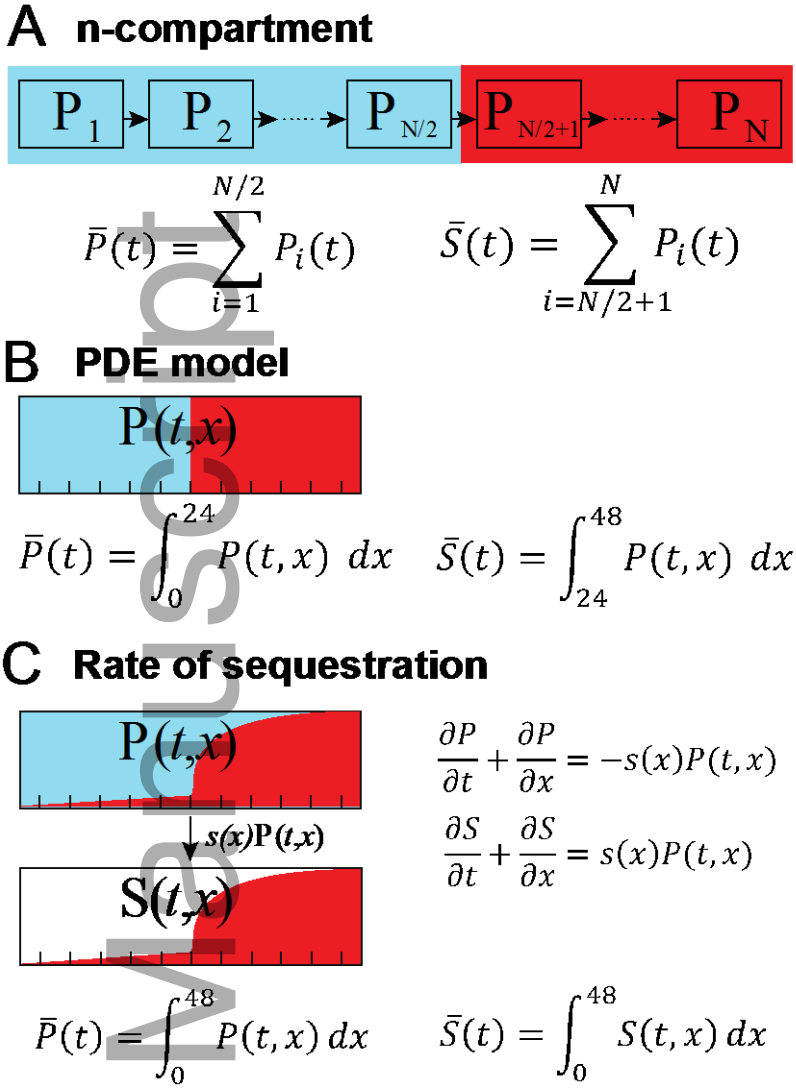

Figure 5: Schematic and equations illustrating how age-structured Plasmodium models can be extended to account for sequestration. (A) Sequestration can be included in the n-compartment model (fig. 3A) by defining the sequestered parasite load, $\bar{S}$, as the sum of all parasite compartments in the second half of the parasite life cycle (shaded red, i.e. P_i where $i > N/2$). The sum of the parasite compartments that correspond to parasites less than half-way through their life cycle (shaded blue, i.e. P_i where $i \leq N/2$), are defined as the total circulating parasite load, $\bar{P}$. (B) In the PDE model (fig. 3B), the total circulating ($\bar{P}$) and sequestered parasite loads ($\bar{S}$) are defined as the integral of the age-density of parasites, $P(t,x)$, over the first and second halves of the parasite life-cycle, respectively. (C) Instead of assuming all parasites sequester instantaneously once they reach a particular age, sequestration can be thought of as a process occurring at some rate, $s(x)$, which also depends on parasite age, x. This model requires the introduction of a new compartment to capture sequestered, S, versus circulating, P, parasites. The total circulating and sequestered parasite loads in this case are simply given by the integral over all parasite ages of the age-density functions for circulating and sequestered parasites respectively.

Box 4: The history of deliberate malaria infection and a resource for modellers

Parasite growth curves, such as that in figure 4, are usually not observable because it is typically unethical to observe infection within an individual without treating them. Prior to the advent of modern antibiotics, some neurosyphilis patients were deliberately infected with Plasmodium so that the malaria induced fevers would assist with controlling their syphilis infections (caused by the bacterium Treponema pallidum) (79-81). These studies produced a unique data set of the daily measurements of parasite numbers within individuals without treatment, that has been long studied (39, 40, 50, 82-86). More recently, a number of groups have established protocols for highly controlled infections of volunteers with Plasmodium parasites to study vaccine and drug efficacy, often referred to as controlled human malaria infections (CHMI) (42, 87-93). These experimental systems use highly sensitive techniques, such as real-time PCR, to quantify very low levels of parasites in the peripheral circulation (94-96). Individuals are then treated before parasitemia reaches a level that is detectable by microscopy (that is, infected RBCs observable on a blood smear using a microscope) or which would cause illness.

Douglas and colleagues have developed and compared a number of modelling approaches to measure the parasite multiplication rate and to estimate initial parasite inoculum using data from CHMI studies (note that they have also made much of this data freely available to the modelling community online, see reference (57)). These include (1) direct estimates of the PMR by taking the ratio of adjacent peaks from the parasite growth curves, (2) fitting an exponential growth curve to the data to estimate the growth rate and converting this to PMR using a simple relationship, (3) fitting an exponential growth model with a sine function to capture the periodicity of infection

(39), and (4) more mechanistic models of parasite replication that consider waves of parasites with normally distributed age structures, moving through the development cycles and producing progeny at the end of the development cycle (35). The first method is limited in that it does not use all available data to estimate the PMR, and so potentially gives wider confidence intervals on estimates. The second method uses more of the available data but disregards the periodic structure of the parasite growth curve. The third model uses all of the data and is able to capture periodicity, but requires more parameters. The fourth model is able to use all of the data and is sympathetic to the underlying biological processes governing the parasites growth curve, but it has twice as many parameters as the exponential growth (second) model, and can be difficult to fit, especially if data is sparse (35). Bejon et al. fitted these models to the their CHMI data and estimated the PMR in each case. They argue that the PMR estimates from each approach yield very similar estimates of the PMR and suggest that the exponential model is sufficient for estimating the PMR in CHMI studies (57).

These methods have been used to analyse and compare the growth rates of experimentally inoculated parasites in immune adults from a malaria endemic region with naïve individuals in the UK. This demonstrated slower growth rate of parasites in immune individuals (PMR ≈2.4) than in malaria naïve individuals (PMR ≈8) (63), consistent with acquired immunity acting at the blood stage.

Fitting the exponential growth model not only provides an estimate of the parasite growth rate (and PMR) but gives an estimate of the starting inoculum of parasites in

the blood, which has been used to assess whether an experimental liver stage vaccine has reduced the release of merozoites from the liver into blood (97).

Using circulating proteins to estimate sequestered parasites

An alternate approach for estimating the number of sequestered pRBCs used the concentration of a protein produced by the parasite (e.g. PfHRP2 or pLDH) in the host circulation (68, 98). In one study, the level of PfHRP2 was combined with a mathematical model of the production of the protein by the parasite and subsequent clearance from host circulation, to provide an estimate of total parasite load in the individuals (68). Using the concentration of PfHRP2, and the mathematical model, it was again shown that this metric of sequestration was a strong predictor of disease severity and death, and was a better predictor than circulating parasite concentration alone.

Measuring parasite sequestration in the mouse

In mice, another interesting method of determining total parasite burden has been genetically-modified rodent Plasmodium parasites (Plasmodium berghei ANKA) that express luciferase (an enzyme found naturally in fireflies, which catalyses a chemical reaction with luciferin, resulting in bioluminescence) (99, 100). Infected, anaesthetised mice are photographed with a sensitive CCD camera, such that the intensity of light emitted provides a measure of total parasite burden (fig. 6). This tool has proved useful as a metric for parasite burden, which can be collected in parallel with measurement of the host's circulating parasitemia (19). However, the bioluminescence is only a relative measure of parasite load over time and, on its own, is not directly comparable to parasite load and concentration in blood. A model to link these would be of value (19). Considerations of the model should include the non-

602 uniform distribution of parasites across the hosts body (with many parasites accumulating in
603 the different organs, causing hot spots of parasites such as in the lung, fig. 6), as well as the
604 transformation of a 3D mouse into a 2D image, resulting in the superposition of many layers
605 of the mouse's body.
606

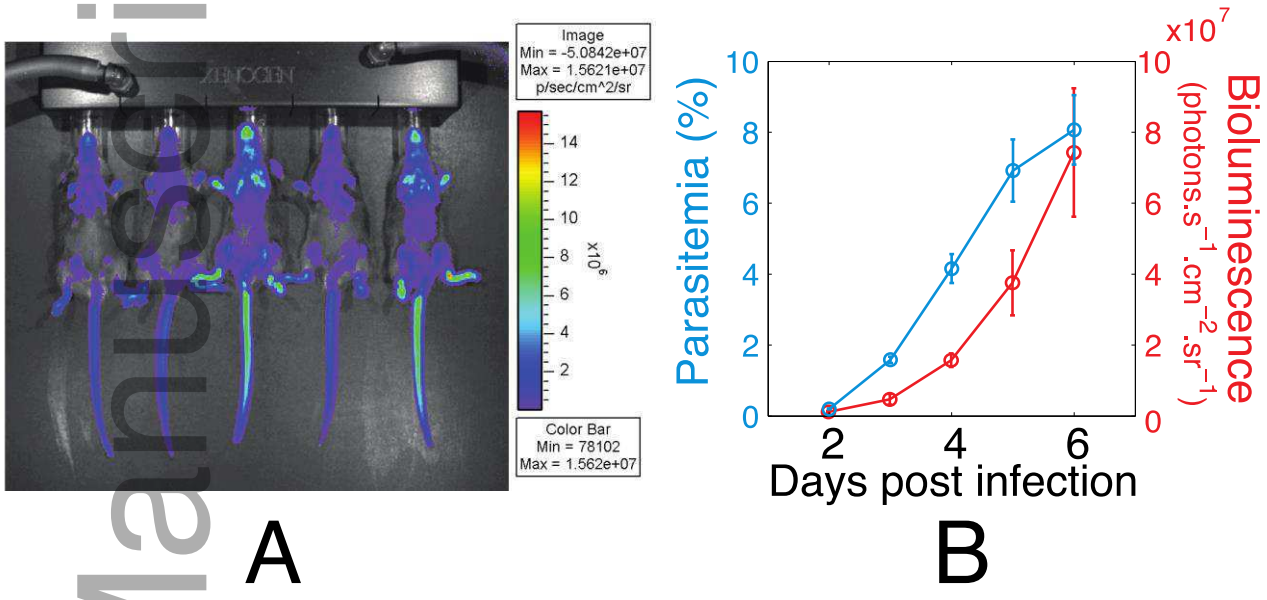

607

608 **Figure 6: Using luciferase to measure total parasite load in mice.** (A) An example of the
609 bioluminescence data collected from C57BL6 mice, infected with a transgenic P. berghei
610 ANKA that expresses luciferase (PbA-Luc). This image was collected on day 6 after
611 infection. Data is from (101). Note the bright appearance of the chest area, which indicates
612 pRBC accumulation in the lungs. (B) A summary figure showing the circulating parasitemia
613 and total bioluminescence measurements (intensity measured as photons per second per
614 square-centimetre per steradian) taken from C57BL6 mice (n=6) infected with PbA-Luc over
615 a 6-day infection. Data from (19).
616

617 **Why hide? The mechanism and purpose of sequestration**

618 Thus far we have made no comment regarding the purpose of sequestration, which may be
619 worthy of discussion. The sequestration of parasites in tissues is not merely passive
620 'trapping' of infected cells. The parasite actively inserts proteins into the infected RBC
621 membrane, making cells 'stick' to the host endothelium. The pRBC surface ligands and host
622 endothelial receptors associated with P. falciparum cytoadherence and sequestration have
623 been studied in detail with some understanding of the main ligands and receptors responsible

(such PfEMP1 (P. falciparum erythrocyte membrane protein 1) and CD36, reviewed in (67)). However, similar to the synchronisation of infection, it is not well established what benefit parasites gain from sequestration. Although a number of hypotheses have been proposed (67), the central paradigm is that sequestration allows parasites to evade host removal of circulating pRBC by the host spleen (75, 102, 103). The spleen is a filtration system for the blood, removing debris, extracellular pathogens, as well as old, damaged or infected RBCs whose deformability is altered (104, 105). Thus, pRBCs are thought to evade circulation through the spleen and splenic removal by adhering to the walls of blood vessels. It is thought that mature stages are more likely to be cleared, and thus parasites sequester mainly in the second half of their cycle (106). This hypothesis is supported by evidence showing that splenectomised individuals have worse outcomes in infection, are susceptible to hyperparasitemia and have slower clearance of infection after drug treatment (104, 107, 108).

Contrary to the above hypothesis, in some experimental systems removing the spleen (splenectomy) causes slower parasite growth rates. This is true in mouse models (100), as well as P. falciparum infected monkeys (109), and suggests that under some circumstances, the spleen promotes parasite proliferation. Furthermore, in vivo imaging of pRBCs in mice (as described above, fig. 6) shows a hot spot of pRBCs in the spleen, suggesting that pRBCs could accumulate in this organ (100). Therefore an alternative hypothesis is that sequestration allows pRBCs to rupture in favourable environments (67). Perhaps locations such as the spleen or lungs, despite containing high concentrations of phagocytic cells, place pRBCs in close proximity to favourable RBC targets. Or perhaps there are multiple benefits to sequestration for the parasite. One study in mice supports the latter suggestion (77). It found that gene knock-out P. berghei parasites, lacking the gene responsible for producing the ligand thought to be involved in sequestration, grew more slowly than wild-type counterparts.

649 The advantage gained by sequestering, was more than could be accounted for by evading host
650 clearance alone, suggesting that sequestration afforded the parasite an additional advantage
651 (77). The benefits of sequestration for pRBCs remains an unresolved question, and a formal
652 comparison of models that consider the various proposed hypotheses (67) might provide new
653 insights and lead to further research in this area.

654 # Host control of parasite proliferation

655 The typical course of acute infection involves growth to a peak of parasitemia, followed by
656 successful resolution of infection involving a decay from this peak. The mechanisms leading
657 to this decrease in parasite numbers include the reduced availability of target cells (target cell
658 limitation), or host immune mechanisms (innate or adaptive) acting directly to reduce parasite
659 numbers. Modelling has been used to explore these mechanisms.
660

661 **Target cell limitation**

662 The replication capacity of a pathogen is often able to exceed the ability of the host to replace
663 uninfected target cells, and as a result the level of infection declines after some peak. Thus,
664 while the slowing of growth or decay of HIV or parasite levels from a peak is often attributed
665 to host immunity, others have argued that target cell limitation may also play a major role
666 (110-113). However, a significant difficulty arises in modelling target cell depletion if
667 infection occurs in a subset of cells, which may be poorly defined or difficult to measure. In
668 HIV this is the case because the virus only targets a subset of $CD4^+$ T cells. In malaria, the
669 preference of some species for a subset of very young RBCs, known as reticulocytes, may
670 also present issues with measuring target cell availability.
671
672
673

Preferences for subsets of RBCs

Some species of Plasmodium parasites such as P. vivax in human infection, and P. berghei in rodent malaria are known to exclusively or preferentially invade reticulocytes. Other species such as P. falciparum are thought to target all RBCs equally, although there is evidence for preferential invasion of a subset of cells (114, 115), especially reticulocytes (116). A number of models that incorporate more sophisticated details of RBC (reticulocyte) production, and preferential targeting of certain RBC stages have been constructed (e.g. fig. 7, (18, 20, 117-120)). These studies have, in most cases, adopted a structure similar to either the many compartment ODE or the PDE models in figure 3, but to capture the age structure of the RBCs rather than the parasites (illustrative model presented in figure 7).

One modelling study investigated the extent of the P. berghei preference for reticulocytes in Balb/c mice (120). This study developed a difference equation model similar in structure to the standard model (fig. 2B), but without explicit consideration of the short-lived merozoite forms, and splitting target cells into two populations, the normocytes (mature erythrocytes) and the preferentially infected reticulocytes. This model also extended the standard model, by more accurately accounting for the production of reticulocytes (following the work of others (119)), allowing for an increased production of new RBCs (reticulocytes) as the host loses its RBCs (fig. 7) (120). During early P. berghei infection a rapid increase in parasite numbers was observed, due to high availability of the preferred target cells (reticulocytes). However, an intermediate phase, characterised by a decline in parasite numbers, occurred as reticulocytes were depleted by infection. The infection-induced anaemia was detected by the host, causing increased production of reticulocytes, increasing target cell availability and driving a second wave of infection. The study of P. berghei estimated an approximate 150 fold preference for reticulocytes over normocytes (120).

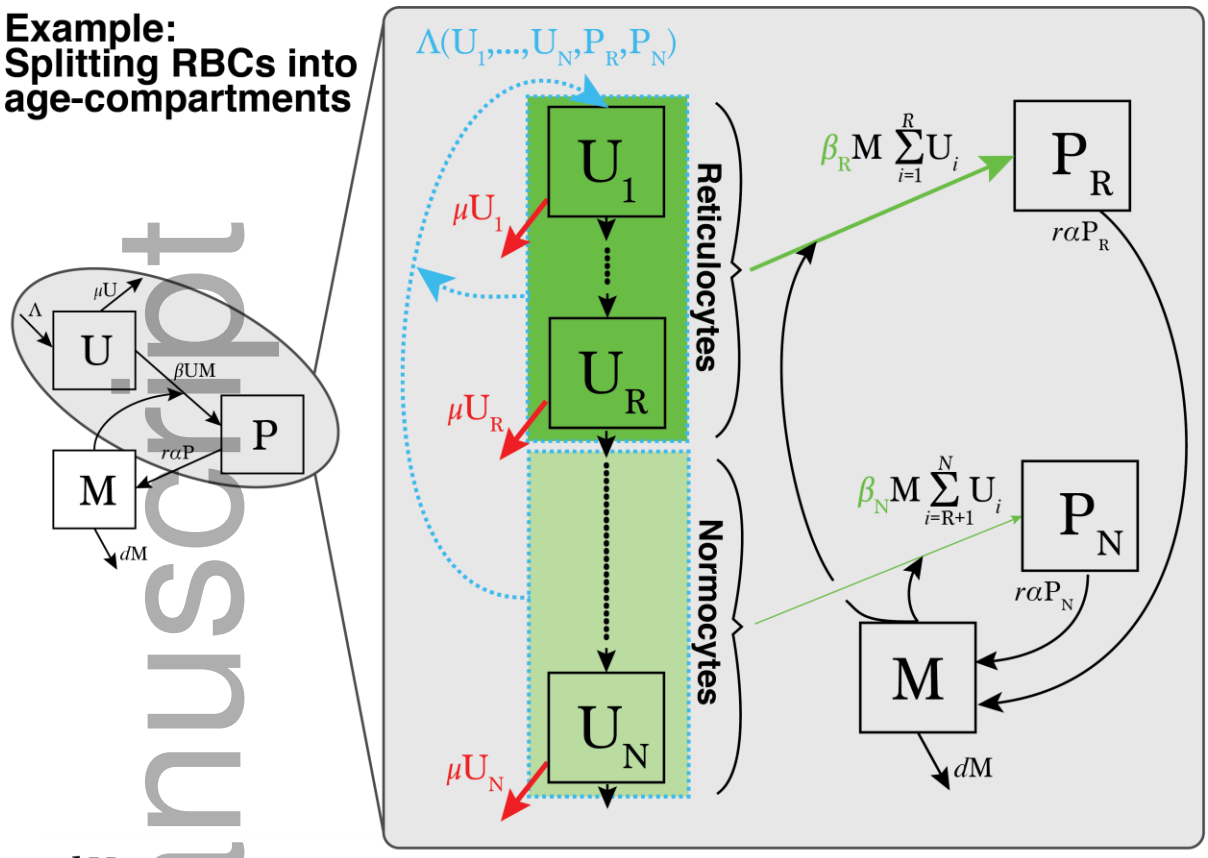

$$\frac{dU_1}{dt} = \underbrace{\Lambda(U_1,\dots,U_N,P_R,P_N)}_{\text{Production of RBCs}} - \underbrace{\omega U_1}_{\text{RBC maturation}} - \beta_R U_1 M - \underbrace{\mu U_1}_{\text{Bystander killing}}$$

$$\frac{dU_i}{dt} = \omega U_{i-1} - \omega U_i - \underbrace{\beta_R M U_i}_{\text{Preferential invasion of reticulocytes}} - \mu U_i, \qquad 1 \le i \le R$$

$$\frac{dU_i}{dt} = \omega U_{i-1} - \omega U_i - \beta_N M U_i - \mu U_i, \qquad R+1 \le i \le N$$

$$\frac{dP_R}{dt} = \beta_R M \sum_{i=1}^{R} U_i - \alpha P_R \qquad \frac{dP_N}{dt} = \beta_N M \sum_{i=R+1}^{N} U_i - \alpha P_N$$

Figure 7: Example model with age-structured target cells and preferential invasion of young RBCs (reticulocytes). An ordinary differential equation (ODE) model extending on the standard model in figure 2B by adding age-structure to the uninfected target RBCs (adapted from (119)). The uninfected RBC compartment from the standard model is split into N discrete cell stages. The rate of transition between stages is given by ω, and chosen such that N/ω is equal to the average life time of an RBC (120 days in humans). Uninfected RBCs in the R^{th} compartment or below are considered reticulocytes, and R is chosen such that R/ω is equal to the average time an RBC spends as a reticulocyte (approximately 6 days in humans). With age-structured target cells it is possible to consider heterogeneity in merozoite invasion of the various subsets of RBCs. For example, in this illustration, merozoites have differing infectivities of reticulocytes (β_R) and normocytes (β_N) – allowing the inclusion of a

711 preference for invasion of reticulocytes. Although not shown here, it is also common to
712 include age-structure of the pRBC compartments as illustrated in figure 3. RBCs are
713 produced at a rate that depends on the total number of RBCs (infected and uninfected),
714 $\Lambda(U_1, \ldots, U_N, P_R, P_N)$, and destroyed at rate μ. The production rate of RBCs increases with
715 anemia (i.e. as total RBCs decrease), often with some delay (e.g. (18, 119, 120)). The
716 increased destruction of 'bystander' uninfected RBCs can be captured in this model by an
717 increase in μ. The other parameters presented here are as described in figure 2.
718

719 The advantage gained by the parasite from targeting reticulocytes is an unanswered question.
720 One modelling study proposed an interesting hypothesis, namely that preferential invasion of
721 reticulocytes may be a mechanism used by the parasite to self-regulate parasite replication, so
722 as to prevent the rapid depletion of targets or harm to the host, which might interfere with the
723 parasites ultimate goal of transmission to a mosquito (118). The parasite preference for
724 reticulocytes also provides an opportunity for host resistance because reduced reticulocyte
725 production can shut down parasite replication before depletion of the mature RBC pool (↓ Λ
726 in figure 7). Patients often show bone marrow suppression during severe P. falciparum
727 malaria, and modelling suggests that this shutdown of reticulocyte production may
728 paradoxically be a protective mechanism against severe anemia (18, 119).
729

730 Indirect loss of target cells (Bystander killing)

731 Another key factor when considering target cell limitation in malaria infections is the idea of
732 bystander killing. This is the idea that more RBCs are lost in a Plasmodium infected host than
733 can be accounted for by the direct infection by parasites (e.g. ↑ μ in figure 7). One study used
734 a mathematical model to estimate the number of RBCs lost due to direct infection by P.
735 falciparum, compared to the total red cell loss (using data from the neurosyphilis studies
736 mentioned in Box 4) (40). Their modelling estimated that approximately 8 bystander
737 uninfected RBCs were lost for each infected RBC over the course of the infection (40). This
738 modelling work was not without its own limitations. For example, the model considered that
739 the destruction of bystander RBCs was constant over the course of infection. However, the

level of bystander destruction may change with time, depending on the nature of the mechanism that causes bystander loss. For example, malaria-induced inflammation may lead to more active filtering of RBC by the spleen, which may then filter and clear both infected and uninfected RBCs more rapidly, leading to the loss of otherwise healthy RBCs. If this is the case, the extent of bystander destruction would change over the course of infection. Alternatively, it has been suggested that debris released from rupture of infected pRBCs leads to destruction of bystander RBCs (121), which would lead to a fixed ratio of bystander death to pRBC rupture. There are a number of experimental studies that have looked at the role of different host immune responses, such as complement and phagocytes, in mediating accelerated pRBC removal, a number of which may provide some evidence of host responses being involved in the destruction of uninfected RBCs (121-124). Exploring these different mechanisms of bystander destruction using modelling could help make sense of the experimental literature on mechanisms and host risk factors associated with severe anaemia.

Innate immune control of parasite replication

Adaptive immunity (antibodies and T cells) typically takes either weeks (in the case of primary infection) or days (in the case of re-infection) to control infection. Prior to this, the host is reliant upon non-specific innate immune mechanisms (innate immunity).

Quantifying the role of innate immunity

A modelling study by Metcalf et al. looked at infection in mice and attempted to dissect the relative roles of target cell limitation, innate immunity and adaptive immunity in controlling infection (112). This study adapted a model from ecology to fit the parasitemia and RBC concentration data from infected mice (112). The model inferred adaptive immunity by changes in the parasite growth rate that could not otherwise be explained by changes in RBC

765 numbers. Further, the study raised the interesting possibility that host immune control might
766 operate partly by reducing RBC numbers (perhaps by limiting production or by 'bsytander'
767 destruction), in order to limit the number of target cells and slow parasite growth (linking
768 host immune responses and target cell limitation as mechanism of host control) (125). This
769 model provides some novel insights and a useful alternative framework for modelling data of
770 the infection kinetics outside of the classical differential equation framework. However, it is
771 also limited by a narrow view of the mechanisms of innate immunity, in particular, assuming
772 that innate immunity is saturable, which has not been shown experimentally.
773
774 Parasite clearance
775 Perhaps the most commonly assumed mechanism of innate host control of parasite growth is
776 the mechanical filtration of pRBCs by the host spleen (104, 105, 107). As mentioned earlier,
777 the spleen mechanically filters RBCs based on their elasticity. It has been observed that
778 unhealthy or infected RBCs have different elastic/deformability properties (126). It might
779 seem strange then that the standard within-host model has no explicit term representing the
780 clearance of pRBCs (fig. 2B). This was because the original model was not concerned with
781 modelling innate host responses and the authors may have assumed that the loss of pRBCs, to
782 clearance instead of rupture, would be encapsulated in a lower average merozoite production
783 per pRBC that rupture (r). However, there is obviously a case for the explicit inclusion of
784 pRBC clearance in models of malaria infection, and many modelling studies have since
785 included pRBC clearance explicitly (17-19, 44, 74, 75, 112, 120).
786

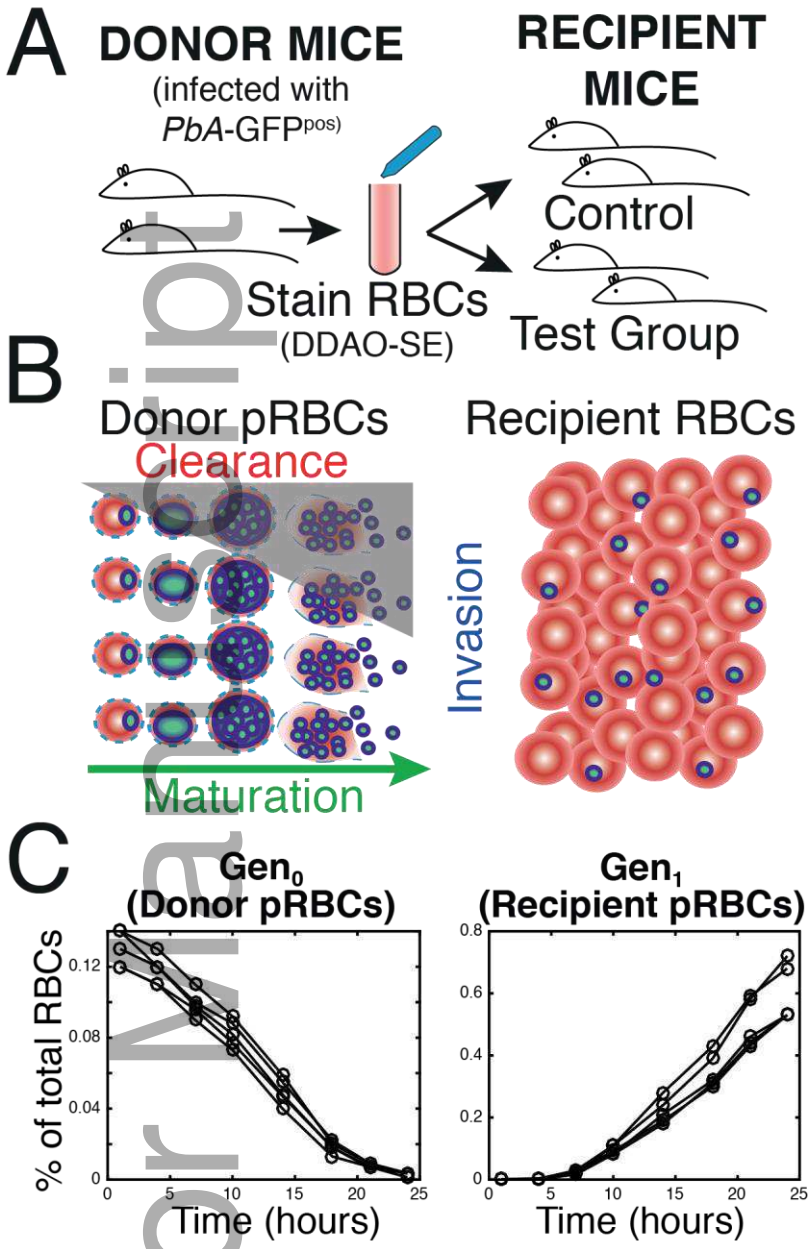

Figure 8: Illustration and data from an adoptive transfer experiment to study parasite clearance and replication in vivo. (A) Adoptive transfer experiments involved harvesting blood from an infected donor mouse. The blood is then stained with a fluorescent dye allowing the pRBCs that originated in the donor mouse to be tracked. The labelled donor pRBCs (as well as some labelled uninfected RBCs) from the donor mouse (Gen_0 pRBCs) are then transfused into groups of recipient mice, which receive various interventions. (B) Illustration of Gen_0 pRBCs maturing and rupturing to release daughter merozoites that will go and infect other RBCs. The recipients' endogenous RBCs make up the vast majority of available RBCs. Therefore, by measuring the number of unlabelled RBCs that become infected we can quantify the progeny of the Gen_0 pRBCs (i.e. Gen_1 pRBCs). (C) Example data from an adoptive transfer experiment, transferring P. berghei ANKA pRBCs from a donor mouse into naïve recipient mice. Data from (48).

Given the relative importance attributed to splenic clearance, there have been limited studies of how the spleen affects pRBCs in vivo. Experimental studies have measured the clearance of radiolabelled infected cells or heat-treated RBC in vivo (127-130), and ex vivo studies have measured the retention of parasites by isolated spleens (106). We recently developed a novel adoptive transfer assay to assess parasite clearance in which blood from infected donor mice is labelled with a fluorescent cytoplasmic dye and transfused into recipient mice (fig. 8A) (48, 131-133). A portion of the labelled RBCs are parasitized, allowing us to track, by flow cytometry, a single labelled generation of pRBCs and monitor their disappearance and clearance in a group of recipient mice (fig. 8B & C). We call this labelled generation of pRBCs Gen_0 parasites. The complication with interpreting this data is that Gen_0 pRBCs can disappear from host circulation for three distinct reasons, host removal of pRBCs, rupture of mature pRBCs, or sequestration of pRBCs. However, when a labelled pRBC disappears because it has ruptured, it should release daughter merozoites, some of which will go on to infect more RBCs. In recipient mice, the majority of the available RBCs are endogenous RBCs (and so are not labelled, fig. 8B). Hence, by looking at the number of endogenous RBCs that become parasitized over time we can track the appearance of the progeny of Gen_0 pRBCs (fig. 8B & C). We constructed a statistical model that looked at the magnitude of the loss of donor (labelled) pRBCs over a given time step and the corresponding appearance of unlabelled parasitized RBCs in order to estimate the number of pRBCs that were lost due to rupture and those that were lost due to host removal (133). This modelling gave an estimate that pRBCs were removed with a 15 hour half-life in naïve mice (no previous infection), i.e. on average 68% of all parasites are removed before they can reach maturity and rupture (133).

How does host clearance change over the course of early infection?

826 In another study we addressed the question of whether pRBC clearance increases from the
827 beginning of infection to the peak of infection. In mouse studies we and others had identified
828 that pRBC growth slows as mice become acutely ill by day 4 or 6 of infection (19). This
829 stage of infection is also marked by increased systemic inflammatory cytokine production
830 and splenic enlargement (19, 134). We hypothesised that slower parasite growth under these
831 conditions resulted from increased splenic clearance of pRBCs. Using our adoptive transfer
832 assay we compared naïve mice to those experiencing an acute infection (day 5 of P. berghei
833 infection, where growth was expected to be slower, fig. 9A) (48). Surprisingly, we found that
834 pRBCs were not cleared faster, but in fact persisted in host circulation for longer under
835 conditions of systemic inflammation and splenomegaly. This is particularly surprising when
836 one considers that these parasites have a 24-hour lifecycle. So, regardless of whether they are
837 removed by the host, they should reach maturity and rupture within 24 hours. In naïve mice
838 we observed that most pRBCs were indeed removed within 24 hours (only 2% remaining at
839 this time), but in acutely infected mice 32% of the transferred donor pRBCs remained 24
840 hours after transfusion (fig. 9B). Using the RNA and DNA content of the pRBCs to
841 determine their developmental stage (rings / trophozoites or schizonts), we observed that
842 pRBCs in acutely infected mice were maturing from the ring stage to the late-stages more
843 slowly. We confirmed this by fitting an extension of the PDE model from figure 3 to the data,
844 which allowed for either altered clearance of parasites or slower maturation of parasites to
845 explain the observed dynamics (fig. 9C). Fitting this model to the data we estimated that in
846 acutely infected mice, pRBCs were taking approximately 37 hours to complete their
847 lifecycle, compared with 24 hours in the control group (48). In addition, our modelling
848 revealed that the slower growth of parasitemia in acutely infected mice could be explained by
849 the observed slower maturation of pRBCs, without requiring any other mechanisms of host
850 control, such as increased clearance or reduced merozoite invasion (fig. 9C). Thus, our

findings revealed a host-mediated mechanism which impaired parasite maturation, and was responsible for slowing parasite growth, with no evidence of increased parasite clearance (48).

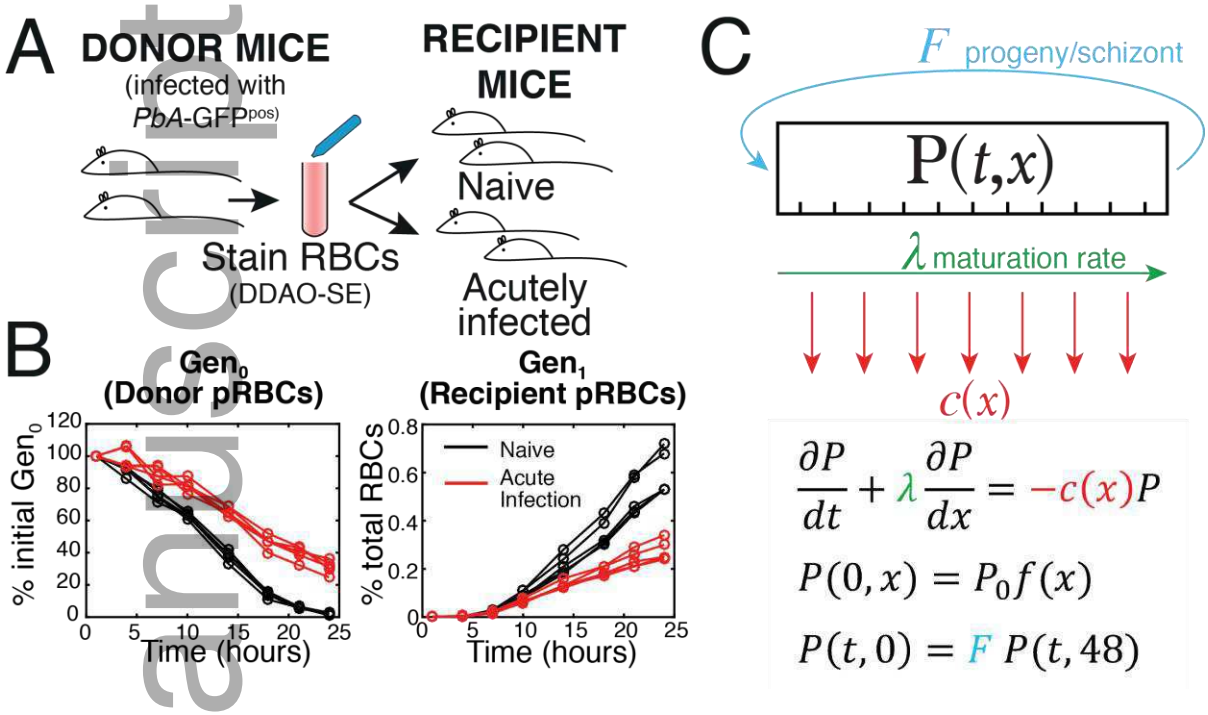

Figure 9: Measuring clearance in acutely infected mice. (A) Outline of the adoptive transfer experiment used to explore host clearance in naïve and acutely (5 day) infected mice. Fluorescently labelled pRBCs from donor mice (Gen_0 pRBCs) were transferred into (n=5) naïve and (n=5) acutely infected mice (48). (B) Acutely infected mice were expected to have slower growth of parasite numbers, which was confirmed by the reduced number of Gen_1 pRBCs observed in acutely infected mice. Surprisingly, rather than observing faster removal of the labelled Gen_0 pRBCs in acutely infected mice, Gen_0 pRBCs persisted in these mice. Further, despite the 24 hour life-cycle of P. berghei ANKA, Gen_0 pRBCs were still present in acutely infected mice after 24 hours. Data from (48). (C) We extended the PDE model from fig. 3B by including a maturation "rate", λ, which scales the amount of aging that occurs in a given time (48). When $\lambda = 1$ parasites age normally and when $\lambda = 0$ parasites do not mature. In this model clearance of pRBCs is given by $c(x)$, and the number of progeny (i.e. successful Gen_1 pRBC that arise) per rupturing schizont is given by F. The initial distribution of parasite stages is given by the probability density function $f(x)$, which we assume to be a normal distribution. Note that this model does not include target cells or merozoites explicitly, differing from the standard model.

Modelling intracellular maturation processes

The above finding highlighted the importance of understanding parasite maturation within RBC, and how it is altered by the host. Parasitised RBCs have historically been categorised into three main developmental stages: rings (young parasite forms), which mature into

trophozoites and finally into mature schizont stages (fig. 1). Some researchers go further to break this categorisation up into more compartments, for example, distinguishing between small rings and large rings, and so on (66). However, this is a morphological description of the asexual parasite development cycle, and underpinning these morphological changes are molecular processes within the infected RBC (23). The maturation of the parasite has also recently been classified based on the transcriptome (135). Perturbation of the malaria lifecycle has now been demonstrated in response to nutrient deprivation, drug treatment (132, 138) and resistance (136), and host innate immunity (48) and nutritional status (141). Given the increasing observation of Plasmodium parasites with altered development within RBCs, developing models to understand the molecular underpinnings of parasite development and how it is perturbed, is likely to have broad applications. In the pursuit of models to describe the molecular processes associated with parasite development within a RBC, the classical models of mammalian cellular developmental, such as that proposed by Smith and Martin (139), are likely to be very informative. Recently, a model inspired by this older model of the mammalian cell cycle was developed to explore parasite development, and in particular the perturbation of this development by drug treatment (140).

Adaptive (acquired) immunity

In malaria endemic areas individuals are repeatedly exposed to infection and can acquire partial immunity to Plasmodium infection. However, this takes many years of exposure, with children under 5 often remaining the most susceptible to malaria in these regions (6, 142). Even with prolonged exposure, immunity is incomplete (not 'sterilising') because immune individuals continue to be infected and carry a low level of parasites (chronic infection), although they are far less likely to succumb to high parasitemias or clinical malaria (i.e. they are immune to clinical illness (143)). Understanding which immune responses are critical in

naturally-acquired immunity will assist in developing effective blood-stage vaccines that generate the same protective responses in susceptible individuals.

Is immunity against the liver or blood stage of Plasmodium infection?

A major debate in malaria immunity is whether naturally-acquired immunity, associated with prolonged exposure, acts at the liver stage to prevent the initiation of blood stage growth, or on blood-stage replication itself to reduce parasite growth and peak levels. For many years it was believed that immune adults may have a lower incidence of infection than children, suggesting that new infections may be blocked at the liver stage. However, recent studies using more sensitive techniques to detect parasites have revealed a hidden pool of low-level infection in adults. Modelling of data on the time-to-infection of a highly exposed population suggest that the frequency of new infection does not differ with age, and that the major impact of prolonged exposure is a reduced growth rate of parasites in blood (144, 145), which leads to prolonged episodes of infection and a higher multiplicity of infection (146) (fig. 10). This is consistent with the observation that the transfer of serum from immune adults, living in malaria endemic regions, into Plasmodium infected children results in a decline in the children's circulating parasitemia (147). This indicates that immune adults carry antibodies (Ab) in their serum that can inhibit blood-stage parasite replication and control infection.

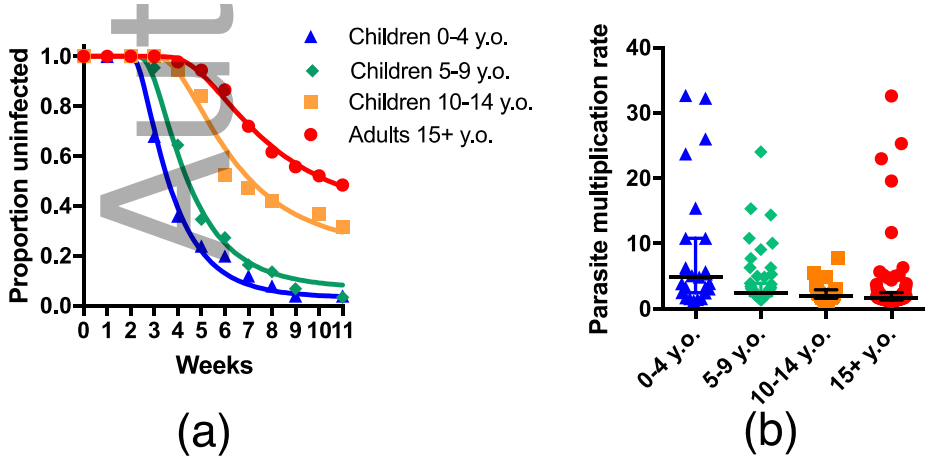

Figure 10: Naturally acquired immunity slows blood-stage P falciparum growth. (a) Naturally acquired immunity leads to increasing time-to detection of infection with age in a highly exposed population. Curve fitting assuming the same infection rate for all ages, and a distribution in PMR for each age group, with a decreased mean PMR with age. (b) Estimated growth rate of blood stage parasitemia in groups of different ages decreases from a PMR of 6 per cycle in children less than 4 years of age to 1.5 per cycle in adults >15 years. Adapted from references (148) and (145).

Considering our approach to understanding immunity – a mechanistic focus

These studies of naturally-acquired immunity represent an interesting contrast between measuring immune responses to infection, versus immunity to infection. That is, the dominant approach for understanding immunity to malaria infection is to measure immune responses, and correlate these with outcomes. A major barrier here is that all immune responses increase with exposure, and thus a response that is a good marker for exposure may appear correlated with protection, even though it plays no mechanistic role in protection. This can manifest in field studies, where responses can also be seen as risk factors for infection, simply because they are found in individuals that are more highly exposed to infection (149, 150). The approach of measuring immune responses and trying to correlate them with clinical outcome might be considered a 'forward approach' to identifying protective responses. It focuses on the immunology (i.e. what the immune responses are doing) of the response and tries to work out which parts are associated with immunity (i.e. actual protection from disease). An alternative approach is to identify what immunity does in terms of changing infection dynamics. For example, since we know older individuals are more immune, can we identify what changes in infection dynamics have occurred, and then look for immune mechanisms that mediate these changes? Thus, the strongly reduced growth rate of blood stage parasitemia with age suggests that measuring parasite blood-stage replication rate as a clinical outcome (rather than frequency of infection or time to infection) may focus our attention on the major mechanisms of naturally acquired immunity (151). Hence, we will

949 now focus our discussion on modelling immunity that acts to slow replication of the asexual
950 blood-stage.
951
952 Within-host models of immunity
953 With little knowledge regarding the precise immune responses associated with protection in
954 naturally acquired immunity, other than a knowledge that immunity slows asexual parasite
955 expansion, how might we model immunity? Generally speaking, from the standard model
956 one might think that a host immune response (adaptive or innate) could act directly against
957 the parasite in a number of possible ways (fig. 11): (i) to destroy merozoites ($\uparrow d$), (ii) to
958 reduce the infectivity of merozoites ($\downarrow \beta$), (iii) to destroy pRBCs ($\uparrow c$), or (iv) to reduce the
959 number of merozoites successfully produced by pRBCs ($\downarrow r$). These different mechanisms
960 are akin to mechanisms in HIV infection that might (i) destroy free virus, (ii) reduce the
961 potential for free virus to successfully infect a target cell (e.g. through Ab binding and
962 neutralisation), (iii) directly kill infected cells (e.g. CD8 cytotoxic killing of infected cells), or
963 (iv) reduce the production of virus by infected cells.
964

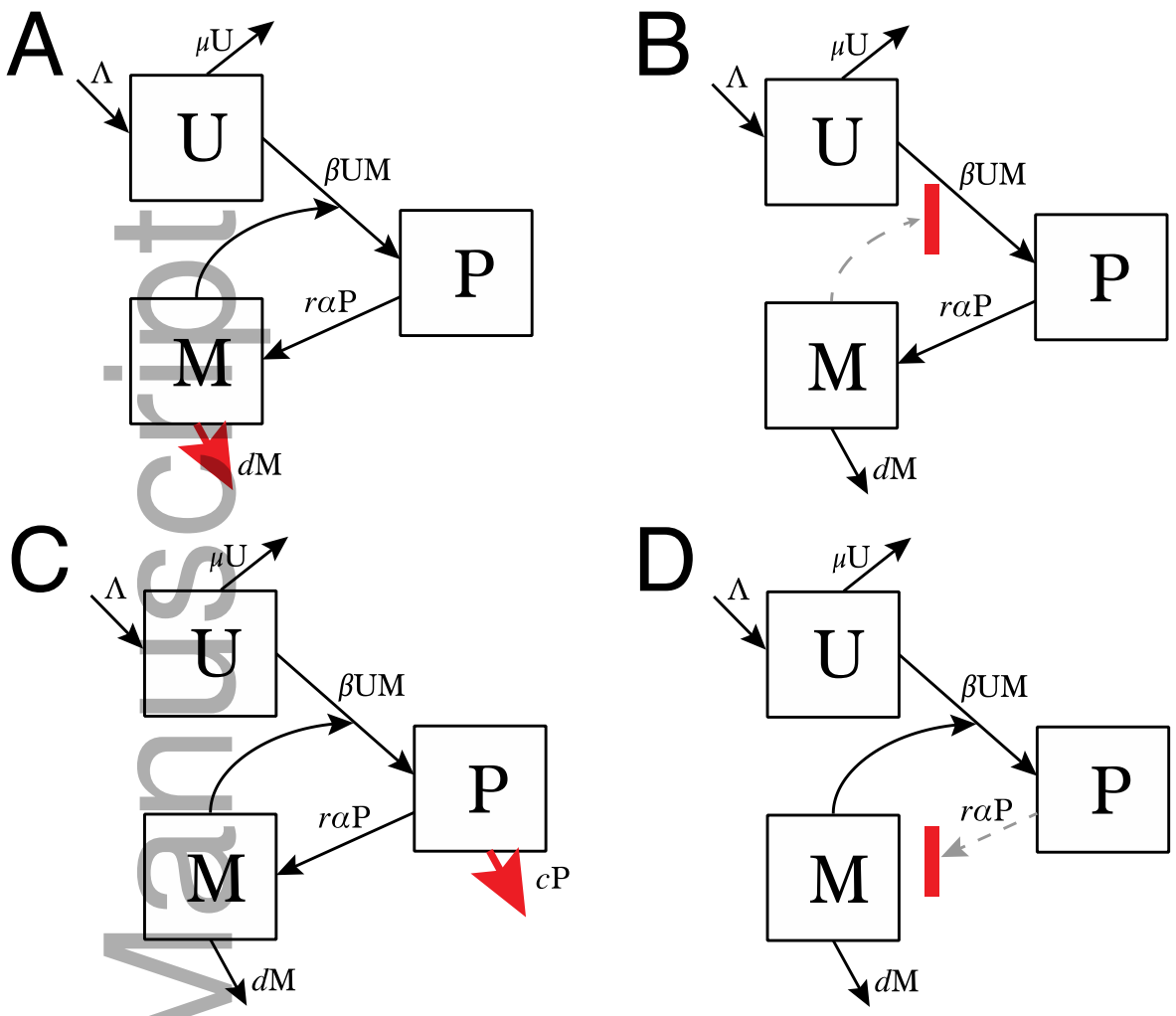

965

966 **Figure 11: Illustration of how immunity might inhibit the parasite lifecycle.** Variables
967 and parameters in this figure are equivalent to those described in figure 2B, except where
968 stated otherwise. (A) Immunity could act by increasing the clearance of merozoites (e.g.
969 phagocytosis), (B) inhibiting merozoite invasion (e.g. neutralisation), (C) causing the
970 clearance of pRBCs (at rate c), or (D) inhibition of merozoite production (e.g. by inhibiting
971 pRBC maturation or blocking rupture). Red arrows and bars indicate the effect of immunity,
972 and dashed arrows indicate an inhibited process.
973

974 In an early model of within-host malaria, Anderson et al. present two models of adaptive
975 immunity, but rather than considering all four of the possibilities above, they compared only
976 immunity that targets merozoites versus immunity that targets both merozoites and pRBCs
977 (fig. 12A & B) (9). In these models, all adaptive immune functions (Ab mediated immunity,
978 cellular immunity, etc) were encapsulated by one state variable, I. In the first model,
979 immunity increased proportionally to the number of merozoites, and acted against merozoites

980 only (fig. 12A). In the second model, immune responses were recruited in proportion to both
981 merozoites and pRBC levels, and the immune responses acted to clear both merozoites and
982 pRBCs (fig. 12B). They observed from their model that immunity that acted against the
983 longer lived pRBCs as well as merozoites would generate a more effective control of
984 infection, and lead to elimination of infection, whereas targeting merozoites alone failed to
985 clear the infection in their model. This model of adaptive immunity has some seemingly
986 reasonable features. For example, it is appropriate that recruitment of immunity depends on
987 both merozoites and pRBCs (fig. 12B). However, it is possible (even likely) that these
988 different parasite stages recruit host responses to differing extents, since it is well known that
989 pRBC rupture causes inflammation as intracellular host and parasite debris is released in to
990 the blood of the host, generating fever and inflammation that could activate innate immune
991 cells. On the other hand, circulating pRBCs carry parasite proteins on the surface of their host
992 cell membranes, but intact pRBCs may elicit a much smaller host response on their own.
993 Hence, the parameter describing the immune stimulation from merozoites (γ_M) and pRBC
994 (γ_P) may differ (fig. 12B), and the challenge becomes determining the appropriate rate at
995 which each parasite stage will elicit host immune responses. Further, this model assumes that
996 all immunity acts generally on all stages of the parasite (i.e. once immunity is recruited,
997 either by pRBCs or merozoites, it affects both pRBCs (ψ_P) and merozoites (ψ_M) (fig. 12B)).
998 However, it is possible that immunity recruited towards merozoites might only act against
999 merozoites and vice versa (fig. 12C).
1000
1001 Since the model by Anderson et al. (9), a number of other models of adaptive immunity have
1002 been developed. Like Anderson et al., most of these models of within-host acquired
1003 immunity encapsulate all immunity as one or maybe two factors (such as cellular and
1004 antibody (152)) (10, 84, 85, 153). Also, while some of these models explicitly assume

schizont rupture is the major factor responsible for stimulating/recruiting immunity (153), most assume recruitment is related to total parasite load (10, 84, 85, 152). However, perhaps more critically, like Anderson et al. (9), most models assume that the immunity generated acts against all stages of the parasite, regardless of whether it was induced by, say, merozoites or pRBCs (fig. 12C). A lack of careful consideration of the stage-specificity of host responses seems like one of the major limitations for these models being able to provide useful insights regarding the mechanisms of immune control.

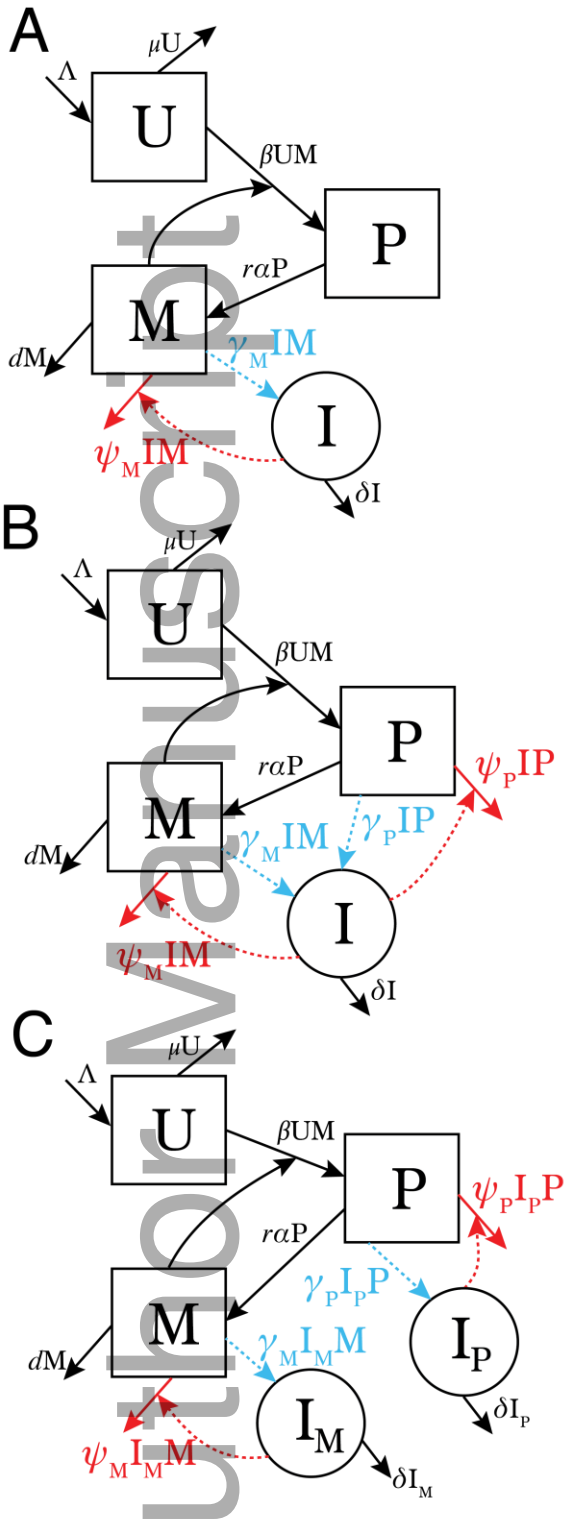

$$\frac{dU}{dt} = \Lambda - \mu U - \beta UM$$

$$\frac{dP}{dt} = \beta UM - \alpha P$$

$$\frac{dM}{dt} = r\alpha P - dM - \psi_M IM$$

$$\frac{dI}{dt} = \gamma_M IM - \delta I$$

$$\frac{dU}{dt} = \Lambda - \mu U - \beta UM$$

$$\frac{dP}{dt} = \beta UM - \alpha P - \psi_P IP$$

$$\frac{dM}{dt} = r\alpha P - dM - \psi_M IM$$

$$\frac{dI}{dt} = \gamma_M IM + \gamma_P IP - \delta I$$

$$\frac{dU}{dt} = \Lambda - \mu U - \beta UM$$

$$\frac{dP}{dt} = \beta UM - \alpha P - \psi_P I_P P$$

$$\frac{dM}{dt} = r\alpha P - dM - \psi_M I_M M$$

$$\frac{dI_M}{dt} = \gamma_M I_M M - \delta I_M$$

$$\frac{dI_P}{dt} = \gamma_P I_P M - \delta I_P$$

Figure 12: Models of parasite stage-specific immune recruitment and action. The three models presented here are extensions of the standard model (fig. 2B), however, in these models immunity, I, is introduced. The immunity state variable, I, encompasses all immune mechanisms that may be acting to control infection. Immunity is recruited by the presence of the parasites, P and M, (terms shown in blue). Immunity then acts to accelerate the removal of parasites (terms shown in red). Solid arrows indicate a change of state, and dashed arrows indicate an interaction without a state-change. (A) & (B) were originally presented in (9). As in the standard model, uninfected red blood cells (RBCs), U, are produced at rate Λ and lost

at rate μ. Production of pRBCs, P, is given by the interaction of merozoites, M and uninfected cells. Parasitised RBCs rupture at rate α, with each rupturing pRBC producing r merozoites. (A) This model assumes all immunity acts to clear merozoites only. The model assumes immunity is recruited at rate $\gamma_M I$, in proportion to the number of merozoites, and that immunity acts to clear merozoites at rate $\psi_M I$. (B) This model is the same as (A), except both merozoites and pRBCs stimulate an immune response and can be targeted by the immune response. Merozoites stimulate and are targeted by an immune response in the same manner as in (A). Parasitised RBCs stimulate an immune response at rate $\gamma_P I$, in proportion to the number of pRBCs. Parasitised RBCs are then cleared by immunity at rate $\psi_P I$. (C) Immunity generated by specific parasite stages is restricted to those stages. Neither of the models shown in (A) or (B), nor more recent models consider the possibility that immunity recruited against merozoites, might not be effective against pRBCs, and vice versa. Hence, we propose a third model identical to (B), expect that we split immunity into immunity that acts against merozoites only, I_M, and immunity that acts against pRBCs only, I_P.

Determining whether immunity acts against the merozoite or pRBCs

A number of in vitro studies have explored how antibodies from immune individuals act against parasite replication in culture (154-159). Given that the inhibitory activity of antibodies is likely dependent on other host immune mechanisms present in vivo, these in vitro systems often add back immune effector mechanisms such as phagocytic cells or complement in order to better replicate the mechanisms available to the host in vivo (154-158). These studies have often emphasised a role for merozoite-specific antibodies. One study found that complement-dependent, antibody-mediated killing of merozoites was a major correlate of immunity in individuals (157). This is consistent with a number of studies that have found the concentration of antibodies against merozoite proteins to be correlated with protection in individuals from endemic areas (though as discussed above, there are difficulties in interpreting these immune correlate studies (160)). Antibodies may act against merozoites in a number of ways, including complement mediated lysis or opsonisation for phagocytosis (both of which would increase merozoite clearance, i.e. d in the standard model shown in figure 11A), or neutralisation (preventing their invasion of new RBC, i.e. reducing β in figure 11B). Data from these in vitro growth inhibitory assays are likely to inform the development of models of immunity.

Antibodies and other immune mechanisms may also directly target the infected RBC, acting to accelerate their removal or impair their development (as was observed in acutely ill mice (48)), either of which could also play a significant role in controlling Plasmodium infection. It has been highlighted that the longer lived pRBCs (which circulate for 24 hours or more) might be a better target for host immunity than the short-lived merozoite (which is infectious for only around 10 minutes) (9). However, this ultimately depends on how effectively immune responses are able to suppress pRBC development or accelerate their clearance. For example, it is possible that the fully exposed merozoite is much more susceptible to antibody binding or neutralisation than the parasite inside a RBC, and thus a given level of antibody may have a much larger effect on merozoites (i.e. parameter ψ_M may be much larger than parameter ψ_P in figure 12B & C). Thus, we need to assess not only the magnitude of the host adaptive response targeting merozoites or pRBCs, but the efficacy of a given level of antibody or other response in reducing parasite replication.

The immune recruitment and effector actions discussed above are generally modelled with simple 'mass action' terms. However, a variety of other approaches including maximum growth rates, density dependent growth and survival, and saturable killing rates are also possible (161-164). Given the amount of uncertainty regarding the targets, mechanisms, and efficacy of host immune control of Plasmodium replication, novel experimental and modelling approaches to quantifying immune control are urgently required (112, 165).

Antigenic variation and cross-reactive immunity in Plasmodium infections

In addition to life-stage-specific immunity, a separate issue is strain-specific immunity. P. falciparum expresses an antigenically diverse family of var genes on the pRBC surface. Each

parasite has a repertoire of around 60 var genes, and an individual strain can switch expression from one variant of the gene to the other during an infection (166). Thus, the response to a single strain may initially target one var variant, which is then switched and a new response must be generated to a new variant (in much the same way as occurs with immune escape in HIV (167, 168)). Importantly, the concept of var gene variation and strain (or variant)-specific immunity also applies to sequential infection with different strains, which may carry or express different var gene variants. Modelling studies have attempted to capture the notion of competing Plasmodium variants within the one individual, with the host responding to each variant with a separate immune response, or the idea of Plasmodium gene switching (var gene switching) as a mechanism of avoid host responses (145, 169, 170). Over multiple exposures, it is expected that some form of cross-reactive immune responses should be elicited, which may act to control new infections (145, 171).

Persistent infection

Many viral infections such as HIV and hepatitis C develop into chronic infections. These viruses persist through their ability to evade immunity, at least partly due to antigenic variation to avoid immune recognition. In contrast, Plasmodium infections frequently manifest as acute infections that lead to illness and treatment (or death) and are usually completely resolved by the host. However, in endemic areas it seems that partially immune adults are able to carry infections for long periods of time at low parasitemias (143, 172). Given that antigenic variation is also a feature of malaria infection, whether by repeated exposures (with some patients re-infected as frequently as once every 10 days (144, 145)), or var gene switching in a single infection, it is plausible that ‘chronic’ malaria infections resemble some chronic viral infections.

Modelling drug treatment

Unlike HIV, Plasmodium infections are typically easily curable with drug treatment. However, the history of antimalarial therapy worldwide is one of repeated cycles of success and failure of new drugs. The Global Malaria Eradication Campaign was launched in 1955, using DDT to reduce mosquito numbers and chloroquine for treating infected individuals. This program initially led to major reductions in the number of malaria cases, however, by 1960 chloroquine resistance appeared (173). New drugs were introduced, including piperaquine (in the 1960s) and mefloquine (in the 1970s and 80s), however drug resistance to each soon followed. Artemisinin (originally known as qinghaosu) and its derivatives were developed in China in the 1970s. These drugs have been adopted as the recommended therapy for the treatment of malaria globally (174), in particular, in combination with partner antimalarials. The artemisinin-based therapies are highly effective, resulting in very rapid declines in parasite burden when administered to infected individuals (175). However, in the last ten years resistance to the artemisinins has emerged and spread across the Greater Mekong Region (176-179).

Modelling antimalarial drug action using traditional pharmacokinetic-pharmacodynamic (PK/PD) models is well established (reviewed in (180)). These models relate the in vivo concentration of an antimalarial with the rate of killing of parasites. Most PK/PD modelling in malaria also, rightly, includes the known differences in antimalarial activity against early-stage parasites (which are usually less susceptible to the action of antimalarials) and late-stage parasites (181-183). However, ongoing development of mechanistic models to better understand antimalarial drug action and resistance are still major research areas, and not without some controversy (138, 184, 185). While there are many similarities to studies of

antiviral drug action in vivo, the complex and synchronised lifecycle of the parasite provides some important challenges to modelling and interpretation which we will discuss below.

The unique shape of the parasite clearance curve

Early modelling studies of drug action in HIV and hepatitis C infection proved remarkably useful in understanding the dynamics of viral replication (13, 186, 187). These studies analysed the decay of virus after drug treatment and applied mechanistic models to interpret the viral lifecycle and drug action. Similar dynamics of decay in circulating parasite numbers after treatment have been observed both in field studies and in studies of experimentally infected patients. The 'parasite clearance curve' is typically more complex than the viral clearance curve, as a result of the more complex lifecycle of the parasite (fig. 13) (102). In particular, approximately one quarter of patients experience a rise in parasite numbers soon after treatment (43). Rises after treatment occur when an individual has late-stage parasites at the time of treatment, and the drug is unable act quickly enough to stop mature stage parasites from rupturing and infecting more RBCs immediately (43). If individuals have many young parasite stages at the time of treatment, the drug has many hours to take effect in order to prevent pRBCs rupturing and releasing more merozoites. The apparent delay between treatment and a decline in parasite numbers in some individuals is called the "lag-phase" (102) (fig. 13). After excluding the lag-phase, the subsequent phase of exponential parasite "clearance" has become an important metric for drug efficacy in malaria, and an online statistical tool has since been developed to estimate the rate of decline of parasite concentrations in individuals (188). The rate of parasite clearance has been used to identify the presence of drug resistance (176) and is currently being used to assess new antimalarial drug candidates (189, 190).

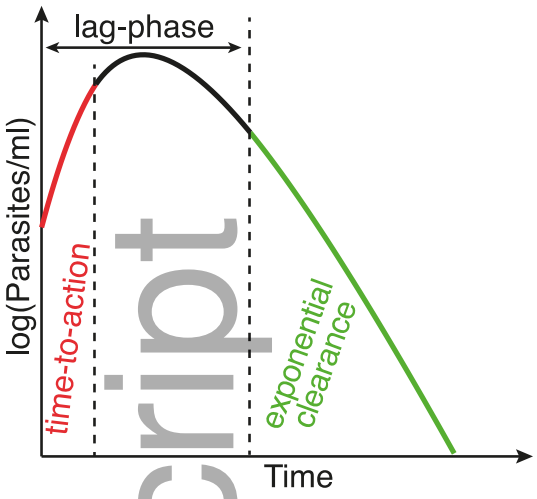

Figure 13: Illustration of a parasite clearance curve, showing the lag-phase. The dynamics of parasites after treatment has become known as the parasite clearance curve (191). After treatment many Plasmodium infected individuals can experience a rise in parasite concentration. This occurs when the individual is harbouring many mature schizonts at the time of treatment. The delay before drug is able to stop parasites maturing enables some schizonts to rupture and release progeny. At some point parasite replication is stopped and pRBC concentration declines. The lag-phase is the time between treatment and the exponential phase of parasite decline.

Interpreting and modelling parasite clearance

Correctly interpreting the exponential decline in parasite numbers after treatment has proved an area of some controversy (138, 184, 185). Given the complex and synchronous lifecycle of the parasite, one may ask why decay would be exponential at all (44, 138, 192)? In HIV dynamic modelling, drug action is interpreted as blocking viral replication, and the exponential decay phase of virus is interpreted as the natural decay rate of (virus producing) infected cells. In malaria treatment the effects of drug are interpreted very differently, with the rate of exponential decay in circulating parasite numbers usually being interpreted as the rate of killing by the drug (fig. 14A). That is, it has been assumed that 'killed' parasites are removed from circulation immediately. This presents a particular issue for interpreting the effects of short-acting drugs. The artemisinin derivatives typically have a short elimination half-life (30 minutes to 1 hour) and are largely cleared from the body by six hours post-treatment. These are typically administered every 24 hours. However, the exponential decay

of parasites continues despite the removal of drug from circulation (illustration in fig. 14A, see (193)).

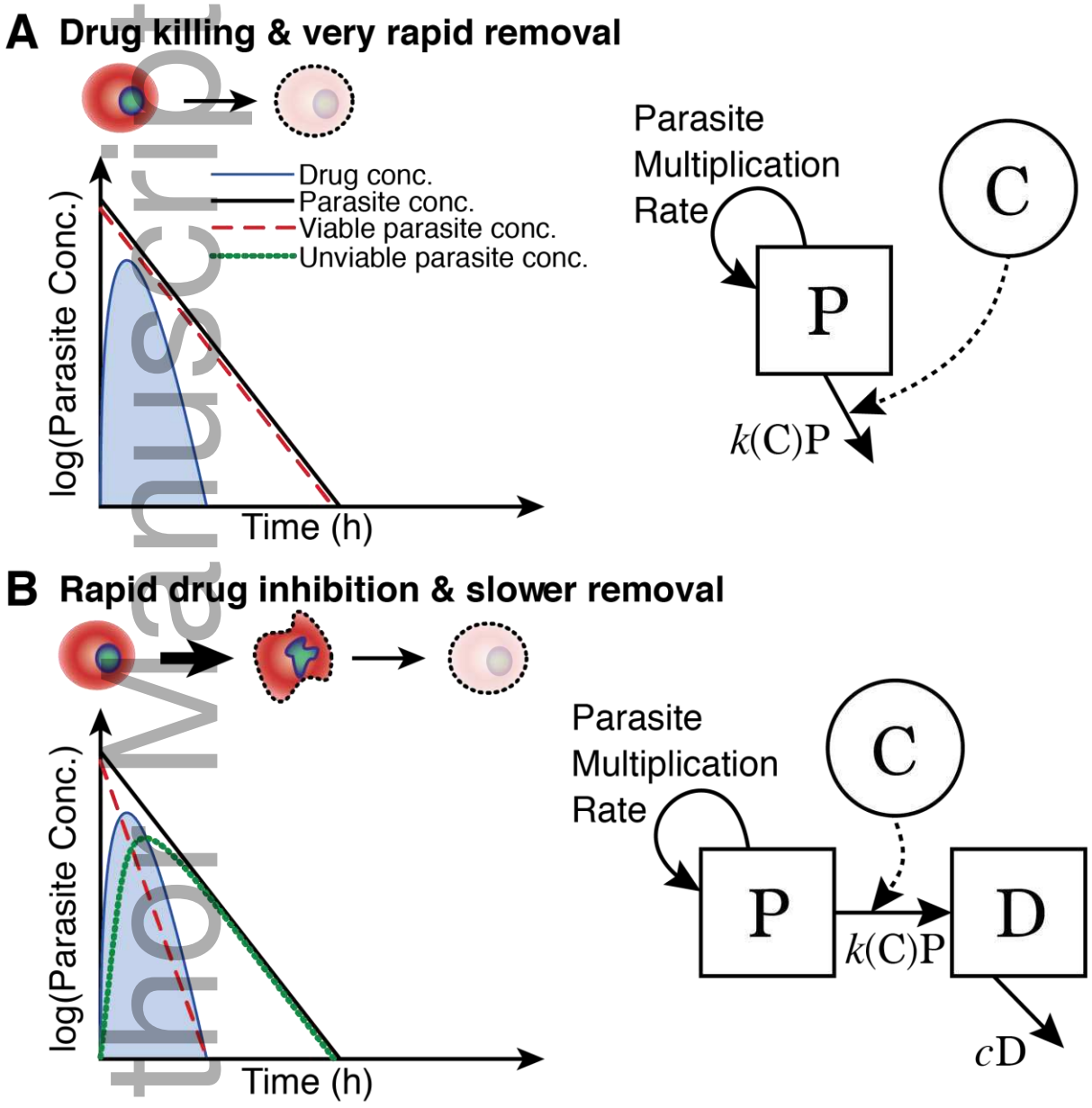

Figure 14: Illustration of two alternative understandings of drug-effect and parasite removal. Here we present an illustration of the decline in parasite concentration after treatment with an antimalarial, highlighting that it is possible to observe parasite concentration declining even once drug has been eliminated from host circulation (193). The solid black line indicates parasite concentration, and the blue shaded region indicates the drug concentration over time. (A) In PK/PD models of antimalarial drug action it is typically assumed that once a drug kills a parasite it is very rapidly removed, such that the overall decline in pRBCs from the host is essentially a measure of the rate of drug-killing (see red-dashed line and solid black line). The mathematical models tend to have a drug killing term, $k(C)$, that depends on the concentration of drug, C, in the host and causes pRBCs to decline

as they are killed. (B) Other modelling studies have suggested that drug-effect and host removal of drug-damaged or killed pRBCs are separate processes. This would mean that the decline in parasite concentration after drug treatment is not a measure of the speed of the drug-effect, but is a measure of the rate of host removal of drug-affected pRBCs (green dotted line versus red dashed line). A mathematical model of this process has an extra compartment, drug-damaged, or dead pRBCs, D. Drug action is still modelled in the same way, as a function of drug concentration, $k(C)$. However, the drug effect does not cause instant removal of the pRBCs but shifts them from the 'healthy' (red dashed line) to drug-affected (damaged) state, where they are subsequently removed at some rate, c.

Most models of drug action in malaria combine the two processes of drug killing of parasites, and the subsequent removal of those killed parasites, by assuming instantaneous removal (fig. 14A) (15, 16, 44, 74). However, several studies have proposed that drug killing of parasites and their removal might be two separate processes, and that the rate of killing might be faster than the rate of clearance of those killed parasites by the host (fig. 14B) (132, 133, 138, 184, 194-196). Under this scenario, the presence of drug for six hours may be sufficient to kill parasites (or perhaps to 'stun' them, since they may appear morphologically normal). These drug-affected (unviable) parasites remain in circulation and are subsequently cleared at an exponential rate (fig. 14B). This reconciles the short duration of drug action with the prolonged clearance of circulating parasites.

Distinguishing between these two processes is very difficult in human studies. However, adoptive transfer studies in mice (fig. 8) allow a dissection of the timing of drug action versus clearance of drug-affected parasites in vivo (132, 133). By removing a proportion of parasites from the mouse soon after treatment and culturing them in vitro, it is clear that after 6 hours of exposure to artesunate in vivo circulating parasites were completely impaired in their development and unable to mature in culture (132). However, these drug affected pRBCs continued to circulate in vivo, and were cleared with a half-life of 6.7 hours (132). This study indicates that drug action to impair or kill pRBCs is very rapid (complete within 6 hours), but that the subsequent host removal of these impaired or killed parasites is considerably slower.

The removal of these drug-affected parasites appeared host-mediated, as removal of phagocytes by clodronate treatment, or splenectomy, significantly reduced the clearance rate (133, 197). This strongly suggests that models should be incorporating drug effect and pRBC clearance as separate processes in vivo.

Incorporating cumulative drug effects on parasite killing

A recent series of in vitro experimental studies have established that a drug's killing activity is not only concentration, but also exposure dependent (138, 183, 198). These have highlighted an important gap in the modelling literature in malaria. Classical models of drug action in malaria, and most PK/PD models generally, have tended to assume that drug killing rates at any point in time are instantaneously related to the drug concentration at that time. This assumption is probably sufficient when considering drug action in HIV, for example, where enzyme inhibition is the major action, and drugs act rapidly to inhibit these enzymes and viral processes. Surprisingly, the mechanisms of action of most common antimalarials are poorly defined, and often ascribed to broad interference with parasite metabolism, and death due to oxidative damage (as a result of the parasite's need for haemoglobin degradation and metabolism) (138, 199). Thus, even if the inhibition of parasite metabolism is rapid, the resulting oxidative damage may take some time to accumulate and kill (or otherwise affect) the parasite. This suggests that the rate of 'killing' of parasites may be time-dependent and exposing a parasite to an antimalarial for longer periods may increase its risk of being killed (137). This concept of accumulated parasite stress, depending on the history of exposure of a parasite to a drug, has recently been modelled (137). Mechanistic models of the action of antimalarials to kill or inhibit parasites are sparse, more modelling of these processes may contribute to unravelling the mechanisms of antimalarial action.

Conclusion

This review has provided an introduction to within-host modelling of malaria infection, with a particular focus on exploring the complexities of the infection in order to highlight the points of difference with the extensive field of viral dynamics modelling. We have attempted to highlight the key challenges and open questions in the field and summarise some of the recent progress towards addressing those challenges. A major obstacle for many modellers in entering a new field of research can be accumulating enough of the necessary background knowledge to determine how their previous modelling experience can be applied with greatest effect. We hope to have provided readers the necessary background knowledge to begin developing models with biological fidelity, and to calibrate and test them with real-world data.

Acknowledgements

This work was supported by the Australian Research Council (grant DP120100064 & DP180103875 (to MPD, DC, AH, DSK), DP170103076 (to JMM, JAS) and FT110100250 (to JMM)), the National Health and Medical Research Council (NH&MRC), Australia (grants 1082022 (to MPD, DC, AH), 1141921 (to DSK), 1080001 (to MPD), 1028634 (to AH), 1100394 (to JAS, JMM), 1104975 (to JAS), 1028641 (to AH) and 1126399 (to AH)). The University of New South Wales provided the International Postgraduate Research Scholarship to RA and a Scientia PhD Scholarship to GRR. This work was supported in part by the Australian Centre for Research Excellence on Malaria Elimination, funded by the National Health and Medical Research Council of Australia 1134989 (to JAS, JMM, JM).

There are no conflicts of interest to declare.

References

1. Guedj J, Rong L, Dahari H, Perelson AS. A perspective on modelling hepatitis C virus infection. J Viral Hepat. 2010;17(12):825-33.
2. Perelson AS, Ribeiro RM. Modeling the within-host dynamics of HIV infection. BMC Biology. 2013;11(1):96.
3. Eaton JW, Johnson LF, Salomon JA, Barnighausen T, Bendavid E, Bershteyn A, et al. HIV treatment as prevention: systematic comparison of mathematical models of the potential impact of antiretroviral therapy on HIV incidence in South Africa. PLoS Med. 2012;9(7):e1001245.
4. Kretzschmar ME, Schim van der Loeff MF, Birrell PJ, De Angelis D, Coutinho RA. Prospects of elimination of HIV with test-and-treat strategy. Proc Natl Acad Sci U S A. 2013;110(39):15538-43.
5. Virlogeux V, Zoulim F, Pugliese P, Poizot-Martin I, Valantin M-A, Cuzin L, et al. Modeling HIV-HCV coinfection epidemiology in the direct-acting antiviral era: the road to elimination. BMC Medicine. 2017;15(1):217.
6. World Health Organization. World malaria report 2017: World Health Organization,; 2017 November 2017.
7. Perelson AS, Neumann AU, Markowitz M, Leonard JM, Ho DD. HIV-1 Dynamics in Vivo: Virion Clearance Rate, Infected Cell Life-Span, and Viral Generation Time. Science. 1996;271(5255):1582.
8. Wei X, Ghosh SK, Taylor ME, Johnson VA, Emini EA, Deutsch P, et al. Viral dynamics in human immunodeficiency virus type 1 infection. Nature. 1995;373(6510):117-22.
9. Anderson RM, May RM, Gupta S. Non-Linear Phenomena in Host-Parasite Interactions. Parasitology. 1989;99:S59-S79.
10. Hellriegel B. Modelling the immune response to malaria with ecological concepts: short-term behaviour against long-term equilibrium. Proc R Soc Lond B Biol Sci. 1992;250:249-56.
11. Hetzel C, Anderson RM. The within-host cellular dynamics of bloodstage malaria: Theoretical and experimental studies. Parasitology. 1996;113:25-38.
12. Nowak M, May RM. Virus Dynamics : Mathematical Principles of Immunology and Virology: Mathematical Principles of Immunology and Virology: Oxford University Press, UK; 2000.
13. Ho DD, Neumann AU, Perelson AS, Chen W, Leonard JM, Markowitz M. Rapid turnover of plasma virions and CD4 lymphocytes in HIV-1 infection. Nature. 1995;373(6510):123-6.
14. Gravenor M, Lloyd A. Reply to: Models for the in-host dynamics of malaria revisited: errors in some basic models lead to large overestimates of growth rates. Parasitology. 1998;117:409-10.
15. Saralamba S, Pan-Ngum W, Maude RJ, Lee SJ, Tarning J, Lindegårdh N, et al. Intrahost modeling of artemisinin resistance in Plasmodium falciparum. Proc Natl Acad Sci U S A. 2011;108(1):397-402.
16. Zaloumis S, Humberstone A, Charman SA, Price RN, Moehrle J, Gamo-Benito J, et al. Assessing the utility of an anti-malarial pharmacokinetic-pharmacodynamic model for aiding drug clinical development. Malar J. 2012;11(1):303.
17. Hoshen MB, Heinrich R, Stein WD, Ginsburg H. Mathematical modelling of the within-host dynamics of Plasmodium falciparum. Parasitology. 2000;121 (Pt 3):227-35.

18. Cromer D, Stark J, Davenport MP. Low red cell production may protect against severe anemia during a malaria infection--insights from modeling. J Theor Biol. 2009;257(4):533-42.
19. Khoury DS, Cromer D, Best SE, James KR, Kim PS, Engwerda CR, et al. Effect of mature blood-stage Plasmodium parasite sequestration on pathogen biomass in mathematical and in vivo models of malaria. Infect Immun. 2014;82(1):212-20.
20. Antia R, Yates A, de Roode JC. The dynamics of acute malaria infections. I. Effect of the parasite's red blood cell preference. Proc R Soc B. 2008;275(1641):1449-58.
21. Alano P, Carter R. Sexual differentiation in malaria parasites. Annu Rev Microbiol. 1990;44:429-49.
22. Frevert U. Sneaking in through the back entrance: the biology of malaria liver stages. Trends in parasitology. 2004;20(9):417-24.
23. Garnham PCC. Malaria parasites of man: life-cycles and morphology (excluding ultrastructure). In: Wernsdorfer WH, McGregor I, editors. Malaria: principles and practice of malariology. 1: Churchill Livingstone; 1988. p. 61-96.
24. Miller LH, Ackerman HC, Su X-z, Wellems TE. Malaria biology and disease pathogenesis: insights for new treatments. Nat Med. 2013;19(2):156-67.
25. Bannister L, Mitchell G. The ins, outs and roundabouts of malaria. Trends in parasitology. 2003;19(5):209-13.
26. Perelson AS. Modelling viral and immune system dynamics. Nat Rev Immunol. 2002;2(1):28-36.
27. Dixit NM, Markowitz M, Ho DD, Perelson AS. Estimates of intracellular delay and average drug efficacy from viral load data of HIV-infected individuals under antiretroviral therapy. Antiviral therapy. 2004;9(2):237-46.
28. Petravic J, Ellenberg P, Chan ML, Paukovics G, Smyth RP, Mak J, et al. Intracellular Dynamics of HIV Infection. J Virol. 2014;88(2):1113-24.
29. Beauchemin CAA, Miura T, Iwami S. Duration of SHIV production by infected cells is not exponentially distributed: Implications for estimates of infection parameters and antiviral efficacy. Scientific Reports. 2017;7:42765.
30. Pearson JE, Krapivsky P, Perelson AS. Stochastic theory of early viral infection: continuous versus burst production of virions. PLoS Comput Biol. 2011;7(2):e1001058.
31. Saul A. Models for the in-host dynamics of malaria revisited: errors in some basic models lead to large over-estimates of growth rates. Parasitology. 1998;117:405-7.
32. Jacquez JA, Simon CP, Koopman J, Sattenspiel L, Perry T. Modeling and analyzing HIV transmission: the effect of contact patterns. Math Biosci. 1988;92(2):119-99.
33. Best KP, A.S. Mathematical modeling of within host Zika virus dynamics. Immunol Rev. 2018;(This issue).
34. Nelson PW, Gilchrist MA, Coombs D, Hyman JM, Perelson AS. An Age-Structured Model of HIV Infection that Allows for Variations in the Production Rate of Viral Particles and the Death Rate of Productively Infected Cells. Mathematical Biosciences & Engineering. 2004;1(2):267-88.
35. White NJ, Chapman D, Watt G. The effects of multiplication and synchronicity on the vascular distribution of parasites in falciparum malaria. Trans R Soc Trop Med Hyg. 1992;86(6):590-7.
36. Garcia CRS, Markus RP, Madeira L. Tertian and Quartan Fevers: Temporal Regulation in Malarial Infection. J Biol Rhythms. 2001;16(5):436-43.

37. Baker HB. Malaria; and the causation of periodic fever. J Amer Med Assoc. 1888;XI(19):651-63.
38. Kwiatkowski D, Greenwood BM. Why is malaria fever periodic? A hypothesis. Parasitology Today. 1989;5(8):264-6.
39. Simpson JA, Aarons L, Collins WE, Jeffery GM, White NJ. Population dynamics of untreated Plasmodium falciparum malaria within the adult human host during the expansion phase of the infection. Parasitology. 2002;124(03).
40. Jakeman G, Saul A, Hogarth W, Collins W. Anaemia of acute malaria infections in non-immune patients primarily results from destruction of uninfected erythrocytes. Parasitology. 1999;119:127-33.
41. Andrews L, Andersen RF, Webster D, Dunachie S, Walther RM, Bejon P, et al. Quantitative real-time polymerase chain reaction for malaria diagnosis and its use in malaria vaccine clinical trials. Am J Trop Med Hyg. 2005;73(1):191-8.
42. McCarthy JS, Sekuloski S, Griffin PM, Elliott S, Douglas N, Peatey C, et al. A pilot randomised trial of induced blood-stage Plasmodium falciparum infections in healthy volunteers for testing efficacy of new antimalarial drugs. PLoS One. 2011;6(8):e21914.
43. Khoury DS, Cromer D, Möhrle JJ, McCarthy JS, Davenport MP. Defining the Effectiveness of Antimalarial Chemotherapy: Investigation of the Lag in Parasite Clearance Following Drug Administration. J Infect Dis. 2016;214(5):753-61.
44. Gravenor MB, Lloyd AL, Kremsner PG, Missinou MA, English M, Marsh K, et al. A model for estimating total parasite load in falciparum malaria patients. J Theor Biol. 2002;217(2):137-48.
45. Beaudry JT, Fairhurst RM. Microvascular sequestration of Plasmodium falciparum. Blood. 2011;117(24):6410.
46. Touré-Ndouo FS, Zang-Edou ES, Bisvigou U, Mezui-Me-Ndong J. Relationship between in vivo synchronicity of Plasmodium falciparum and allelic diversity. Parasitology international. 2009;58(4):390-3.
47. Boyle MJ, Wilson DW, Richards JS, Riglar DT, Tetteh KKA, Conway DJ, et al. Isolation of viable Plasmodium falciparum merozoites to define erythrocyte invasion events and advance vaccine and drug development. Proc Natl Acad Sci U S A. 2010;107(32):14378-83.
48. Khoury DS, Cromer D, Akter J, Sebina I, Elliott T, Thomas BS, et al. Host-mediated impairment of parasite maturation during blood-stage Plasmodium infection. Proc Natl Acad Sci U S A. 2017;114(29):7701-6.
49. Babbitt SE, Altenhofen L, Cobbold SA, Istvan ES, Fennell C, Doerig C, et al. Plasmodium falciparum responds to amino acid starvation by entering into a hibernatory state. Proc Natl Acad Sci U S A. 2012;109(47):E3278-87.
50. Kwiatkowski D, Nowak M. Periodic and chaotic host-parasite interactions in human malaria. Proc Natl Acad Sci U S A. 1991;88(12):5111-3.
51. Mideo N, Reece SE, Smith AL, Metcalf CJE. The Cinderella syndrome: why do malaria-infected cells burst at midnight? Trends in parasitology. 2013;29(1):10-6.
52. O'Donnell AJ, Schneider P, McWatters HG, Reece SE. Fitness costs of disrupting circadian rhythms in malaria parasites. Proceedings Biological sciences. 2011;278(1717):2429-36.
53. Gautret P, Deharo E, Tahar R, Chabaud AG, Landau I. The adjustment of the schizogonic cycle of Plasmodium chabaudi chabaudi in the blood to the circadian rhythm of the host. Parasite. 1995;2(1):69-74.

54. Prior KF, van der Veen DR, O'Donnell AJ, Cumnock K, Schneider D, Pain A, et al. Timing of host feeding drives rhythms in parasite replication. PLoS Pathog. 2018;14(2):e1006900.
55. Hirako IC, Assis PA, Hojo-Souza NS, Reed G, Nakaya H, Golenbock DT, et al. Daily Rhythms of TNFalpha Expression and Food Intake Regulate Synchrony of Plasmodium Stages with the Host Circadian Cycle. Cell Host Microbe. 2018.
56. Deharo E, Coquelin F, Chabaud A, Landau I. The erythrocytic schizogony of two synchronized strains of *Plasmodium berghei*, NK65 and ANKA, in normocytes and reticulocytes. Parasitol Res. 1996;82(2):178-82.
57. Douglas AD, Edwards NJ, Duncan CJA, Thompson FM, Sheehy SH, O'Hara GA, et al. Comparison of modeling methods to determine liver-to-blood inocula and parasite multiplication rates during controlled human malaria infection. J Infect Dis. 2013;208(2):340-5.
58. Carvalho LJdM, Alves FA, de Oliveira SG, do Valle RdR, Fernandes AAM, Muniz JAPC, et al. Severe anemia affects both splenectomized and non-splenectomized Plasmodium falciparum-infected Aotus infulatus monkeys. Mem Inst Oswaldo Cruz. 2003;98(5):679-86.
59. Langreth SG, Peterson E. Pathogenicity, stability, and immunogenicity of a knobless clone of Plasmodium falciparum in Colombian owl monkeys. Infect Immun. 1985;47(3):760-6.
60. Pye D, O'Brien CM, Franchina P, Monger C, Anders RF. Plasmodium falciparum infection of splenectomized and intact Guyanan Saimiri monkeys. J Parasitol. 1994;80(4):558-62.
61. White NJ, Turner GDH, Medana IM, Dondorp AM, Day NPJ. The murine cerebral malaria phenomenon. Trends in parasitology. 2010;26(1):11-5.
62. Craig AG, Grau GE, Janse C, Kazura JW, Milner D, Barnwell JW, et al. The role of animal models for research on severe malaria. PLoS Pathog. 2012;8(2):e1002401.
63. Douglas AD, Andrews L, Draper SJ, Bojang K, Milligan P, Gilbert SC, et al. Substantially Reduced Pre-patent Parasite Multiplication Rates Are Associated With Naturally Acquired Immunity to Plasmodium falciparum. J Infect Dis. 2011;203(9):1337-40.
64. Duncan CJ, Sheehy SH, Ewer KJ, Douglas AD, Collins KA, Halstead FD, et al. Impact on malaria parasite multiplication rates in infected volunteers of the protein-in-adjuvant vaccine AMA1-C1/Alhydrogel+CPG 7909. PLoS One. 2011;6(7):e22271.
65. Dietz K, Raddatz G, Molineaux L. Mathematical model of the first wave of plasmodium falciparum asexual parasitemia in non-immune and vaccinated individuals. Am J Trop Med Hyg. 2006;75(2 suppl):46-55.
66. Silamut K, White NJ. Relation of the stage of parasite development in the peripheral blood to prognosis in severe falciparum malaria. Trans R Soc Trop Med Hyg. 1993;87(4):436-43.
67. Sherman IW, Eda S, Winograd E. Cytoadherence and sequestration in Plasmodium falciparum: defining the ties that bind. Microbes and Infection. 2003;5(10):897-909.
68. Dondorp AM, Desakorn V, Pongtavornpinyo W, Sahassananda D, Silamut K, Chotivanich K, et al. Estimation of the total parasite biomass in acute falciparum malaria from plasma PfHRP2. PLoS medicine. 2005;2(8):e204.
69. Haque A, Best SE, Amante FH, Ammerdorffer A, de Labastida F, Pereira T, et al. High parasite burdens cause liver damage in mice following *Plasmodium berghei* ANKA infection independently of CD8(+) T cell-mediated immune pathology. Infect Immun. 2011;79(5):1882-8.

70. Haque A, Best SE, Unosson K, Amante FH, de Labastida F, Anstey NM, et al. Granzyme B Expression by CD8(+) T Cells Is Required for the Development of Experimental Cerebral Malaria. J Immunol. 2011;186(11):6148-56.
71. McQuillan JA, Mitchell AJ, Ho YF, Combes V, Ball HJ, Golenser J, et al. Coincident parasite and CD8 T cell sequestration is required for development of experimental cerebral malaria. Int J Parasitol. 2011;41(2):155-63.
72. Turner GD, Morrison H, Jones M, Davis TM, Looareesuwan S, Buley ID, et al. An immunohistochemical study of the pathology of fatal malaria. Evidence for widespread endothelial activation and a potential role for intercellular adhesion molecule-1 in cerebral sequestration. The American journal of pathology. 1994;145(5):1057-69.
73. Tom S, Armstrong SJ, Richard H. Attributable fraction estimates and case definitions for malaria in endemic. Stat Med. 1994;13(22):2345-58.
74. Gravenor M, van Hensbroek M, Kwiatkowski D. Estimating sequestered parasite population dynamics in cerebral malaria. Proc Natl Acad Sci U S A. 1998;95(13):7620-4.
75. Cromer D, Best SE, Engwerda C, Haque A, Davenport M. Where have all the parasites gone? Modelling early malaria parasite sequestration dynamics. PLoS One. 2013;8(2):e55961.
76. Carvalho BO, Lopes SCP, Nogueira PA, Orlandi PP, Bargieri DY, Blanco YC, et al. On the Cytoadhesion of Plasmodium vivax-Infected Erythrocytes. J Infect Dis. 2010;202(4):638-47.
77. Fonager J, Pasini EM, Braks JAM, Klop O, Ramesar J, Remarque EJ, et al. Reduced CD36-dependent tissue sequestration of Plasmodium-infected erythrocytes is detrimental to malaria parasite growth in vivo. The Journal of experimental medicine. 2012;209(1):93-107.
78. Udomsangpetch R, Pipitaporn B, Silamut K, Pinches R, Kyes S, Looareesuwan S, et al. Febrile temperatures induce cytoadherence of ring-stage Plasmodium falciparum-infected erythrocytes. Proc Natl Acad Sci U S A. 2002;99(18):11825-9.
79. Matz PB. The treatment of neurosyphilis by "inoculation malaria" in the United States Veterans Bureau. J Nerv Ment Dis. 1928;68:113-33.
80. O Leary PA. Treatment of neurosyphilis by malaria - Report on the three years observation of the first one hundred patients treated. J Amer Med Assoc. 1927;89:95-100.
81. O'Leary P, Goeckerman WH, Parker ST. Treatment of neurosyphilis by malaria - A preliminary report. Arch Dermatol Syph. 1926;13(3):301-20.
82. Gravenor M, Mclean AR, Kwiatkowski D. The Regulation of Malaria Parasitemia - Parameter Estimates for a Population-Model. Parasitology. 1995;110:115-22.
83. Molineaux L, Trauble M, Collins WE, Jeffery GM, Dietz K. Malaria therapy reinoculation data suggest individual variation of an innate immune response and independent acquisition of antiparasitic and antitoxic immunities. Trans R Soc Trop Med Hyg. 2002;96(2):205-9.
84. McKenzie FE, Bossert WH. An integrated model of Plasmodium falciparum dynamics. J Theor Biol. 2005;232(3):411-26.
85. Gurarie D, Karl S, Zimmerman PA, King CH, St Pierre TG, Davis TM. Mathematical modeling of malaria infection with innate and adaptive immunity in individuals and agent-based communities. PLoS One. 2012;7(3):e34040.
86. McKenzie FE, Jeffery GM, Collins WE. Plasmodium vivax blood-stage dynamics. J parasitology. 2002;88(3):521-35.

87. Griffin P, Pasay C, Elliott S, Sekuloski S, Sikulu M, Hugo L, et al. Safety and Reproducibility of a Clinical Trial System Using Induced Blood Stage Plasmodium vivax Infection and Its Potential as a Model to Evaluate Malaria Transmission. PLoS neglected tropical diseases. 2016;10(12):e0005139.
88. McCarthy JS, Griffin PM, Sekuloski S, Bright AT, Rockett R, Looke D, et al. Experimentally induced blood-stage Plasmodium vivax infection in healthy volunteers. J Infect Dis. 2013;208(10):1688-94.
89. Payne RO, Griffin PM, McCarthy JS, Draper SJ. Plasmodium vivax Controlled Human Malaria Infection - Progress and Prospects. Trends Parasitol. 2017;33(2):141-50.
90. Roestenberg M, de Vlas SJ, Nieman A-E, Sauerwein RW, Hermsen CC. Efficacy of preerythrocytic and blood-stage malaria vaccines can be assessed in small sporozoite challenge trials in human volunteers. J Infect Dis. 2012;206(3):319-23.
91. Roestenberg M, McCall M, Hopman J, Wiersma J, Luty AJF, van Gemert GJ, et al. Protection against a Malaria Challenge by Sporozoite Inoculation. N Engl J Med. 2009;361(5):468-77.
92. Roestenberg M, Teirlinck AC, McCall MBB, Teelen K, Makamdop KN, Wiersma J, et al. Long-term protection against malaria after experimental sporozoite inoculation: an open-label follow-up study. Lancet. 2011;377(9779):1770-6.
93. Spring MD, Cummings JF, Ockenhouse CF, Dutta S, Reidler R, Angov E, et al. Phase 1/2a study of the malaria vaccine candidate apical membrane antigen-1 (AMA-1) administered in adjuvant system AS01B or AS02A. PLoS One. 2009;4(4):e5254.
94. Rockett RJ, Tozer SJ, Peatey C, Bialasiewicz S, Whiley DM, Nissen MD, et al. A real-time, quantitative PCR method using hydrolysis probes for the monitoring of Plasmodium falciparum load in experimentally infected human volunteers. Malar J. 2011;10:48.
95. Schneider P, Wolters L, Schoone G, Schallig H, Sillekens P, Hermsen R, et al. Real-time nucleic acid sequence-based amplification is more convenient than real-time PCR for quantification of Plasmodium falciparum. J Clin Microbiol. 2005;43(1):402-5.
96. Hermsen CC, Telgt DSC, Linders EHP, van de Locht LATF, Eling WMC, Mensink EJBM, et al. Detection of Plasmodium falciparum malaria parasites in vivo by real-time quantitative PCR. Mol Biochem Parasitol. 2001;118(2):247-51.
97. Bejon P, Andrews L, Andersen RF, Dunachie S, Webster D, Walther M, et al. Calculation of liver-to-blood inocula, parasite growth rates, and preerythrocytic vaccine efficacy, from serial quantitative polymerase chain reaction studies of volunteers challenged with malaria sporozoites. J Infect Dis. 2005;191(4):619-26.
98. Seydel KB, Milner DA, Kamiza SB, Molyneux ME, Taylor TE. The Distribution and Intensity of Parasite Sequestration in Comatose Malawian Children. J Infect Dis. 2006;194(2):208-5.
99. Franke-Fayard B, Waters AP, Janse CJ. Real-time in vivo imaging of transgenic bioluminescent blood stages of rodent malaria parasites in mice. Nature protocols. 2006;1(1):476-85.
100. Amante FH, Haque A, Stanley AC, Rivera FdL, Randall LM, Wilson YA, et al. Immune-Mediated Mechanisms of Parasite Tissue Sequestration during Experimental Cerebral Malaria. J Immunol. 2010;185(6):3632-42.
101. Haque A, Best SE, Amante FH, Mustafah S, Desbarrieres L, de Labastida F, et al. CD4+ natural regulatory T cells prevent experimental cerebral malaria via CTLA-4 when expanded in vivo. PLoS Pathog. 2010;6(12):e1001221.
102. White NJ. Malaria parasite clearance. Malar J. 2017;16(1):88.

103. Buffet PA, Safeukui I, Milon G, Mercereau-Puijalon O, David PH. Retention of erythrocytes in the spleen: a double-edged process in human malaria. Curr Opin Hematol. 2009;16(3):157-64.
104. Buffet PA, Safeukui I, Deplaine G, Brousse V, Prendki V, Thellier M, et al. The pathogenesis of Plasmodium falciparum malaria in humans: insights from splenic physiology. Blood. 2011;117(2):381-92.
105. Del Portillo HA, Ferrer M, Brugat T, Martin-Jaular L, Langhorne J, Lacerda MVG. The role of the spleen in malaria. Cell Microbiol. 2012;14(3):343-55.
106. Safeukui I, Correas J-M, Brousse V, Hirt D, Deplaine G, Mule S, et al. Retention of *Plasmodium falciparum* ring-infected erythrocytes in the slow, open microcirculation of the human spleen. Blood. 2008;112(6):2520-8.
107. Chotivanich K, Udomsangpetch R, McGready R, Proux S, Newton P, Pukrittayakamee S, et al. Central role of the spleen in malaria parasite clearance. J Infect Dis. 2002;185(10):1538-41.
108. Demar M, Legrand E, Hommel D, Esterre P, Carme B. Plasmodium falciparum malaria in splenectomized patients: two case reports in French Guiana and a literature review. Am J Trop Med Hyg. 2004;71(3):290-3.
109. David PH, Hommel M, Miller LH, Udeinya IJ, Oligino LD. Parasite sequestration in Plasmodium falciparum malaria: spleen and antibody modulation of cytoadherence of infected erythrocytes. Proc Natl Acad Sci U S A. 1983;80(16):5075-9.
110. Phillips AN. Reduction of HIV Concentration during Acute Infection: Independence from a Specific Immune Response. Science. 1996;271(5248):497-9.
111. Davenport MP, Zhang L, Shiver JW, Casmiro DR, Ribeiro RM, Perelson AS. Influence of peak viral load on the extent of CD4+ T-cell depletion in simian HIV infection. J Acquir Immune Defic Syndr. 2006;41(3):259-65.
112. Metcalf CJE, Graham AL, Huijben S, Barclay VC, Long GH, Grenfell BT, et al. Partitioning regulatory mechanisms of within-host malaria dynamics using the effective propagation number. Science. 2011;333(6045):984-8.
113. De Boer RJ, Perelson AS. Target Cell Limited and Immune Control Models of HIV Infection: A Comparison. J Theor Biol. 1998;190(3):201-14.
114. Silamut K, Phu NH, Whitty C, Turner GD, Louwrier K, Mai NT, et al. A quantitative analysis of the microvascular sequestration of malaria parasites in the human brain. The American journal of pathology. 1999;155(2):395-410.
115. Simpson JA, Silamut K, Chotivanich K, Pukrittayakamee S, White NJ. Red cell selectivity in malaria: a study of multiple-infected erythrocytes. Trans R Soc Trop Med Hyg. 1999;93(2):165-8.
116. Pasvol G, Weatherall DJ, Wilson RJ. The increased susceptibility of young red cells to invasion by the malarial parasite Plasmodium falciparum. Br J Haematol. 1980;45(2):285-95.
117. Thakre N, Fernandes P, Mueller AK, Graw F. Examining the Reticulocyte Preference of Two Plasmodium berghei Strains during Blood-Stage Malaria Infection. Front Microbiol. 2018;9:166.
118. Kerlin DH, Gatton ML. Preferential invasion by Plasmodium merozoites and the self-regulation of parasite burden. PLoS One. 2013;8(2):e57434.
119. McQueen PG, McKenzie FE. Age-structured red blood cell susceptibility and the dynamics of malaria infections. Proc Natl Acad Sci U S A. 2004;101(24):9161-6.

120. Cromer D, Evans KJ, Schofield L, Davenport MP. Preferential invasion of reticulocytes during late-stage Plasmodium berghei infection accounts for reduced circulating reticulocyte levels. Int J Parasitol. 2006;36(13):1389-97.
121. Dasari P, Fries A, Heber SD, Salama A, Blau IW, Lingelbach K, et al. Malarial anemia: digestive vacuole of Plasmodium falciparum mediates complement deposition on bystander cells to provoke hemophagocytosis. Med Microbiol Immunol. 2014;203(6):383-93.
122. Evans KJ, Hansen DS, van Rooijen N, Buckingham LA, Schofield L. Severe malarial anemia of low parasite burden in rodent models results from accelerated clearance of uninfected erythrocytes. Blood. 2006;107(3):1192-9.
123. Matthews K, Duffy SP, Myrand-Lapierre ME, Ang RR, Li L, Scott MD, et al. Microfluidic analysis of red blood cell deformability as a means to assess hemin-induced oxidative stress resulting from Plasmodium falciparum intraerythrocytic parasitism. Integr Biol (Camb). 2017;9(6):519-28.
124. Gallo V, Skorokhod OA, Schwarzer E, Arese P. Simultaneous determination of phagocytosis of Plasmodium falciparum-parasitized and non-parasitized red blood cells by flow cytometry. Malar J. 2012;11(1):428.
125. Metcalf CJE, Long GH, Mideo N, Forester JD, Bjornstad ON, Graham AL. Revealing mechanisms underlying variation in malaria virulence: effective propagation and host control of uninfected red blood cell supply. Journal of the Royal Society, Interface / the Royal Society. 2012;9(76):2804-13.
126. Herricks T, Seydel KB, Molyneux M, Taylor T, Rathod PK. Estimating physical splenic filtration of *Plasmodium falciparum*-infected red blood cells in malaria patients. Cell Microbiol. 2012;14(12):1880-91.
127. Looareesuwan S, Ho M, Wattanagoon Y, White NJ, Warrell DA, Bunnag D, et al. Dynamic alteration in splenic function during acute falciparum malaria. N Engl J Med. 1987;317(11):675-9.
128. Quinn TC, Wyler DJ. Intravascular clearance of parasitized erythrocytes in rodent malaria. The Journal of clinical investigation. 1979;63(6):1187-94.
129. Wyler DJ, Quinn TC, Chen LT. Relationship of alterations in splenic clearance function and microcirculation to host defense in acute rodent malaria. The Journal of clinical investigation. 1981;67(5):1400-4.
130. Smith LP, Hunter KW, Oldfield EC, Strickland GT. Murine malaria: blood clearance and organ sequestration of Plasmodium yoelii-infected erythrocytes. Infect Immun. 1982;38(1):162-7.
131. Khoury DS, Cromer D, Best SE, James KR, Sebina I, Haque A, et al. Reduced erythrocyte susceptibility and increased host clearance of young parasites slows *Plasmodium* growth in a murine model of severe malaria. Sci Rep. 2015;5:9412.
132. Khoury DS, Cromer D, Elliott T, Soon MSF, Thomas BS, James KR, et al. Characterizing the effect of antimalarial drugs on the maturation and clearance of murine blood-stage Plasmodium parasites *in vivo*. Int J Parasitol. 2017;47(14):913-22.
133. Aogo RA, Khoury DS, Cromer D, Elliott T, Akter J, Fogg LG, et al. Quantification of host-mediated parasite clearance during blood-stage Plasmodium infection and anti-malarial drug treatment in mice. Int J Parasitol. 2018:(In Press).
134. Randall LM, Amante FH, McSweeney KA, Zhou Y, Stanley AC, Haque A, et al. Common strategies to prevent and modulate experimental cerebral malaria in mouse strains with different susceptibilities. Infect Immun. 2008;76(7):3312-20.

135. Bozdech Z, Llinás M, Pulliam BL, Wong ED, Zhu J, DeRisi JL. The Transcriptome of the Intraerythrocytic Developmental Cycle of Plasmodium falciparum. PLoS Biol. 2003;1(1):e5.
136. Mok S, Ashley EA, Ferreira PE, Zhu L, Lin Z, Yeo T, et al. Population transcriptomics of human malaria parasites reveals the mechanism of artemisinin resistance. Science. 2014.
137. Cao P, Klonis N, Zaloumis S, Dogovski C, Xie SC, Saralamba S, et al. A dynamic stress model explains the delayed drug effect in artemisinin treatment of Plasmodium falciparum. Antimicrob Agents Chemother. 2017;61(12):e00618-17.
138. Dogovski C, Xie SC, Burgio G, Bridgford J, Mok S, McCaw JM, et al. Targeting the Cell Stress Response of *Plasmodium falciparum* to Overcome Artemisinin Resistance. PLoS Biol. 2015;13(4):e1002132.
139. Smith JA, Martin L. Do Cells Cycle? Proceedings of the National Academy of Sciences. 1973;70(4):1263.
140. Cao P, Klonis N, Zaloumis S, Khoury DS, Cromer D, Davenport MP, et al. A mechanistic model quantifies artemisinin-induced parasite growth retardation in blood-stage Plasmodium falciparum infection. J Theor Biol. 2017;430:117-27.
141. Mancio-Silva L, Slavic K, Grilo Ruivo MT, Grosso AR, Modrzynska KK, Vera IM, et al. Nutrient sensing modulates malaria parasite virulence. Nature. 2017;547(7662):213-6.
142. Mogeni P, Williams TN, Fegan G, Nyundo C, Bauni E, Mwai K, et al. Age, Spatial, and Temporal Variations in Hospital Admissions with Malaria in Kilifi County, Kenya: A 25-Year Longitudinal Observational Study. PLoS medicine. 2016;13(6):e1002047.
143. Portugal S, Tran TM, Ongoiba A, Bathily A, Li S, Doumbo S, et al. Treatment of Chronic Asymptomatic Plasmodium falciparum Infection Does Not Increase the Risk of Clinical Malaria Upon Reinfection. Clin Infect Dis. 2017;64(5):645-53.
144. Pinkevych M, Petravic J, Chelimo K, Vulule J, Kazura JW, Moormann AM, et al. Decreased growth rate of P. falciparum blood stage parasitemia with age in a holoendemic population. J Infect Dis. 2014;209(7):1136-43.
145. Pinkevych M, Petravic J, Chelimo K, Kazura JW, Moormann AM, Davenport MP. The dynamics of naturally acquired immunity to Plasmodium falciparum infection. PLoS Comput Biol. 2012;8(10):e1002729.
146. Pinkevych M, Petravic J, Bereczky S, Rooth I, Färnert A, Davenport MP. Understanding the Relationship Between Plasmodium falciparum Growth Rate and Multiplicity of Infection. Journal of Infectious Diseases. 2014.
147. Cohen S, Carrington S, Mcgregor IA. Gamma-Globulin and Acquired Immunity to Human Malaria. Nature. 1961;192(480):733-7.
148. Pinkevych M, Petravic J, Chelimo K, Vulule J, Kazura JW, Moormann AM, et al. Decreased growth rate of P. falciparum blood stage parasitemia with age in a holoendemic population. Journal of Infectious Diseases. 2014;209(7):1136-43.
149. What you see is not what you get: implications of the brevity of antibody responses to malaria antigens and transmission heterogeneity in longitudinal studies of malaria immunity., (2009).
150. Antibodies to Plasmodium falciparum Antigens Predict a Higher Risk of Malaria But Protection From Symptoms Once Parasitemic., (2011).
151. Pinkevych M, Chelimo K, Vulule J, Kazura JW, Moormann AM, Davenport MP. Time-to-infection by Plasmodium falciparum is largely determined by random factors. BMC Med. 2015;13:19.

152. Chiyaka C, Garira W, Dube S. Modelling Immune Response and Drug Therapy in Human Malaria Infection. Computational and Mathematical Methods in Medicine. 2008;9(2):143-63.
153. McQueen PG. Population dynamics of a pathogen: the conundrum of vivax malaria. Biophys Rev. 2010;2(3):111-20.
154. Celada A, Cruchaud A, Perrin LH. Opsonic activity of human immune serum on in vitro phagocytosis of Plasmodium falciparum infected red blood cells by monocytes. Clin Exp Immunol. 1982;47(3):635-44.
155. Osier FHA, Feng G, Boyle MJ, Langer C, Zhou J, Richards JS, et al. Opsonic phagocytosis of Plasmodium falciparummerozoites: mechanism in human immunity and a correlate of protection against malaria. BMC Medicine. 2014;12(1):108.
156. Bouharoun-Tayoun H, Oeuvray C, Lunel F, Druilhe P. Mechanisms underlying the monocyte-mediated antibody-dependent killing of Plasmodium falciparum asexual blood stages. The Journal of experimental medicine. 1995;182(2):409-18.
157. Boyle MJ, Reiling L, Feng G, Langer C, Osier FH, Aspeling-Jones H, et al. Human Antibodies Fix Complement to Inhibit Plasmodium falciparum Invasion of Erythrocytes and Are Associated with Protection against Malaria. Immunity. 2015;42(3):580-90.
158. Mugyenyi CK, Elliott SR, Yap XZ, Feng G, Boeuf P, Fegan G, et al. Declining Malaria Transmission Differentially Impacts the Maintenance of Humoral Immunity to Plasmodium falciparum in Children. J Infect Dis. 2017;216(7):887-98.
159. Langreth SGR, R. Antigenicity of the infected-erythrocyte and merozoite surfaces in Falciparum malaria. J Exp Med. 1979;150(5):1241-54.
160. Fowkes FJI, Richards JS, Simpson JA, Beeson JG. The relationship between anti-merozoite antibodies and incidence of Plasmodium falciparum malaria: A systematic review and meta-analysis. PLoS medicine. 2010;7(1):e1000218.
161. Davenport MP, Fazou C, McMichael AJ, Callan MFC. Clonal Selection, Clonal Senescence, and Clonal Succession: The Evolution of the T Cell Response to Infection with a Persistent Virus. The Journal of Immunology. 2002;168(7):3309-17.
162. de Boer RJ, Oprea M, Antia R, Murali-Krishna K, Ahmed R, Perelson AS. Recruitment times, proliferation, and apoptosis rates during the CD8(+) T-cell response to lymphocytic choriomeningitis virus. J Virol. 2001;75(22):10663-9.
163. Gadhamsetty S, Marée AFM, Beltman JB, De Boer RJ. A general functional response of cytotoxic T lymphocyte-mediated killing of target cells. Biophys J. 2014;106(8):1780-91.
164. De Boer RJ. Which of Our Modeling Predictions Are Robust? PLoS Comput Biol. 2012;8(7):e1002593.
165. Mideo N, Savill NJ, Chadwick W, Schneider P, Read AF, Day T, et al. Causes of variation in malaria infection dynamics: insights from theory and data. Am Nat. 2011;178(6):E174-E88.
166. Kyes SA, Kraemer SM, Smith JD. Antigenic variation in Plasmodium falciparum: gene organization and regulation of the var multigene family. Eukaryot Cell. 2007;6(9):1511-20.
167. Althaus CL, De Boer RJ. Dynamics of Immune Escape during HIV/SIV Infection. PLOS Computational Biology. 2008;4(7):e1000103.
168. van Deutekom HW, Wijnker G, de Boer RJ. The rate of immune escape vanishes when multiple immune responses control an HIV infection. J Immunol. 2013;191(6):3277-86.

169. Paget-Mcnicol S, Gatton M, Hastings I, Saul A. The Plasmodium falciparum var gene switching rate, switching mechanism and patterns of parasite recrudescence described by mathematical modelling. Parasitology. 2002;124(03).
170. Holding T, Recker M. Maintenance of phenotypic diversity within a set of virulence encoding genes of the malaria parasite Plasmodium falciparum. J R Soc Interface. 2015;12(113):20150848.
171. Recker M, Nee S, Bull PC, Kinyanjui S, Marsh K, Newbold C, et al. Transient cross-reactive immune responses can orchestrate antigenic variation in malaria. Nature. 2004;429:555.
172. Nguyen T-N, von Seidlein L, Nguyen T-V, Truong P-N, Hung SD, Pham H-T, et al. The persistence and oscillations of submicroscopic Plasmodium falciparum and Plasmodium vivax infections over time in Vietnam: an open cohort study. Lancet Infect Dis. 2018;18(5):565-72.
173. MOORE DV, LANIER JE. Observations on two Plasmodium falciparum infections with an abnormal response to chloroquine. The American journal of tropical medicine and hygiene. 1961;10:5-9.
174. World Health Organization. Guidelines for the treatment of malaria. Italy: World Health Organization; 2015 May 01.
175. Jiang J-B, Guo X-B, Li G-Q, Cheung Kong Y, Arnold K. Antimalarial activity of mefloquine and qinghaosu. Lancet. 1982;320(8293):285-8.
176. Dondorp AM, Nosten F, Yi P, Das D, Phyo AP, Tarning J, et al. Artemisinin resistance in *Plasmodium falciparum* malaria. N Engl J Med. 2009;361(5):455-67.
177. Amaratunga C, Lim P, Suon S, Sreng S, Mao S, Sopha C, et al. Dihydroartemisinin–piperaquine resistance in *Plasmodium falciparum* malaria in Cambodia: a multisite prospective cohort study. Lancet Infect Dis. 2016;16(3):357-65.
178. Phyo AP, Nkhoma S, Stepniewska K, Ashley EA, Nair S, McGready R, et al. Emergence of artemisinin-resistant malaria on the western border of Thailand: a longitudinal study. Lancet. 2012;379(9830):1960-6.
179. Ashley EA, Dhorda M, Fairhurst RM, Amaratunga C, Lim P, Suon S, et al. Spread of Artemisinin Resistance in Plasmodium falciparum Malaria. N Engl J Med. 2014;371(5):411-23.
180. Simpson JA, Zaloumis S, DeLivera AM, Price RN, McCaw JM. Making the most of clinical data: reviewing the role of pharmacokinetic-pharmacodynamic models of anti-malarial drugs. The AAPS journal. 2014;16(5):962-74.
181. Geary TG, Divo AA, Jensen JB. Stage specific actions of antimalarial drugs on Plasmodium falciparum in culture. Am J Trop Med Hyg. 1989;40(3):240-4.
182. Wilson DW, Langer C, Goodman CD, McFadden GI, Beeson JG. Defining the timing of action of antimalarial drugs against *Plasmodium falciparum*. Antimicrob Agents Chemother. 2013;57(3):1455-67.
183. Klonis N, Xie SC, McCaw JM, Crespo-Ortiz MP, Zaloumis SG, Simpson JA, et al. Altered temporal response of malaria parasites determines differential sensitivity to artemisinin. Proc Natl Acad Sci U S A. 2013;110(13):5157-62.
184. Hastings IM, Kay K, Hodel EM. How robust are malaria parasite clearance rates as indicators of drug effectiveness and resistance? Antimicrob Agents Chemother. 2015.
185. White NJ, Watson J, Ashley EA. Split dosing of artemisinins does not improve antimalarial therapeutic efficacy. Sci Rep. 2017;7(1):12132.

186. Dixit NM, Layden-Almer JE, Layden TJ, Perelson AS. Modelling how ribavirin improves interferon response rates in hepatitis C virus infection. Nature. 2004;432(7019):922-4.
187. Neumann AU, Lam NP, Dahari H, Gretch DR, Wiley TE, Layden TJ, et al. Hepatitis C Viral Dynamics in Vivo and the Antiviral Efficacy of Interferon-α Therapy. Science. 1998;282(5386):103.
188. Flegg JA, Guerin PJ, White NJ, Stepniewska K. Standardizing the measurement of parasite clearance in *falciparum* malaria: the parasite clearance estimator. Malar J. 2011;10:339.
189. McCarthy JS, Lotharius J, Rückle T, Chalon S, Phillips MA, Elliott S, et al. Safety, tolerability, pharmacokinetics, and activity of the novel long-acting antimalarial DSM265: a two-part first-in-human phase 1a/1b randomised study. Lancet Infect Dis. 2017;17(6):626-35.
190. McCarthy JS, Ruckle T, Djeriou E, Cantalloube C, Ter-Minassian D, Baker M, et al. A Phase II pilot trial to evaluate safety and efficacy of ferroquine against early Plasmodium falciparum in an induced blood-stage malaria infection study. Malar J. 2016;15:469.
191. White NJ. The parasite clearance curve. Malar J. 2011;10:278.
192. Hoshen MB, Na-Bangchang K, Stein WD, Ginsburg H. Mathematical modelling of the chemotherapy of Plasmodium falciparum malaria with artesunate: postulation of 'dormancy', a partial cytostatic effect of the drug, and its implication for treatment regimens. Parasitology. 2000;121 (Pt 3):237-46.
193. Saunders D, Khemawoot P, Vanachayangkul P, Siripokasupkul R, Bethell D, Tyner S, et al. Pharmacokinetics and pharmacodynamics of oral artesunate monotherapy in patients with uncomplicated Plasmodium falciparum malaria in western Cambodia. Antimicrob Agents Chemother. 2012;56(11):5484-93.
194. Svensson U, Alin MH, Karlsson MO, Bergqvist Y, Ashton M. Population pharmacokinetic and pharmacodynamic modelling of artemisinin and mefloquine enantiomers in patients with falciparum malaria. Eur J Clin Pharmacol. 2002;58(5):339-51.
195. Gordi T, Xie R, Jusko WJ. Semi-mechanistic pharmacokinetic/pharmacodynamic modelling of the antimalarial effect of artemisinin. Br J Clin Pharmacol. 2005;60(6):594-604.
196. Hietala SF, Martensson A, Ngasala B, Dahlstrom S, Lindegardh N, Annerberg A, et al. Population pharmacokinetics and pharmacodynamics of artemether and lumefantrine during combination treatment in children with uncomplicated falciparum malaria in Tanzania. Antimicrob Agents Chemother. 2010;54(11):4780-8.
197. Khoury DS, Cromer D, Elliott T, Soon MSF, Thomas BS, James KR, et al. Characterising the effect of antimalarial drugs on the maturation and clearance of murine blood-stage Plasmodium parasites in vivo. Int J Parasitol. 2017;47(14):913-22.
198. Yang T, Xie SC, Cao P, Giannangelo C, McCaw J, Creek DJ, et al. Comparison of the Exposure Time Dependence of the Activities of Synthetic Ozonide Antimalarials and Dihydroartemisinin against K13 Wild-Type and Mutant Plasmodium falciparum Strains. Antimicrob Agents Chemother. 2016;60(8):4501-10.
199. Klonis N, Crespo-Ortiz MP, Bottova I, Abu-Bakar N, Kenny S, Rosenthal PJ, et al. Artemisinin activity against *Plasmodium falciparum* requires hemoglobin uptake and digestion. Proc Natl Acad Sci U S A. 2011;108(28):11405-10.

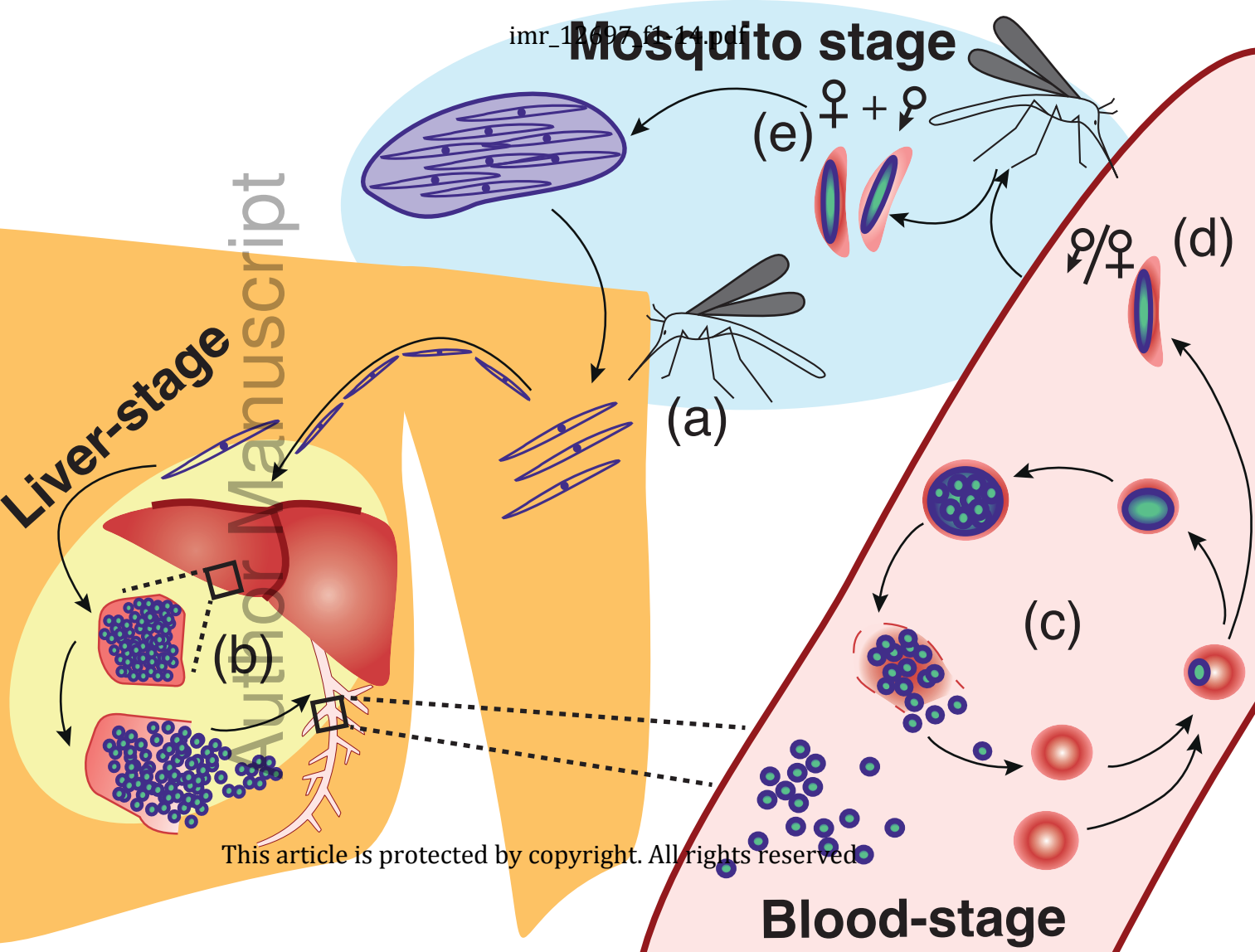

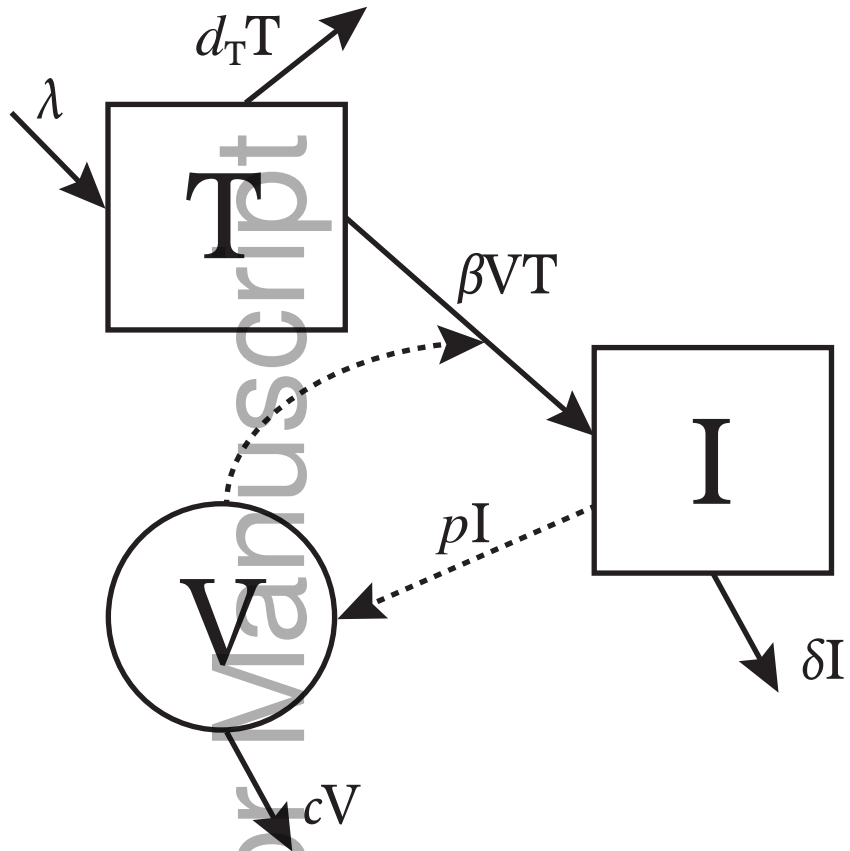

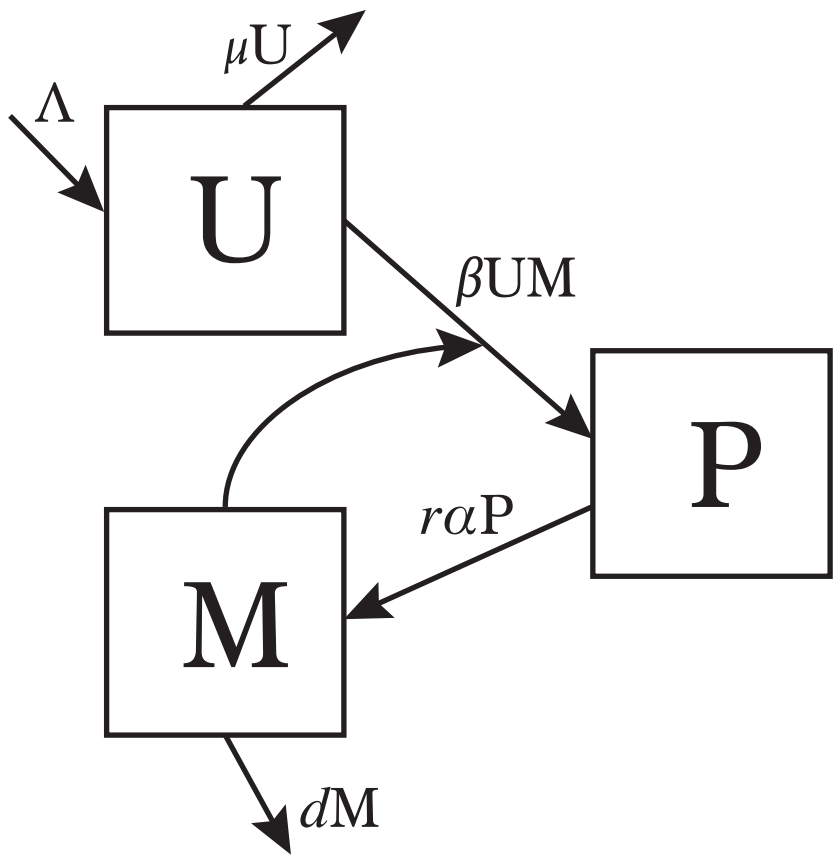

T cells: $\frac{dT}{dt} = \lambda - d_T T - \beta VT$

RBCs: $\frac{dU}{dt} = \Lambda - \mu U - \beta UM$

Infected cells: $\frac{dI}{dt} = \beta VT - \delta I$

pRBCs: $\frac{dP}{dt} = \beta UM - \alpha P$

Free virus: $\frac{dV}{dt} = pI - cV$

Meroz-oites: $\frac{dM}{dt} = r\alpha P - dM$

A n-compartment

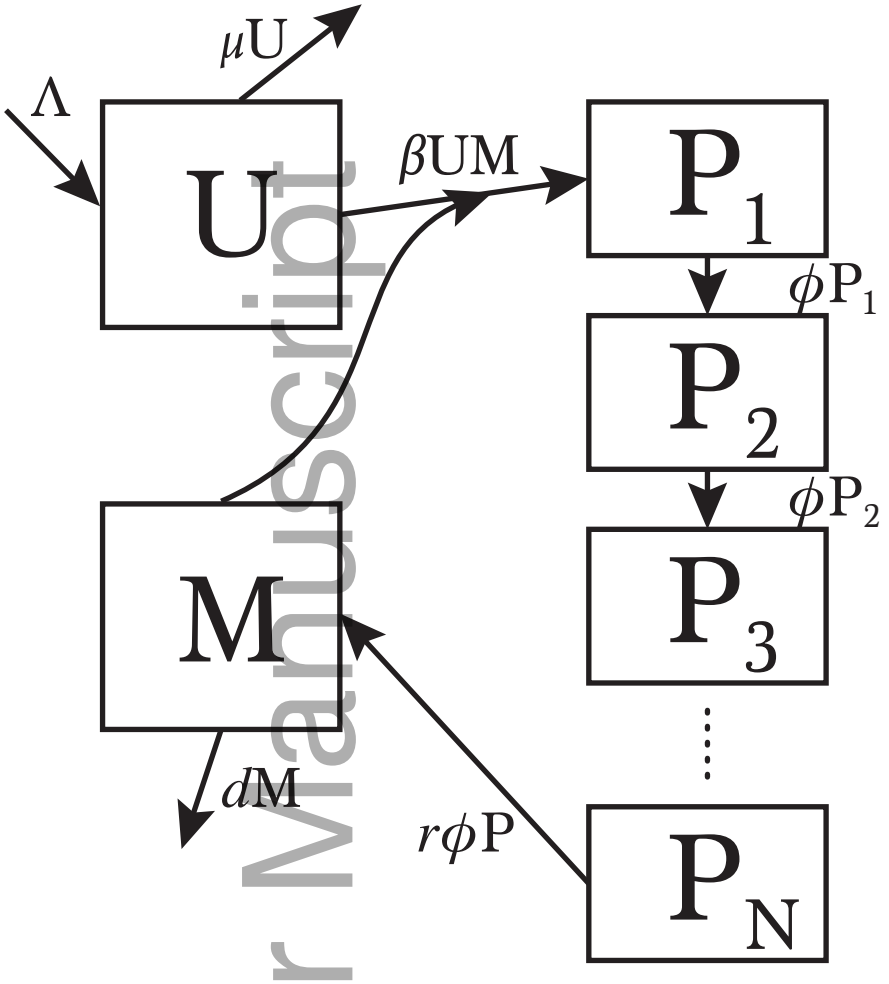

$$\frac{dP_1}{dt} = \beta UM - \phi P_1$$

$$\frac{dP_i}{dt} = \phi P_{i-1} - \phi P_i$$

$$i = 2, \ldots, N$$

$$\frac{dM}{dt} = r\phi P_N - dM$$

B PDE model

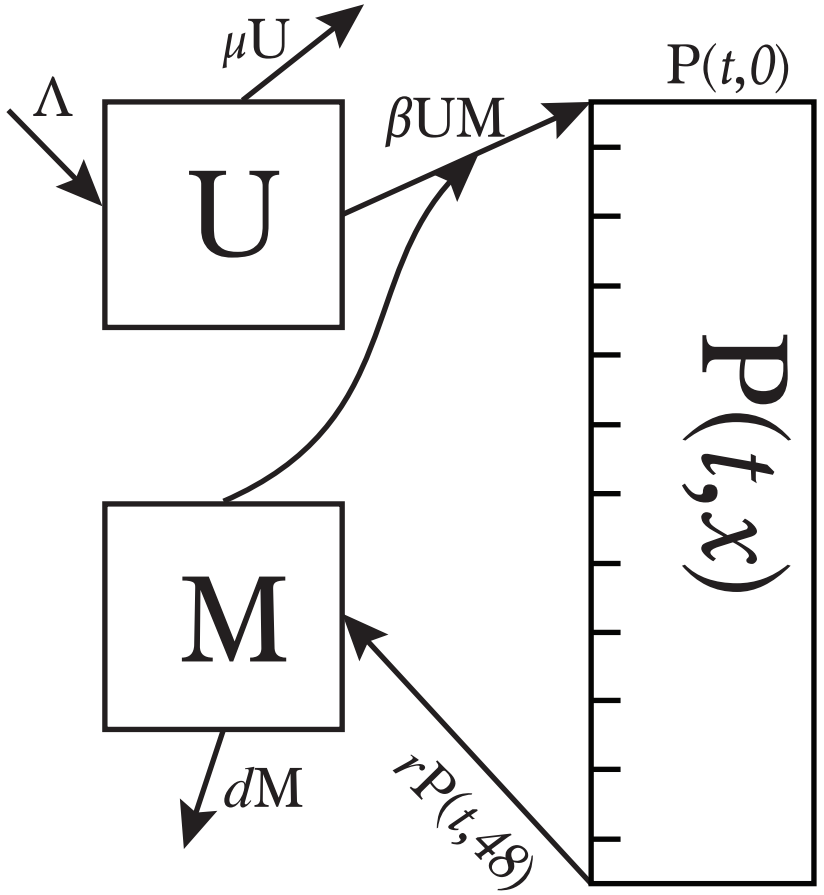

$$\frac{\partial P}{\partial t} + \frac{\partial P}{\partial x} = 0$$

$$P(t,0) = \beta UM$$

$$\frac{dM}{dt} = rP(t,48) - dM$$

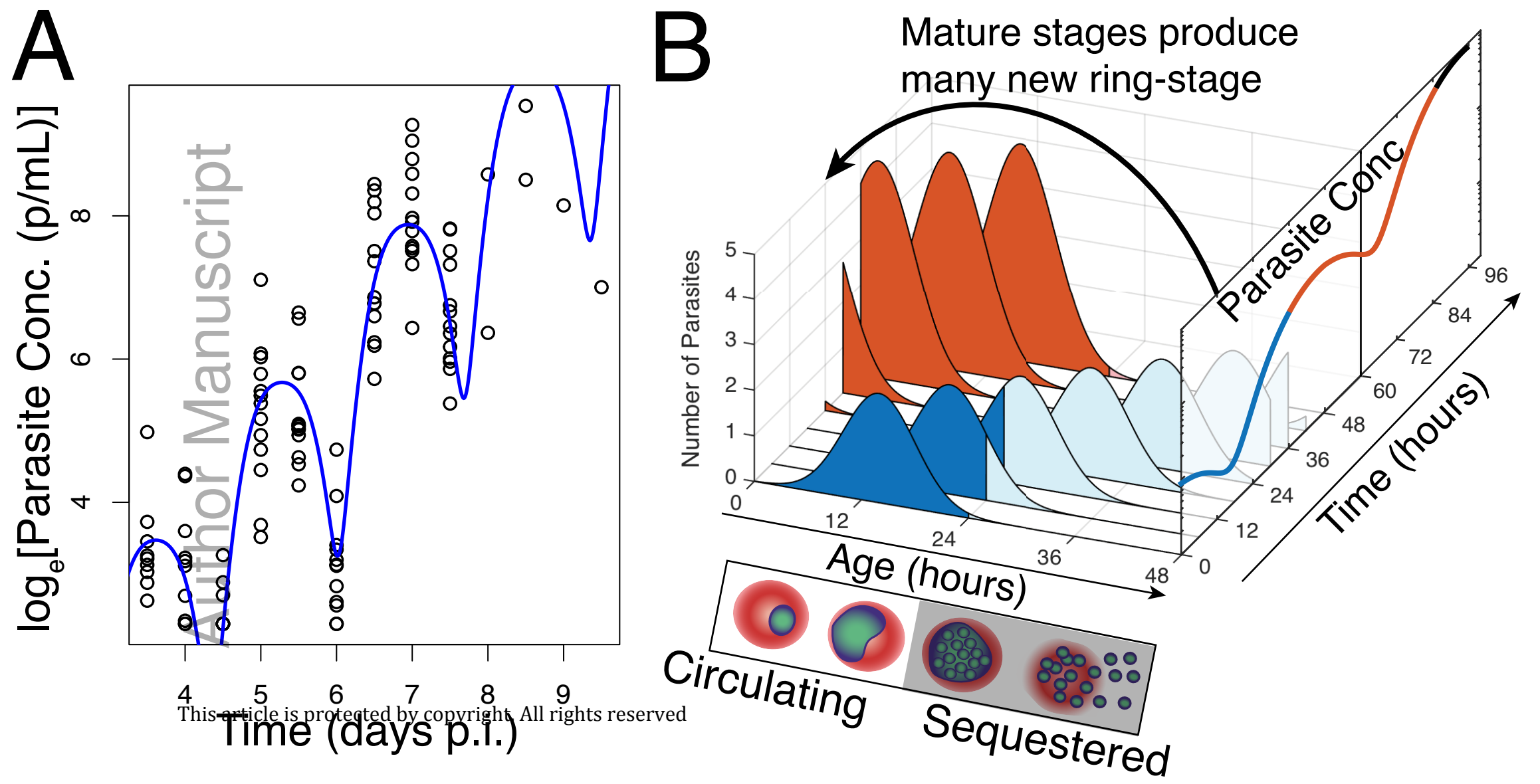

A n-compartment

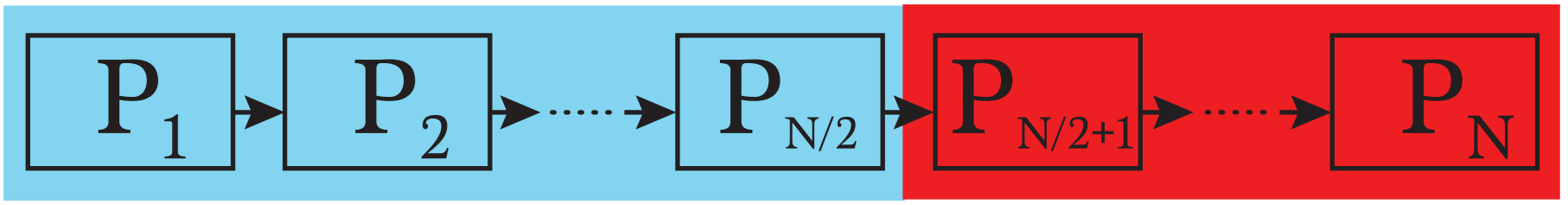

$$\bar{P}(t) = \sum_{i=1}^{N/2} P_i(t) \qquad \bar{S}(t) = \sum_{i=N/2+1}^{N} P_i(t)$$

B PDE model

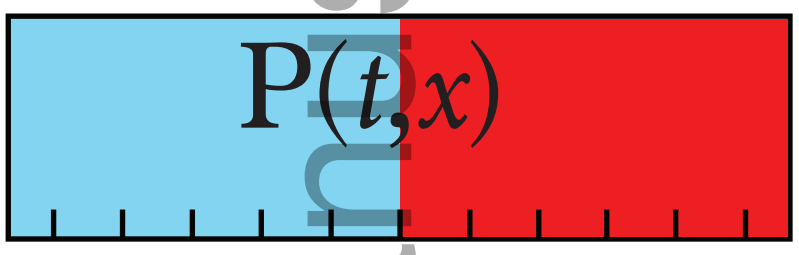

$$\bar{P}(t) = \int_0^{24} P(t,x)\ dx \qquad \bar{S}(t) = \int_{24}^{48} P(t,x)\ dx$$

C Rate of sequestration

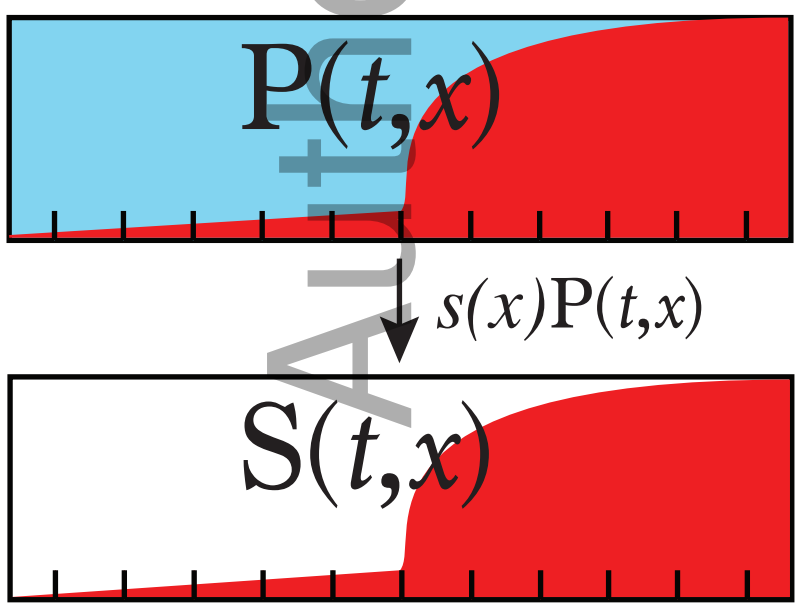

$$\frac{\partial P}{\partial t} + \frac{\partial P}{\partial x} = -s(x)P(t,x)$$

$$\frac{\partial S}{\partial t} + \frac{\partial S}{\partial x} = s(x)P(t,x)$$

$$\bar{P}(t) = \int_0^{48} P(t,x)\ dx \qquad \bar{S}(t) = \int_0^{48} S(t,x)\ dx$$

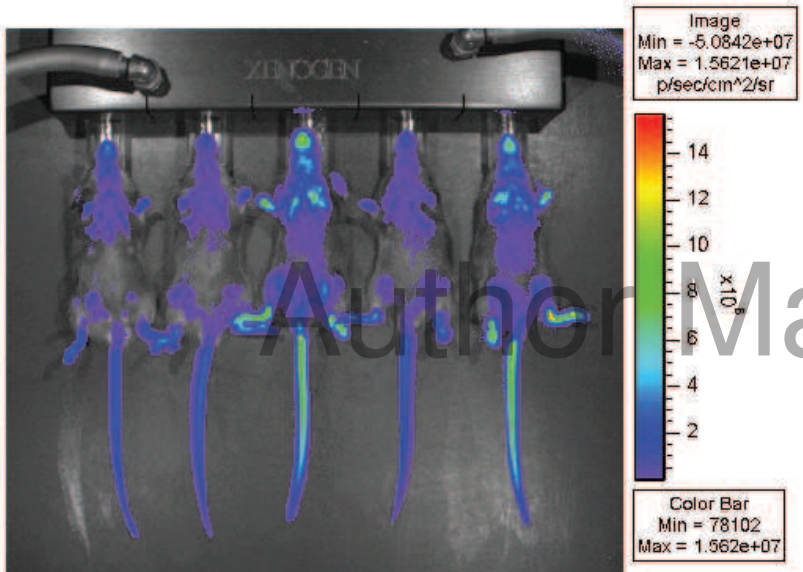

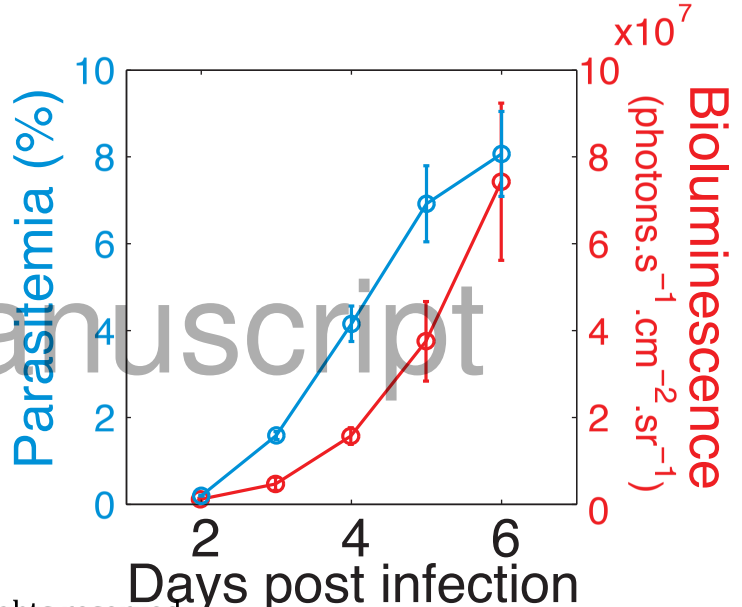

A

B

Example: Splitting RBCs into age-compartments

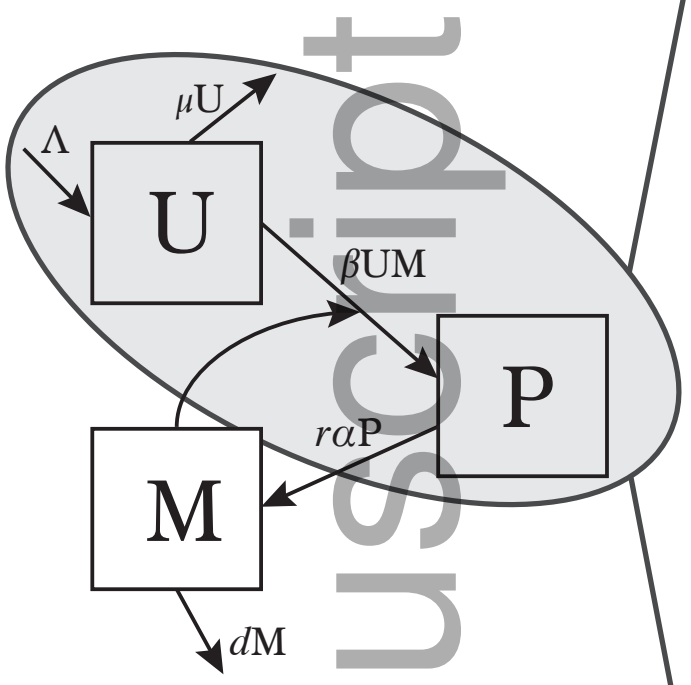

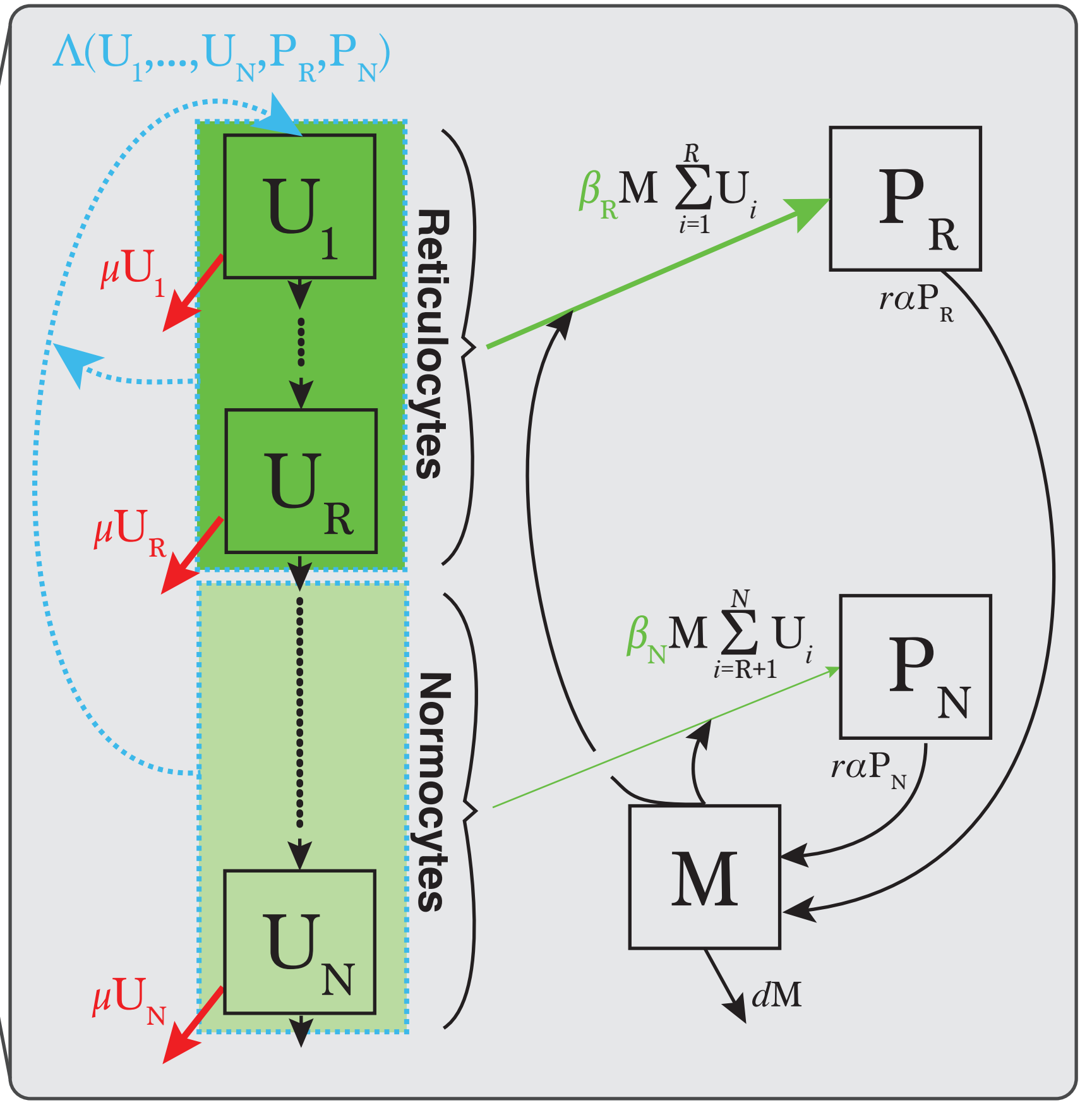

$$\frac{dU_1}{dt} = \underbrace{\Lambda(U_1,\dots,U_N,P_R,P_N)}_{\text{Production of RBCs}} - \underbrace{\omega U_1}_{\text{RBC maturation}} - \beta_R U_1 M - \underbrace{\mu U_1}_{\text{Bystander killing}}$$

$$\frac{dU_i}{dt} = \omega U_{i-1} - \omega U_i - \underbrace{\beta_R M U_i}_{\text{Preferential invasion of reticulocytes}} - \mu U_i, \qquad 1 \le i \le R$$

$$\frac{dU_i}{dt} = \omega U_{i-1} - \omega U_i - \beta_N M U_i - \mu U_i, \qquad R+1 \le i \le N$$

$$\frac{dP_R}{dt} = \beta_R M \sum_{i=1}^{R} U_i - \alpha P_R \qquad \frac{dP_N}{dt} = \beta_N M \sum_{i=R+1}^{N} U_i - \alpha P_N$$

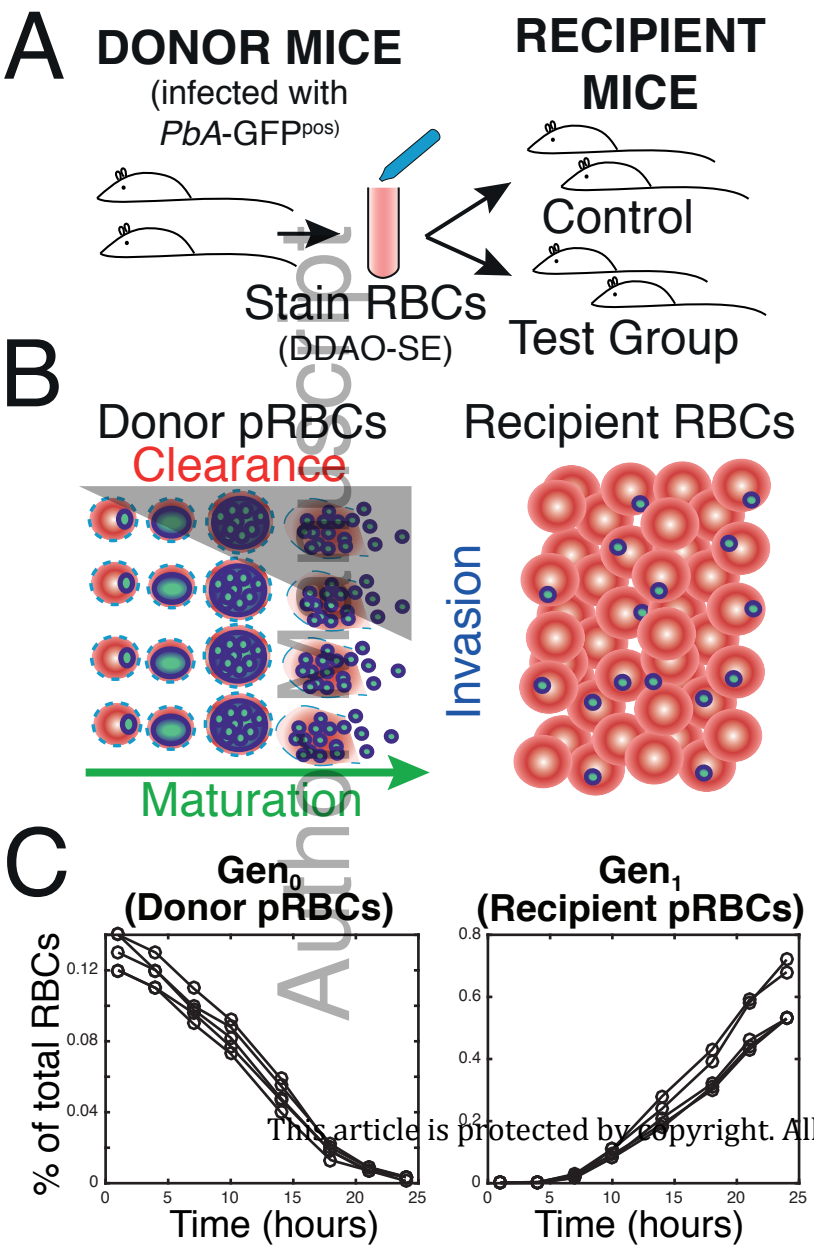

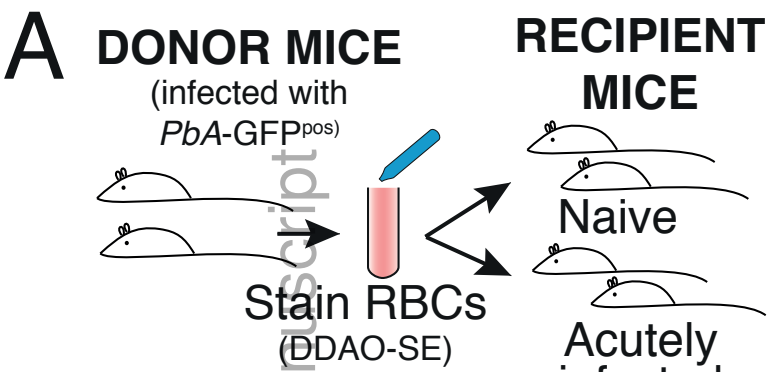

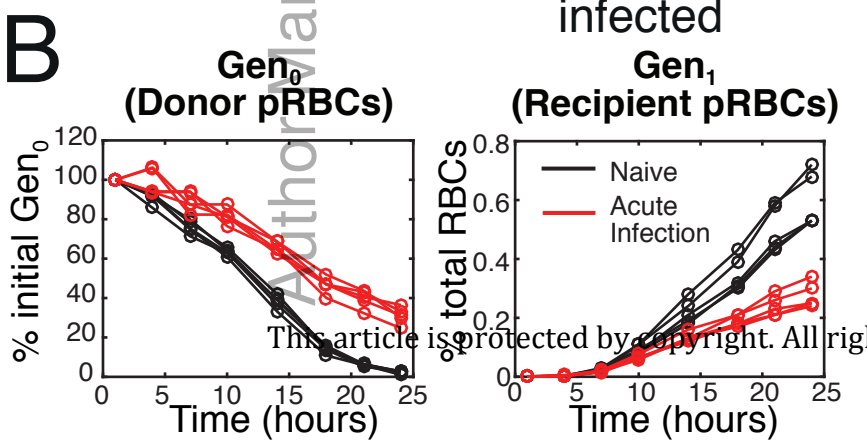

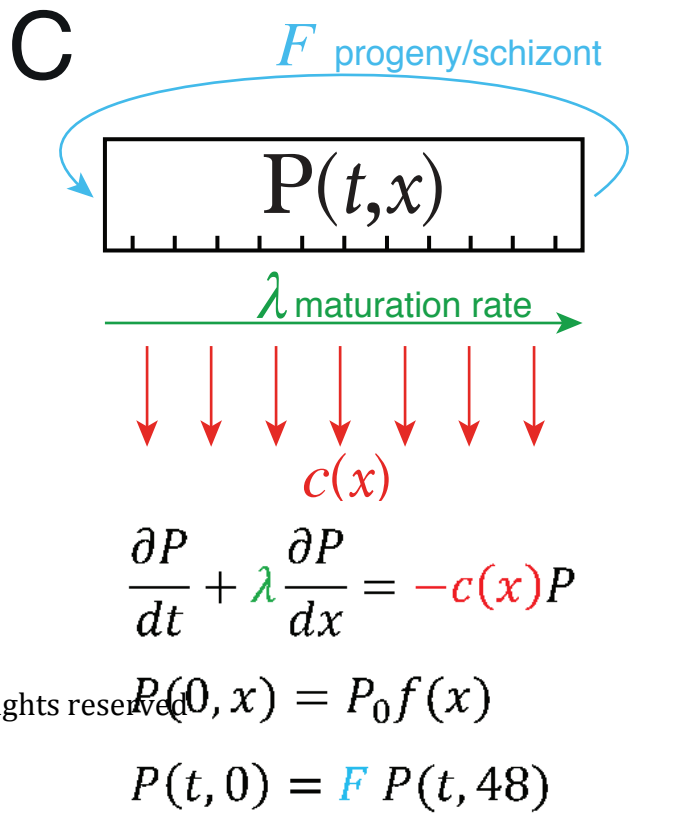

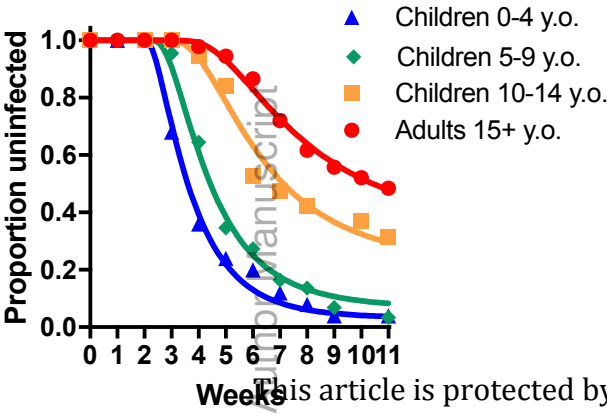

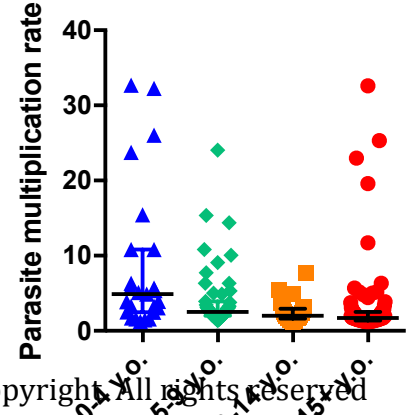

(a) (b)

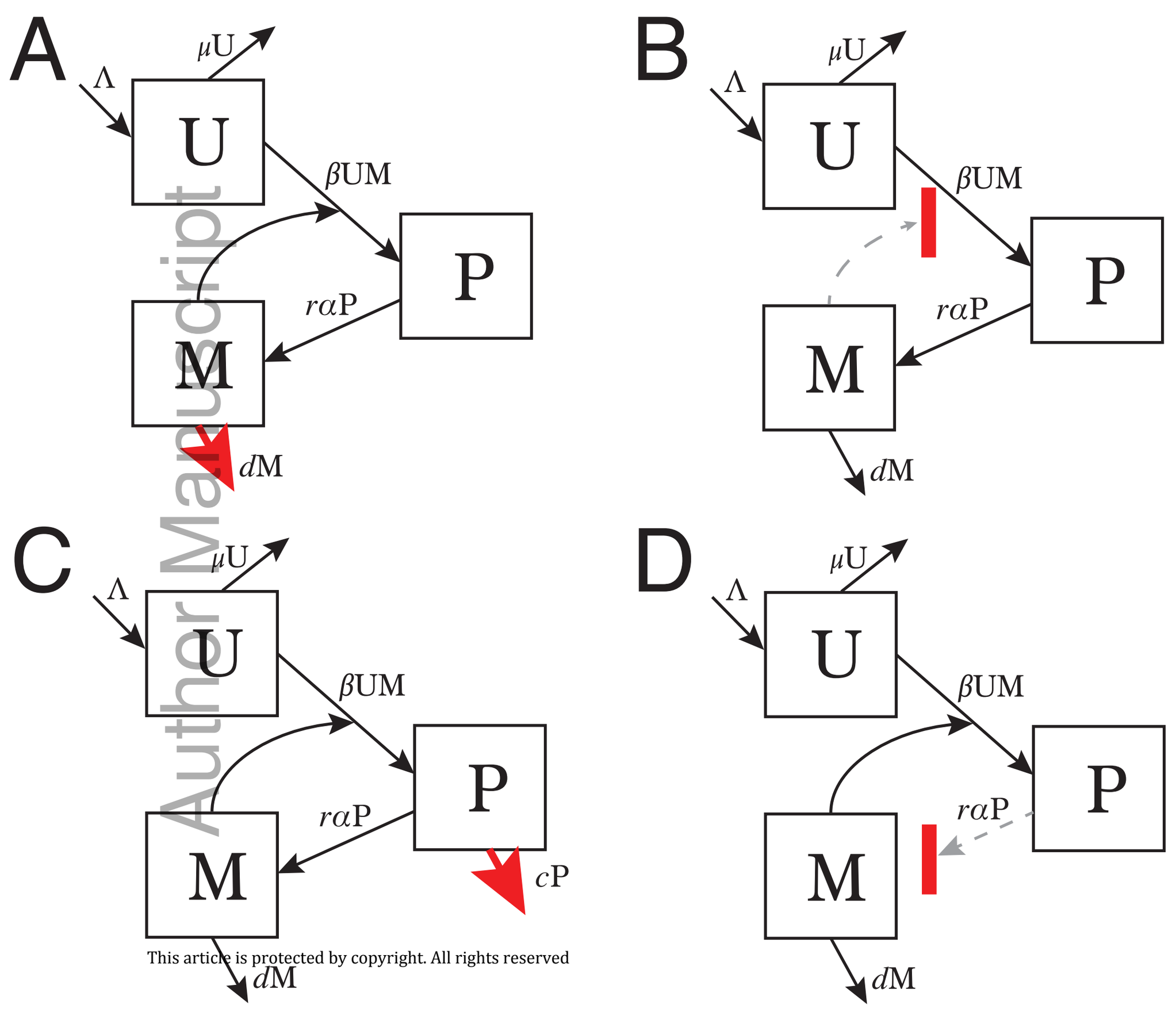

A

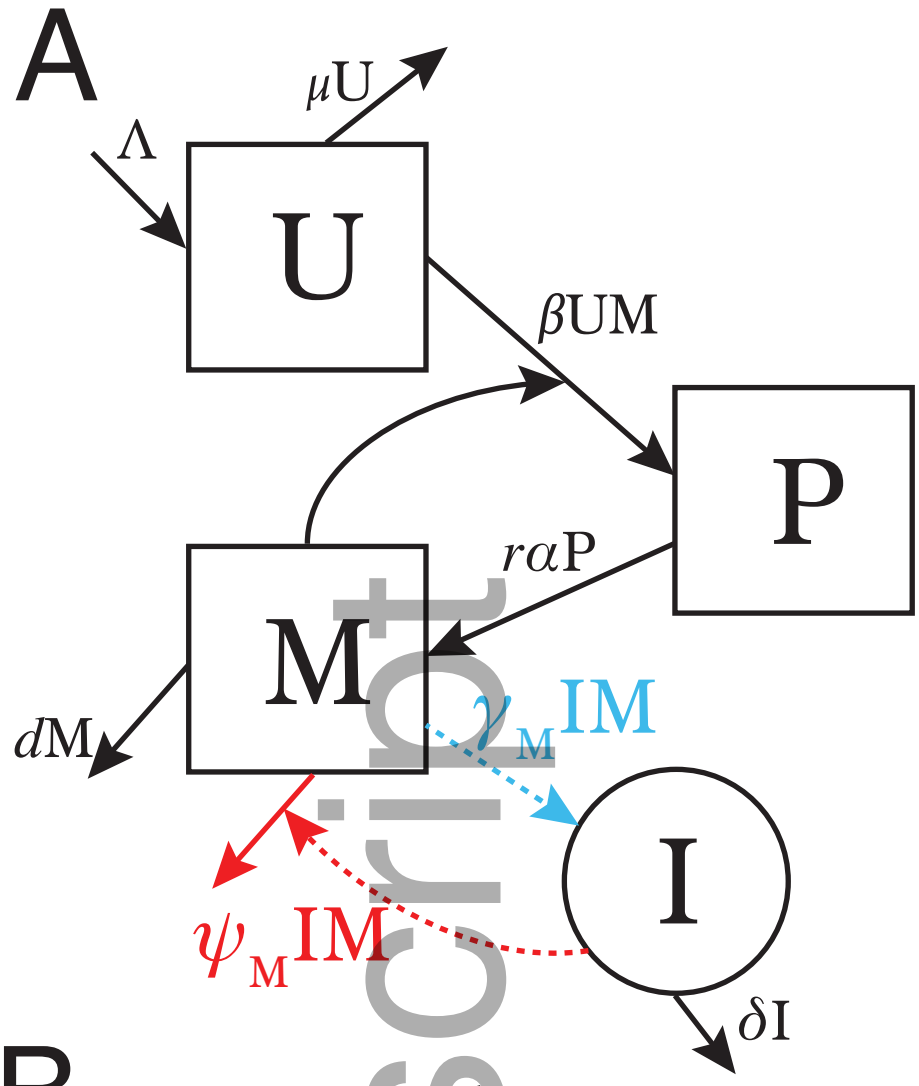

$$\frac{dU}{dt} = \Lambda - \mu U - \beta UM$$

$$\frac{dP}{dt} = \beta UM - \alpha P$$

$$\frac{dM}{dt} = r\alpha P - dM - \psi_M IM$$

$$\frac{dI}{dt} = \gamma_M IM - \delta I$$

B

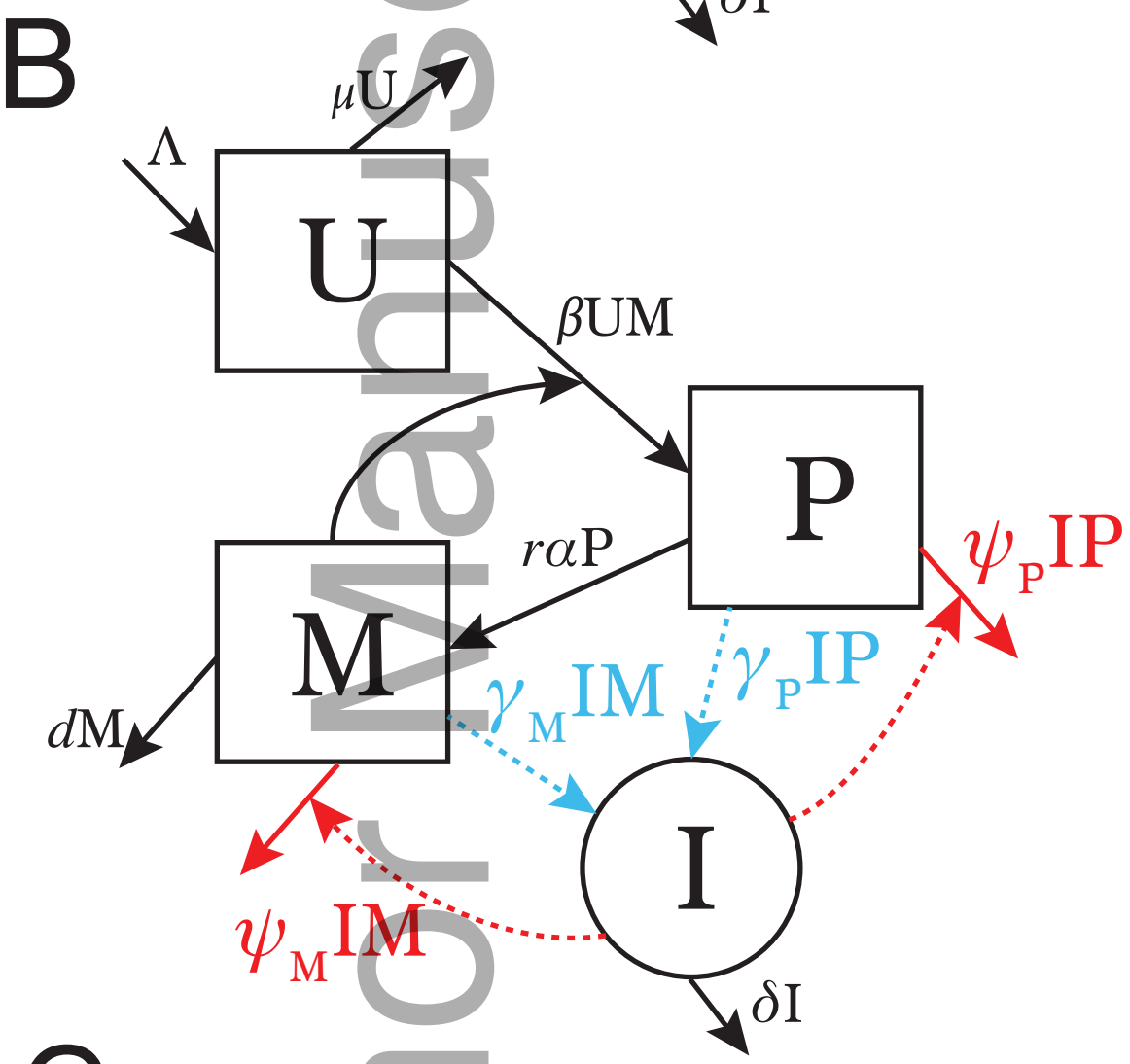

$$\frac{dU}{dt} = \Lambda - \mu U - \beta UM$$

$$\frac{dP}{dt} = \beta UM - \alpha P - \psi_P IP$$

$$\frac{dM}{dt} = r\alpha P - dM - \psi_M IM$$

$$\frac{dI}{dt} = \gamma_M IM + \gamma_P IP - \delta I$$

C

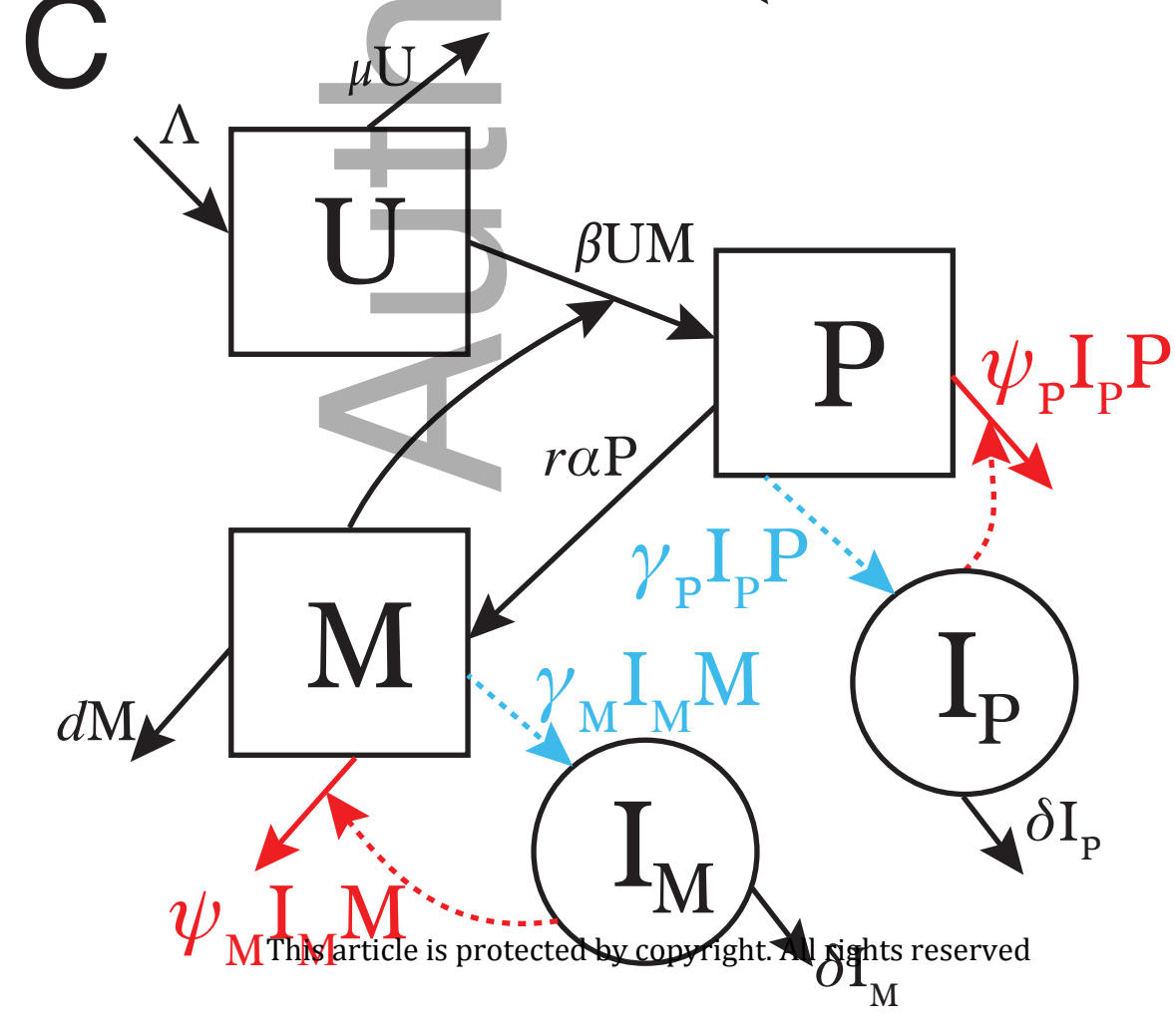

$$\frac{dU}{dt} = \Lambda - \mu U - \beta UM$$

$$\frac{dP}{dt} = \beta UM - \alpha P - \psi_P I_P P$$

$$\frac{dM}{dt} = r\alpha P - dM - \psi_M I_M M$$

$$\frac{dI_M}{dt} = \gamma_M I_M M - \delta I_M$$

$$\frac{dI_P}{dt} = \gamma_P I_P M - \delta I_P$$

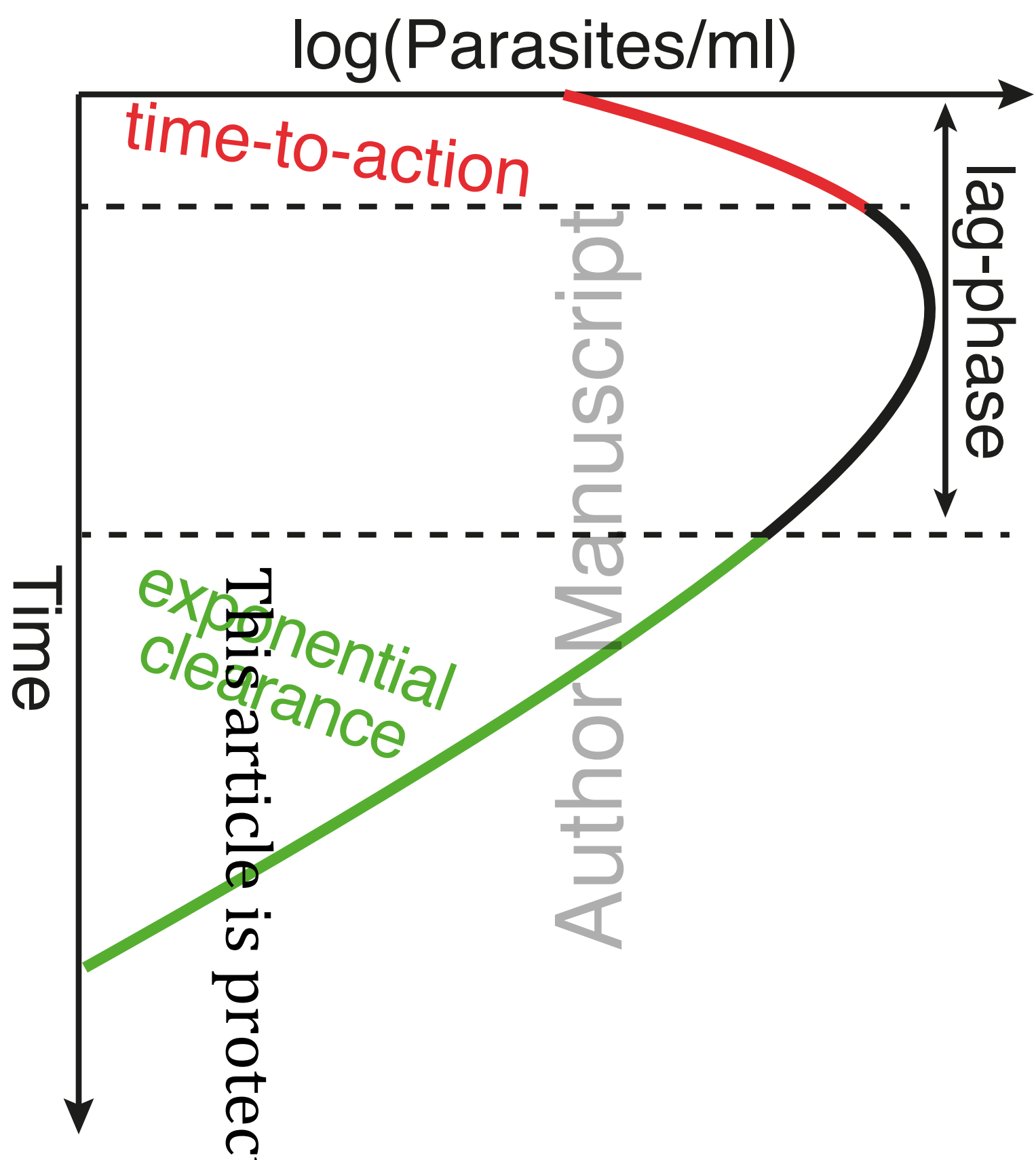
log(Parasites/ml)
time-to-action
lag-phase
Time
exponential clearance
This article is protec
Author Manuscript

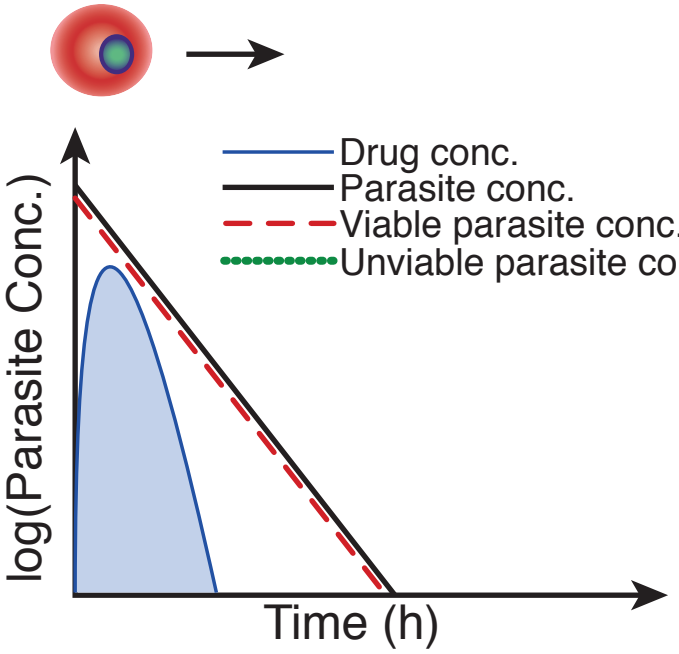
Drug conc.
Parasite conc.
Viable parasite conc.
Unviable parasite conc.
log(Parasite Conc.)
Time (h)

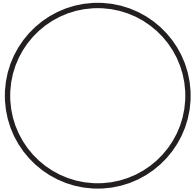

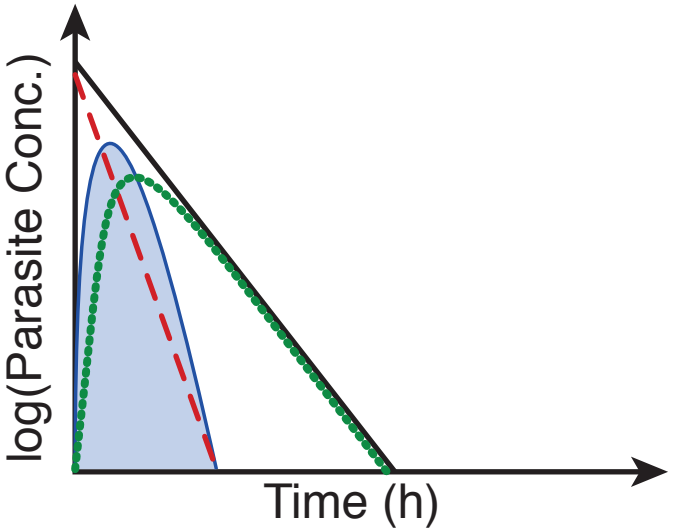
log(Parasite Conc.)
Time (h)